# PROCESSING AND CHARACTERIZATION OF FLY ASH – QUARTZ COATINGS

**A**

**THESIS SUBMITTED IN PARTIAL FULFILLMENT**

**OF THE REQUIREMENT FOR THE DEGREE OF**

**MASTER OF TECHNOLOGY**

in

**Metallurgical & Materials Engineering**

**By**

**SWETAPADMA PRAHARAJ**


**DEPARTMENT OF METALLURGICAL & MATERIALS ENGINEERING**

**NATIONAL INSTITUTE OF TECHNOLOGY, ROURKELA**

**2009**

# PROCESSING AND CHARACTERIZATION OF FLY ASH – QUARTZ COATINGS

**A**
**THESIS SUBMITTED IN PARTIAL FULFILLMENT**
**OF THE REQUIREMENT FOR THE DEGREE OF**

**MASTER OF TECHNOLOGY**

in

**Metallurgical & Materials Engineering**

**By**

**SWETAPADMA PRAHARAJ**

**Under the Guidance of**
**Prof. S C Mishra**

and

**Under the Co-Guidance of**
**Prof. Alok Satapathy**


**DEPARTMENT OF METALLURGICAL & MATERIALS ENGINEERING**

**NATIONAL INSTITUTE OF TECHNOLOGY, ROURKELA**
**2009**

**Department of Metallurgical and Materials Engineering**
**National Institute of Technology**
**Rourkela – 769 008**

# CERTIFICATE

This is to certify that thesis entitled, "**PROCESSING AND CHARACTERIZATION OF FLYASH-QUARTZ COATINGS"** submitted by **Mrs. SWETAPADMA PRAHARAJ** in partial fulfillment of the requirements for the award of **Master of Technology** Degree in **Metallurgical and Materials Engineering** at **National Institute of Technology**, Rourkela (Deemed University) is an authentic work carried out by her under our supervision and guidance.

To the best of our knowledge, the matter embodied in this thesis has not been submitted to any other university/ institute for award of any Degree or Diploma.

**Dr. Alok Satapathy**
**Asst. Professor**
Dept. of Mechanical Engg.
National Institute of Technology
Rourkela

**Dr. S.C.Mishra**
**Professor**
Dept. of Metallurgical and Materials Engg.
National Institute of Technology
Rourkela.

# ACKNOWLEDGEMENT

I avail this opportunity to extend my hearty indebtedness to my guide **Prof. S. C. Mishra** for his invaluable guidance, untiring efforts and meticulous attention at all stages during my course of work. I would also like to convey my deep regards to my co-guide **Prof. Alok Satapathy** for his patience, constant motivation and regular monitoring of the work and inputs, for which this work has come to fruition.

I express my gratitude to **Prof. B B Verma, Head of the Department** for providing me the necessary facilities in the department.

My sincere regards to **Dr. P.V.A Padmanavan** and **Dr. K.P.Sreekumar,** Laser and Plasma Division, BARC, for availing me the laboratory facilities.

I am also thankful to **Mrs Tabasum Ara Begum, Sri Hemram, Sri Udayanath Sahu, Sri Rajesh Pattnaik, and Sri Samir Pradhan,** Metallurgical & Materials Engineering, Technical assistants, for their co-operation in experimental work.

Special thanks to **Sri Nadiya Bihari Nayak,** Department of Metallurgical and Materials Engineering for being so supportive and helpful in every possible way.

**SWETAPADMA PRAHARAJ**

# CONTENTS

**Page No.**

## Abstract

*Fly ash emerges as the major waste material of many thermal power plants. It mainly comprises of oxides of silicon, aluminium, iron, and titanium along with some other minor constituents. The present investigation explores the coating potential of this industrial waste. It envisages the processing and characterization of a series of plasma sprayed coatings made with fly ash premixed with quartz, which is a low cost mineral available in plenty. These materials do not belong to the so-called "plasma sprayable" category. These have been deposited on mild steel and copper substrates by atmospheric plasma spraying. Utilization of such kind of industrial waste as coating material minimizes the cost of plasma spray deposition process, which posed to be the major hindrance to its wide spread application due to high cost of the spray grade powders.*

*Using atmospheric plasma spraying system coatings are deposited on metal substrates at different operating power levels of the plasma torch ranging from 11kW to 21kW and then characterization of the coatings is carried out. The properties of the coating depend on the materials used, operating condition and the process parameters. The plasma spraying process is controlled by the parameter interdependencies, co-relations and individual effect on coating characteristics. The particle sizes of the raw materials used for coating are characterized using Laser particle size analyzer. Deposition efficiency is an important factor that determines the techno economics of the process. It is evaluated for the deposited coatings. Coating interface bond strength is evaluated using coating pull out method, confirming to ASTM C-633 standard. In view of tribological applications, hardness is one of the most required mechanical properties. Hardness measurement is done on the polished cross section of the samples using Leitz Micro-Hardness Tester. Coating porosity is measured by image analysis technique. To ascertain the phases present and phase changes / transformation taking place during plasma spraying, XRD analysis is made. Coating surface & interface morphology is studied with Scanning Electron Microscope.*

*To study the suitability of the coatings for wear resistance application, wear properties of these coatings are studied. The erosion wear behaviour of these coatings is evaluated with solid particle erosion tests under various operating conditions. In order to control the wear loss in such a process, one of the challenges is to recognize parameter interdependencies; correlations and their individual effects on wear so that the coating can*

*be useful for tribological application. Statistical analysis of the experimental results using Taguchi experimental design is presented. Spraying parameters such as impact angle, size of the erodent, standoff distance and impact velocity are identified as the significant factors affecting the coating erosion wear. Other statistical techniques like ANN and SYSTAT have also been very much useful in predicting the experimental data with a larger domain. This work establishes that fly ash-quartz mixture can be used as a potential coating material suitable for depositing plasma spray coating. It also opens up a new pathway for value added utilization of this industrial waste and low-grade ore mineral.*

****

## LIST OF FIGURES

# LIST OF TABLES

# Chapter 1

# Introduction

- Background
- Objectives of the present piece of investigation

# CHAPTER 1
# INTRODUCTION

## 1.1 BACKGROUND

The incessant quest for higher efficiency and productivity across the entire spectrum of manufacturing and engineering industries has ensured that most modern-day components are subjected to increasingly harsh environments during routine operation. Critical industrial components are, therefore, prone to more rapid degradation as the parts fail to withstand the rigors of aggressive operating conditions and this has been taking a heavy toll of industry's economy. In an overwhelmingly large number of cases, the accelerated deterioration of parts and their eventual failure has been traced to material damage brought about by hostile environments and also by high relative motion between mating surfaces, corrosive media, extreme temperatures and cyclic stresses. Simultaneously, research efforts focused on the development of new materials for fabrication are beginning to yield diminishing returns and it appears unlikely that any significant advances in terms of component performance and durability can be made only through development of new alloys. As a result of the above, the concept of incorporating engineered surfaces by various surface modification techniques, capable of combating the accompanying degradation phenomena like wear, corrosion and fatigue to improve component performance, reliability and durability has gained increasing acceptance in recent years.

Surface modification is a generic term now applied to a large field of diverse technologies that can be gainfully harnessed to achieve increased reliability and enhanced performance of industrial components. The recognition that a vast majority of engineering components fail catastrophically in service through surface related phenomena has further fuelled this approach and led to the development of the broad interdisciplinary area of surface modifications. Hence various surface modification techniques have been adopted. With this regard, protecting the surface with a protective coating is one of the challenging areas of industrial research now days. A protective coating is deposited to act as a barrier between the surfaces of the component and the aggressive environment that it is exposed to during operation is now globally acknowledged to be an attractive means to significantly reduce/suppress damage to the actual component by acting as the first line of defense. Coating is a layer of material formed naturally or synthetically or deposited artificially on

the surface of an object made of another material with the aim of obtaining required technical or decorative properties.

The development of surface engineering has been dynamic largely on account of the fact that it is a discipline of science and technology that is being increasingly relied upon to meet all the key modern day technological requirements: material savings, enhanced efficiencies, environmental friendliness etc. The overall utility of the surface engineering approach is further augmented by the fact that modifications to the component surface can be metallurgical, mechanical, chemical or physical. At the same time, the engineered surface can span at least five orders of magnitude in thickness and three orders of magnitude in hardness.

Existing surface treatment processes fall under three broad categories:

**a) Overlay coatings:**

This category incorporates a very wide variety of coating processes wherein a material different from the bulk is deposited on the substrate. The coating is distinct from the substrate in the as-coated condition and there exists a clear boundary at the substrate/coating interface. The adhesion of the coating to the substrate is a major issue.

**b) Diffusion coatings:**

Chemical interaction of the coating-forming element(s) with the substrate by diffusion is involved in this category. New elements are diffused into the substrate surface, usually at elevated temperatures so that the composition and properties of outer layers are changed as compared to those of the bulk e.g. carburizing, nitriding, cyaniding, boronizing, chromizing etc.

**c) Thermal or Mechanical modification of the surface:**

In this case, the existing metallurgy of the component surface is changed in the near-surface region either by thermal or mechanical means, usually to increase its hardness. The type of coating to be provided depends on the application. There are many techniques available, e.g. electroplating, vapor depositions, thermal spraying etc. Of all these techniques, thermal spraying is popular for its wide range of applicability, adhesion of coating with the substrate and durability. It has gradually emerged as the most industrially useful method of developing a variety of coatings, to enhance the quality of new components as well as to reclaim worn/wrongly machined parts.

Surface modification technologies have grown rapidly, both in terms of finding better solutions and in the number of technology variants available, to offer a wide range of quality and cost. The significant increase in the availability of coating process of wide

ranging complexity that are capable of depositing a plethora of coatings and handling components of diverse geometry today, ensures that components of all imaginable shape and size can be coated economically. Surface modification today is best defined as “the design of substrate and surface together as a system to give a cost effective performance enhancement, of which neither is capable on its own”. The development of a suitable high performance coating on a component fabricated using an appropriate high mechanical strength metal/alloy offers a promising method of meeting both the bulk and surface property requirements of virtually all imagined applications. The newer surfacing techniques, along with the traditional ones, are eminently suited to modify a wide range of engineering properties. The properties that can be modified by adopting the surface engineering approach include tribological, mechanical, thermo-mechanical, electrochemical, optical, electrical, electronic, magnetic/acoustic and biocompatible properties.

In selecting a coating material it is necessary to consider the uses to which it will be put. Factors to be considered include:

**a)** The properties of the coating material itself-its melting point, hardness, vapor pressure, density and thermal expansion coefficient.

**b)** The resistance of the coating material to the attack expected.

**c)** The compatibility of the coating and substrate over the temperature range of the expected application. This includes the minimizing of thermal stresses, by matching thermal expansion coefficients, and the provision of good coating substrate adhesion. Some inter diffusion may be desirable, but an excessive amount, such as may occur with silicon plating at high temperatures, may only lead to bulk diffusion and alloy formation; and

**d)** The cost ultimately whether or not a particular coating will be used, depends on the trade-off between the benefits to be gained and the additional cost to be incurred.

Driven by technological need and fuelled by exciting possibilities, novel methods for applying coatings by **thermal spraying** and their applications have been proliferated in recent years. The type of thermal spraying depends on the type of heat source employed and consequently flame spraying (FS), high velocity oxy-fuel spraying (HVOF), plasma spraying (PS) etc. come under the umbrella of thermal spraying. Plasma spraying utilizes the exotic properties of the plasma medium to impart new functional properties to conventional and non-conventional materials and is considered as one highly versatile and technologically sophisticated thermal spraying technique.

Plasma spraying, one of the thermal spraying processes, is increasingly popular owing to its versatility in spraying a large number of materials and is being researched well. It is a very large industry with applications in corrosion, abrasion and temperature resistant coatings and the production of monolithic and near net shapes [1]. The process can be applied to coat on variety of substrates of complicated shape and size using metallic, ceramic and /or polymeric consumables. The production rate of the process is very high and the coating adhesion is also adequate. Since the process is almost material independent, it has a very wide range of applicability, e.g., as thermal barrier coating, wear resistant coating etc. Thermal barrier coatings are provided to protect the base material, e.g., internal combustion engines, gas turbines etc. at elevated temperatures. Zirconia ($ZrO_2$) is a conventional thermal barrier coating material. As the name suggests, wear resistant coatings are used to combat wear especially in cylinder liners, pistons, valves, spindles, textile mill rollers etc. alumina ($Al_2O_3$), titania ($TiO_2$) and zirconia ($ZrO_2$) are the some of the conventional wear resistant coating materials [2].

Plasma spraying is a surface modification technique that combines particle melting, rapid solidification and consolidation in a single process. Because of their higher strength-to-weight ratio and superior wear-resistant properties, ceramics are preferred in most tribological applications. The ceramic materials can be applied for the overlay coating due to the higher gas enthalpy of the thermal plasma jet. The suitability of a ceramic coating on metal substrates depends on (i) the adherence strength at coating substrate interface, and (ii) stability at operating conditions.

One of the major limitations of the process is a relatively high price of the plasma sprayable consumables. Plasma spraying has certain unique advantages over other competing surface engineering techniques. By virtue of the high temperature (10,000 - 15,000$^0$K) and high enthalpy available in the thermal plasma jet, any powder, which melts without decomposition or sublimation, can be coated keeping the substrate at room temperature. The coating process is fast and the thickness can go from a few tens of microns to a few mm. Very intricate shapes of the materials can be coated by this method. Plasma spraying is extensively used in hi-tech industries like aerospace, nuclear energy as well as conventional industries like textiles, chemicals, plastics and paper to develop a suitable surface coating to improve the component life span at operating environment mainly wear resistant coatings in crucial components. Thus, complex structural parts with improved properties and increased life span can be established [3].

For a long time, Silica and aluminous-silicate bricks are preferred as refractory materials in many industrial applications, due to their high wear resistance and load bearing capacity at high temperatures [4]. During the last decade, although a large number of investigations have been carried out for development of plasma spray ceramic coatings, not much effort has been made to use low-grade raw materials for plasma spray purposes [5]. In the recent past, efforts have been made to deposit fly ash coatings on metal substrates by premixing with aluminium powder and also with titania bearing ore mineral. [6,7]. In the present investigation, the plasma spray deposition of alumino-silicate composite coatings onto metal substrates is done using industrial waste i.e. fly ash so that the limitation in applications/adoption of plasma spray coatings due to the high cost of the spray grade powders required for coating could be addressed [8]. Quartz, a low grade mineral which is plentily available in India, is premixed with fly ash to further decrease the cost of raw materials used for coating. Conventional atmospheric plasma spray technique has been used to develop coatings of these materials. The coating process is based on the creation of a plasma jet to melt a feedstock powder [3]. Powder particles are injected with the aid of a carrier gas; they gain their velocity and temperature by thermal and momentum transfers from the plasma jet. At the surface of the substrate, particles flatten and solidify rapidly forming a stack of lamellae.

Here the coatings (fly ash-quartz) have been characterized for their thickness, hardness, porosity, adhesion strength and microstructure. The significant phase changes associated with the plasma processing during the coating deposition have been studied. In addition, the coating deposition efficiencies at various operating conditions have also been evaluated.

To study the suitability of the coatings for wear resistance application, wear properties of these coatings is evaluated. The erosion wear behavior is one of the less studied areas in case of ceramic coatings. This aspect is studied in the present work using a solid particle erosion test and the capabilities of the coatings to sustain the erosive attack have been assessed. Erosion wear tests were carried out on the coatings to ensure its applicability under various operating conditions. In order to control the wear loss in such a process, one of the challenges is to recognize parameter interdependencies; correlations and their individual effects on wear so that the coating can be useful for tribological application. A qualitative analysis of the experimental results with regard to erosion wear rate using statistical techniques is presented. The analysis is aimed at identifying the operating variables/factors significantly influencing the erosion wear rate of fly ash-quartz on metals. Factors are identified in accordance to their influence on the coating erosion wear rate.

## 1.2 OBJECTIVES OF THE PRESENT PIECE OF INVESTIGATION

The objectives of the present investigation are as follows:

- To explore the coating potential of fly ash - quartz on metal substrates by plasma spraying.

- To develop a series of plasma sprayed coatings from fly ash – quartz on metal substrates and to find coating deposition efficiency, porosity and thickness etc.

- X-ray diffraction studies for phase analysis.

- Micro-structural characterization to evaluate the soundness of coating.

- Mechanical properties i.e. to evaluate the micro-hardness and interface bond strength of coatings.

- To assess the capability of the coatings to combat wear with special references to solid particle erosion wear.

- To analyze the experimental results using statistical techniques so as to identify the significant factors/interactions influencing coating erosion wear rate.

# Chapter 2

# Literature Survey

- Preamble
- Surface engineering and modification
- Techniques of surface modification
- Thermal spraying
- Plasma spraying
- Industrial applications of plasma spraying
- Wear
- Types of wear
- Symptoms of wear
- Recent trends in material wear research
- Wear resistant coatings
- Utilization of fly ash as wear resistant coatings
- Erosion wear of ceramic coatings

# CHAPTER 2
# LITERATURE SURVEY

## 2.1 PREAMBLE

This chapter deals with the literature survey of the broad topic of interest namely the development of surface modification technology for tribological applications. This treatise embraces various coating techniques with a special reference to plasma spraying, the coating materials and their characteristics. It gives a complete description of the coating formation process by plasma spraying. The performances of wear resistant coatings under various conditions have been reviewed critically along with the corresponding failure mechanisms. It also presents a review of the wear, types of wear, symptoms of wear and recent trends in metal wear research along with erosion wear behaviour of ceramic coatings, which is the material of interest in this work.

## 2.2 SURFACE ENGINEERING AND MODIFICATION

Surface engineering is a multidisciplinary activity intended to tailor the properties of the surfaces of engineering components so that their function and serviceability can be improved. Surface engineering is defined as "treatment of the surface and near surface regions of a material to allow the surface to perform functions that are distinct from those functions demanded from the bulk of the material" [9]. An engineering component usually fails when its surface cannot withstand the external forces or environment to which it is subjected. Wear, corrosion, fatigue and creep can cause environmental degradation of the surface over time. Surface engineering involves altering the properties of the surface in order to reduce the degradation over time. This is accomplished by making the surface robust to the environment in which it will be used. The desired properties or characteristics of the surface engineered components are:

- Improved corrosion resistance through barrier or sacrificial protection.
- Improved oxidation and/or sulfidation resistance.
- Improved wear resistance.
- Reduced frictional energy losses.
- Improved mechanical properties for e.g. enhanced fatigue or toughness.
- Improved electronic or electrical properties.
- Improved thermal insulation.

- Improved aesthetic appearance.

These properties can be enhanced metallurgically, mechanically, chemically or by adding a coating.

Surface engineering techniques are being used in the automotive, aerospace, missile, power, electronic, biomedical, textile, petroleum, petrochemical, chemical, steel, power, cement, machine tools, construction industries. Almost all types of materials, including metals, ceramics, polymers, and composites can be coated on similar or dissimilar materials. In 1995, surface engineering was a £10 billion market in the United Kingdom. Coatings, to make surface life robust from wear and corrosion, was approximately half the market.

Surface modification is a relatively new term that has come up in the last two decades or so which aims at improving the functionality of surface properties of engineering materials keeping the economic factors in mind [10]. 'Surface Engineering' is the name of the discipline – surface modification is the philosophy behind it. To elucidate the matter an example can be taken. Tungsten carbide cobalt composite is a very popular cutting tool material, and is well known for its high hardness and wear resistance. If a thin coating of TiN is applied on to the WC-Co insert, its capabilities increase considerably [11]. Actually a cutting tool, in action, is subjected to a high degree of abrasion, and TiN is more capable of combating abrasion. On the other hand, TiN is extremely brittle, but the relatively tough core of WC-Co composite protects it from fracture. Thus, through a surface modification process we assemble two (or more) materials by the appropriate method and exploit the qualities of both [12]. It is a very versatile tool for technological development provided it is applied judiciously keeping the following restrictions in mind:

- The technological value addition should justify the cost.
- The choice of technique must be technologically appropriate.
- The coating – surface treatment should not impair the properties of the bulk material.

## 2.3 TECHNIQUES OF SURFACE MODIFICATION

In recent years, there has been a paradigm shift in surface engineering from age-old electroplating to processes such as vapor phase deposition, diffusion, thermal spray & welding using advanced heat sources like plasma, laser, ion, electron, microwave, solar beams, pulsed arc, pulsed combustion, spark, friction and induction. Hence, today a large number of commercially available technologies are present in the industrial scenario. An overview of such technologies is presented below (Fig.2.1):

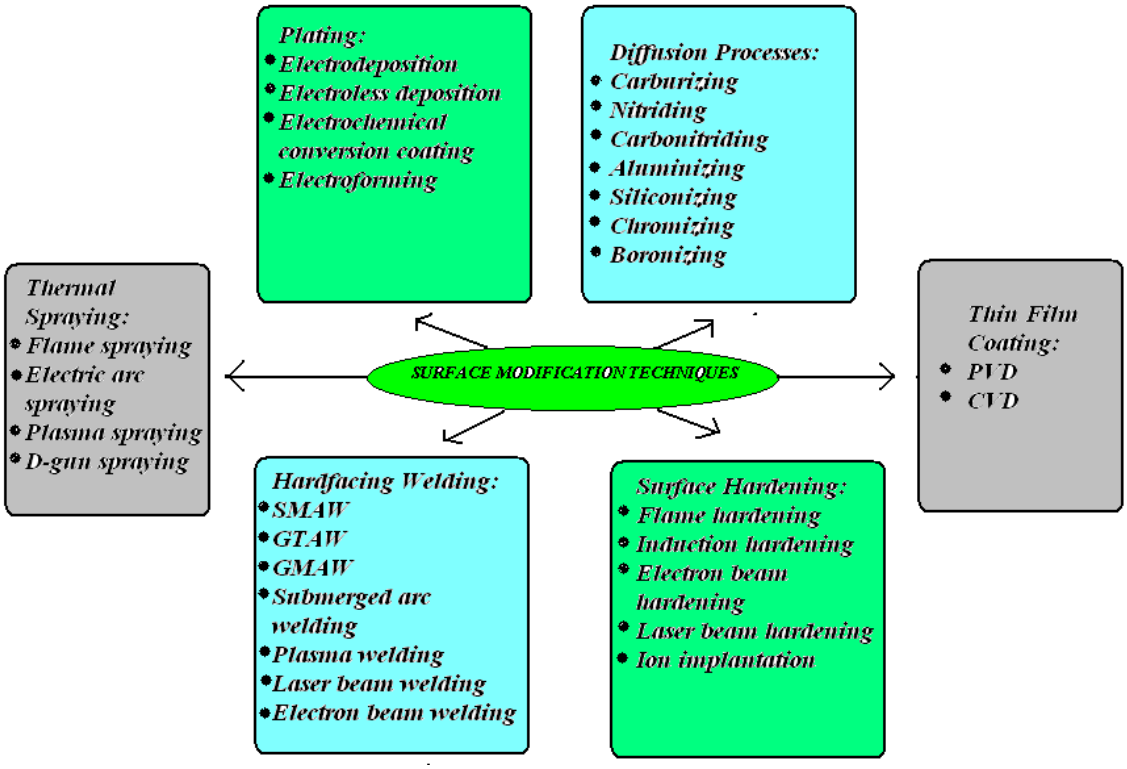


**Figure 2.1** Various forms of surface modification techniques

## 2.4 THERMAL SPRAYING

Thermal spraying is the common name for a vast gallery of techniques for coating deposition. It is the generic category of material processing technique that apply consumables in the form of a finely divided molten or semi molten droplets to produce a coating onto the substrate kept in front of the impinging jet. The melting of the consumables may be accomplished in a number of ways, and the consumable can be introduced into the heat source in wire or powder form. Thermal spray consumables can be metallic, ceramic or polymeric substances. Any material can be sprayed as long as it can be melted by the heat source employed and does not undergo degradation during heating [13].

This technology is uniquely important to an ever-increasing engineering community, for its (i) improved spray footprint definition versus wide spray beam; (ii) high throughput versus competitive techniques; (iii) significantly improved process control; (iv) lower cost-per-mass of applied material, together with overall competitive economics. Thermal spray coatings have been produced for at least 40 years, but the last decade has seen a virtual revolution in the capability of the technology to produce truly high performance coatings of

a great range of materials on many different substrates [14]. The various advantages of thermal spraying technology are listed as:

- Comprehensive choice of coating materials; metals, alloys, ceramics, cermets and carbides.
- Thick coatings can be applied at high deposition rates.
- Coatings are mechanically bonded to the substrate – can often spray coating materials which are metallurgically incompatible with the substrate, e.g. materials with high melting point than the substrate.
- Components can be sprayed with little or no pre - and post - heat treatment, and component distortion is minimal.
- Parts can be rebuilt quickly and at low cost and usually at a fraction of price of a replacement.
- By using a premium material for the thermal spray coating, coated components can outlive new parts.
- Thermal spray coatings can be applied both manually and automatically.

The main principle behind thermal spraying is to melt material feedstock (wire or powder) to accelerate the melt to impact on a substrate where rapid solidification and deposit build up occur. Thus, a heat source and a means of accelerating the material are required. This is pictured schematically in Fig.2.2 (a) [15]. A three-dimensional figure showing a thermal spray coating is given in Fig.2.2 (b).

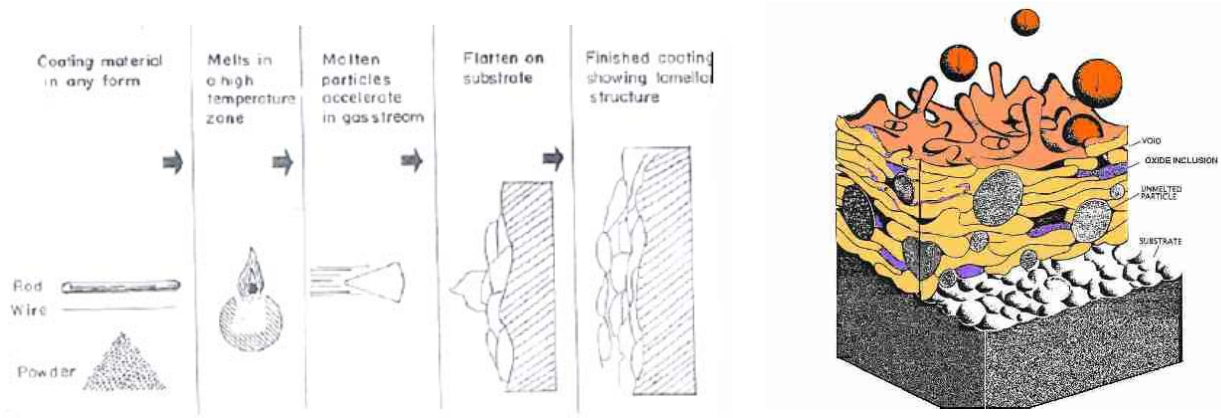


**(a)** **(b)**

**Figure 2.2. (a)** Schematic diagram showing coating formation; **(b)** three-dimensional view of a thermal spray coating.

The nature of bonding at the coating-substrate interface is not completely understood. It is normally assumed that bonding occurs by the mechanical interlocking. Under this circumstance it is generally possible to ignore the metallurgical compatibility [13]. This is an extremely significant feature of thermal spraying. Another interesting aspect of thermal spraying is that the surface temperature seldom exceeds $200^0$C. Hard metal or ceramic coating can be applied to thermosetting plastics. Stress related distortion problems are also not so significant. The spraying action is achieved by the rapid expansion of combustion gases (which transfer the momentum to the molten droplets) or by a separate supply of compressed air. There are two basic ways of generating heat required for melting the consumables [16,17]. They are (i) combustion of a fuel gas and (ii) high energy arc processes, shown in Fig.2.3.

.

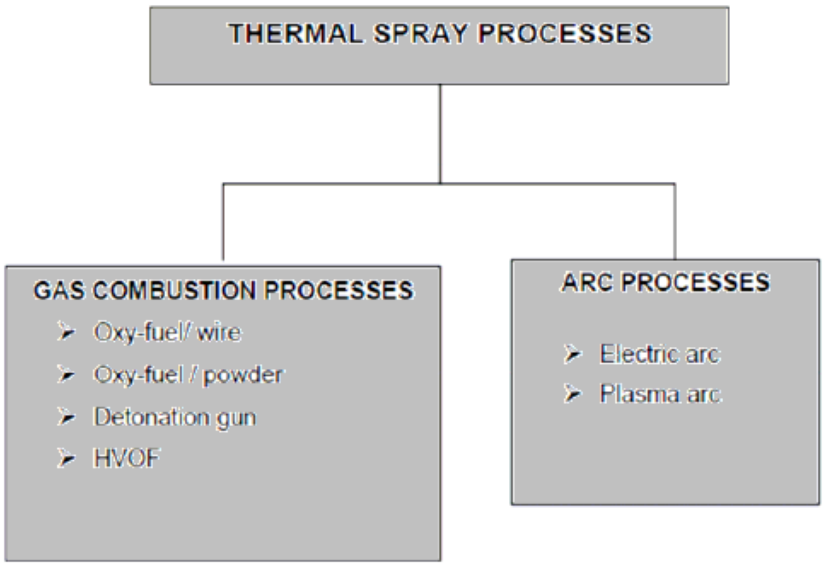


**Figure 2.3** Categorization of various thermal spray processes based on the heat source used.

Processes available for thermal spraying have been developed specifically for a purpose and fall into two categories-high and low energy processes. The key processes and their energy sources are summarized in Table 2.1 [17].

**Table 2.1** Thermal spraying processes

| Processes | | Energy sources | Different nomenclature |
|---|---|---|---|
| Low energy processes | Flame spraying | Chemical | Oxyfuel gas-powder spraying |
| | | | Oxyfuel gas-wire spraying |
| | | | Metallizing |
| | Arc spraying | Electrical | Electric arc spraying |
| | | | Twin-wire arc spraying |
| | | | Metallizing |
| High energy processes | Plasma spraying | Electrical | Atmosphereic plasma spraying (APS) |
| | | | Vacuum plasma spraying (VPS) |
| | | | Low pressure plasma spraying (LPPS) |
| | | | Water stabilized plasma spraying |
| | | | Inductive plasma spraying |
| | Detonation flame spraying | Chemical | D-gun |
| | High velocity oxyfuel spraying | Chemical | HVOF spraying |
| | | | High velocity oxygen fuel spraying |
| | | | High velocity flame spraying |
| | | | High velocity air fuel |

## 2.5 PLASMA SPRAYING

Plasma spraying is one of the most widely used thermal spraying processes which finds a lot of applications due to its versatility of spraying a wide range of materials (metallic and non metallic) and hence more suitable for spraying of high melting point materials like refractory ceramics, cermets etc [18,19]. A schematic diagram of plasma spray process is shown in Fig. 2.4.

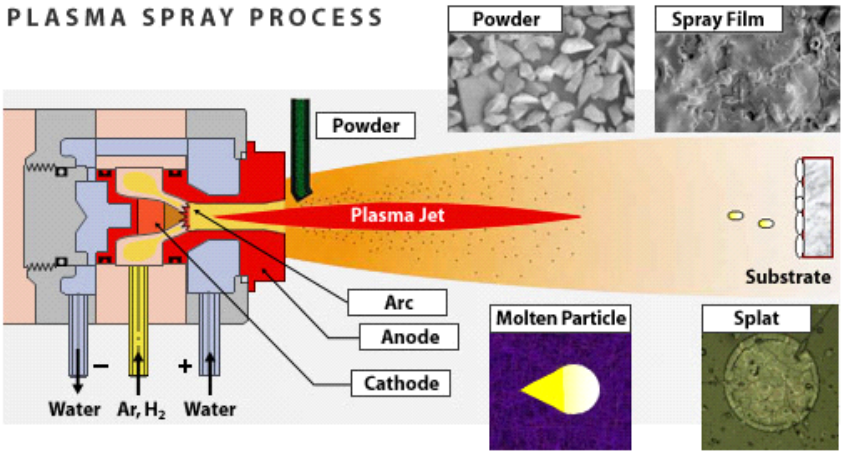


**Figure 2.4** Conventional plasma spraying process.

An arc is created between thoriated tungsten cathode and an annular copper anode (both water cooled). Plasma generating gas is forced to pass through the annular space between the electrodes. While passing through the arc, the gas undergoes ionization in the high temperature environment resulting plasma. The ionization is achieved by collisions of electrons of the arc with the neutral molecules of the gas. The plasma protrudes out of the electrode encasement in the form of a flame. The consumable material, in the powdered form, is poured into the flame in metered quantity. The powders melt immediately and absorb the momentum of the expanding gas and rush towards the target to form a thin deposited layer. The next layer deposits onto the first immediately after and thus the coating builds up layer by layer [12,13]. Temperature in the plasma arc can be as high as $10,000^0$C and is capable of melting anything. Elaborate cooling arrangement is required to protect the plasmatron (i.e. the plasma generator) from excess heating. The equipment consists of the following modules [13]:

- **The plasmatron:** It is the device which houses the electrodes and in which the plasma reaction takes place. It has the shape of a gun and it is connected to the water cooled power supply cables, powder supply hose and gas supply hose.

- **The power supply unit:** Normally plasma arc works in a low voltage (30-60 Volts) and high current (300-700 Amps), DC ambient. The available power (AC, 3 phase, 440Volts) must be transformed and rectified to suit the reactor. This is taken care of by the power supply unit.
- **The powder feeder:** The powder is kept inside a hopper. A separate gas line directs the career gas that fluidizes the powder and carries it to the plasma arc. The flow rate of the powder can be controlled precisely.
- **The coolant and water supply unit:** It circulates water into the plasmatron, the power supply unit and the power cables. Units capable of supplying refrigerated water are also available.
- **The control unit:** Important functions (current control, gas flow rate control etc.) are performed by the control unit. It also consists of relays and solenoid valves and other interlocking arrangements essential for safe running of the equipment. For e.g. an arc can only be started if the coolant supply is on and water pressure and flow rate is adequate.

An arrangement of plasma spraying equipment is shown in Fig. 2.5.

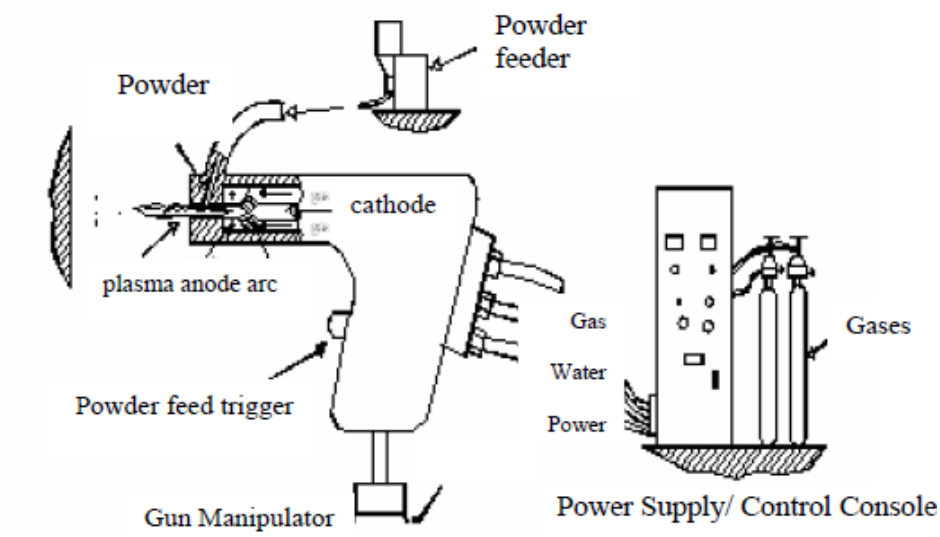


**Figure 2.5** Arrangement for plasma spraying.

The key features of plasma spraying processes are:

- Deposits metals, ceramics or any combination of these materials.
- Forms microstructure with fine, equiaxed grains and without columnar boundaries.
- Produces deposits that do not change in composition with thickness (length of deposition time).

- Can change from depositing a metal to a continuously varying mixture of metals ceramics (i.e. functionally graded materials).
- High deposition rates (>4kg/h).
- Fabricates freestanding forms of virtually any material or any materials combination.
- Process materials in virtually any environment e.g. air, reduced pressure inert gas, high pressure etc.

### 2.5.1 Requirements for Plasma Spraying

**Roughness of the substrate surface:**

A rough surface provides a good coating adhesion. A rough surface provides enough room for anchorage of the splats facilitating bonding through mechanical interlocking. A rough surface is generally created by shot blasting technique. The shots are kept inside a hopper, and compressed air is supplied at the bottom of the hopper. The shots are taken afloat by the compressed air stream into a hose and ultimately directed to an object kept in front of the exit nozzle of the hose. The shots used for this purpose are irregular in shape, highly angular in nature, and made up of hard material like alumina, silicon carbide, etc. Upon impact they create small craters on the surface by localized plastic deformation, and finally yield a very rough and highly worked surface. The roughness obtained is determined by shot blasting parameters, i.e., shot size, shape and material, air pressure, standoff distance between nozzle and the job, angle of impact, substrate material etc [20]. The effect of shot blasting parameters on the adhesion of plasma sprayed alumina has been studied [21]. Mild steel serves as the substrate material. The adhesion increases proportionally with surface roughness and the parameters listed above are of importance. A significant time lapse between shot blasting and plasma spraying causes a marked decrease in bond strength [22].

**Cleanliness of the substrate surfaces:**

The substrate to be sprayed on must be free from any dirt or grease or any other material that might prevent intimate contact of the splat and the substrate. For this purpose the substrate must be thoroughly cleaned (ultrasonically, if possible) with a solvent before spraying. Spraying must be conducted immediately after shot blasting and cleaning. Otherwise on the nascent surfaces, oxide layers tend to grow quickly and moisture may also affect the surface. These factors deteriorate the coating quality drastically [22].

**Bond coat:**

Materials like ceramic cannot be sprayed directly onto metals, owing to a large difference between their thermal expansion coefficients (α). Ceramics have a much lower value of "α" and hence undergo much less shrinkage as compared to the metallic base to form a surface in compression. If the compressive stress exceeds a certain limit, the coating gets peeled off. To alleviate this problem a suitable material, usually metallic of intermediate a value is plasma sprayed onto the substrate followed by the plasma spraying of ceramics. Bond coat may render itself useful for metallic topcoats as well. Molybdenum is a classic example of bond coat for metallic topcoats. Molybdenum adheres very well to the steel substrate and develops a somewhat rough top surface ideal for the topcoat spraying. The choice of bond coats depends upon the application. For example, in wear application, an alumina and Ni-AI top and bond coats combination can be used [23]. In thermal barrier application, CoCrAlY or Ni-AI bond coat [24] and zirconia topcoat are popular. Ceramic coatings when subjected to hertzian loading deform elastically and the metallic substrate deforms plastically. During unloading, elastic recovery of the coating takes place, whereas for the metallic substrate a permanent set has already taken place. Owing to this elastoplastic mismatch the coating tends to spall off at the interface. A bond coat can reduce this mismatch as well.

**Cooling water:**

For cooling purpose distilled water was used, whenever possible. Normally a small volume of distilled water is recirculated into the gun and. it is cooled by an external water supply from a large tank. Sometime water from a large external tank is pumped directly into the gun [13].

### 2.5.2 Process Parameters in Plasma Spraying

In plasma spraying one has to deal with a lot of process parameters, which determine the degree of particle melting, adhesion strength and deposition efficiency of the powder. Deposition efficiency is the ratio of amount of powder deposited to the amount fed to the gun. An elaborate listing of these parameters and their effects are reported in the literature [25].

Some important parameters and their roles are listed below:

**Arc power:**

It is the electrical power drawn by the arc. The power is injected into the plasma gas, which in turn heats the plasma stream. Part of the power is dissipated as radiation and also by the gun cooling water. Arc power determines the mass flow rate of a given powder that can be effectively melted by the arc. Deposition efficiency improves to a certain extent with an increase in arc power, since it is associated with an enhanced particle melting [22, 25, 26]. However, increasing power beyond a certain limit may not cause a significant improvement. On the contrary, once a complete particle melting is achieved, a higher gas temperature may prove to be harmful. In the case of steel, at some point vaporization may take place lowering the deposition efficiency.

**Plasma gas:**

Normally nitrogen or argon doped with about 10% hydrogen or helium is used as a plasma gas. The major constituent of the gas mixture is known as primary gas and the minor is known as the secondary gas. The neutral molecules are subjected to the electron bombardment resulting in their ionization. Both temperature and enthalpy of the gas increase as it absorbs energy. Since nitrogen and hydrogen are diatomic gases, they first undergo dissociation followed by ionization. Thus they need higher energy input to enter the plasma state. This extra energy increases the enthalpy of the plasma. On the other hand, the mono-atomic plasma gases, i.e. argon or helium, approach a much higher temperature in the normal enthalpy range. Good heating ability is expected from them for such high temperature [27]. In addition, hydrogen followed by helium has a very high specific heat, and therefore is capable of acquiring very high enthalpy. When argon is doped with helium the spray cone becomes quite narrow which is especially useful for spraying on small targets.

**Carrier gas:**

Usually the primary gas itself is used as a carrier gas. The flow rate of the career gas is an important factor. A very low flow rate cannot convey the powder effectively to the plasma jet, and if the flow rate is very high then the powders might escape the hottest region of the jet. There is an optimum flow rate for each powder at which the fraction of unmelted powder is minimum and hence the deposition efficiency is maximum [25].

**Mass flow rate of powder:**

Ideal mass flow rate for each powder has to be determined. Spraying with a lower mass flow rate keeping all other conditions constant results in under utilization and slow coating buildup. On the other hand, a very high mass flow rate may give rise to an incomplete melting resulting in a high amount of porosity in the coating. The un-melted powders may bounce off from the substrate surface as well keeping the deposition efficiency low [25].

**Torch to base distance:**

It is the distance between the tip of the gun and the substrate surface. A long distance may result in freezing of the melted particles before they reach the target, whereas a short standoff distance may not provide sufficient time for the particles in flight to melt [22, 25]. The relationship between the coating properties and spray parameters in spraying alpha alumina has been studied in details. It is found that the porosity increases and the thickness of the coating (hence deposition efficiency) decreases with an increase in standoff distance. The usual alpha phase to gamma-phase transformation during plasma spraying of alumina has also been restricted by increasing this distance. A larger fraction of the un-melted particles go in the coating owing to an increase in torch to base distance.

**Spraying angle:**

This parameter is varied to accommodate the shape of the substrate. In coating alumina on mild steel substrate, the coating porosity is found to increase as the spraying angle is increased from 30° to 60°. Beyond 60°, the porosity level remains unaffected by a further increase in spraying angle. The spraying angle also affects the adhesive strength of the coating. The influence of spraying angle on the cohesive strength of chromia, zirconia 8wt% yittria and molybdenum has been investigated, and it has been found that the spraying angle does not have much influence on the cohesive strength of the coatings [28].

**Substrate cooling:**

During a continuous spraying, the substrate might get heated up and may develop thermal-stress related distortion accompanied by a coating peel-off. This is especially true in situations where thick deposits are to be applied. To reduce the substrate temperature, it is kept cool by an auxiliary air supply system. In addition, the cooling air jet removes the unmelted particles from the coated surface and helps to reduce the porosity [22].

**Powder related variables:**

These variables are powder shape, size and size distribution, processing history, phase composition etc. They constitute a set of extremely important parameters. For example, in a given situation if the powder size is too small it might get vaporized. On the other hand a very large particle may not melt substantially and therefore will not deposit. The shape of the powder is also quite important. A spherical powder will not have the same characteristics as the angular ones, and hence both could not be sprayed' using the same set of parameters [29].

**Angle of power injection:**

Powders can be injected into the plasma jet perpendicularly, coaxially, or obliquely. The residence time of the powders in the plasma jet will vary with the angle of injection for a given carrier gas flow rate. The residence time in turn will influence the degree of melting of a given powder. For example, to melt high melting point materials a long residence time and hence oblique injection may prove to be useful. The angle of injection is found to influence the cohesive and adhesive strength of the coatings as well [13].

### 2.5.3 Mechanism of Coating Formation in Plasma Spraying Process

Since coatings are formed by the impact of a stream of particles striking the substrate, the major factors which control the structure of a particular coating are the temperature, velocity and size distribution of the incident particles. Ideally all the particles which strike the substrate would be completely molten. Unmolten particles will bounce off reducing the deposition efficiency and partly melted particles are incorporated within the deposit modifying its microstructure and properties [30]. Coatings are formed by the build up of successive layers of liquid droplets which flatten and solidify on impact to give lamellar microstructure.

When a liquid droplet strikes the surface at low velocity, it flattens to a disc which then retracts passing through the equillibrium shape of spherical cap to form a cone and the spreads again to the final equillibrium shape determined by the static surface tension forces. At high impact velocities, however radially flowing thin sheet of liquid becomes unstable and disintegrates at the edge into many small droplets i.e. splashing occurs (Fig 2.6). Its cooling rate then rapidly increases by conduction into the substrate. The cooling rates achieved are of the order of $10^6$-$10^7$ $Ksec^{-1}$ [31]. P. Fauchais et al. also made a study on coating generation and predicted a model for calculating the splat-quenching rate [19]. It

was also found experimentally that some metastable phases are formed during cooling, like γ-alumina rather than α-alumina which was explained on the basis of nucleation kinetics: γ-alumina was easily nucleated because of lower interfacial energy between crystal and the liquid and at sufficiently rapid cooling rates, the metastable form is retained at room temperature [32, 33]. It was suggested that the mechanical behaviour of the coatings is limited to the degree of contact between the lamellae within the coatings and between the lamellae and the substrate rather than the nature of bonds in regions of good contact. This study was made on alumina coatings. The low apparent area of

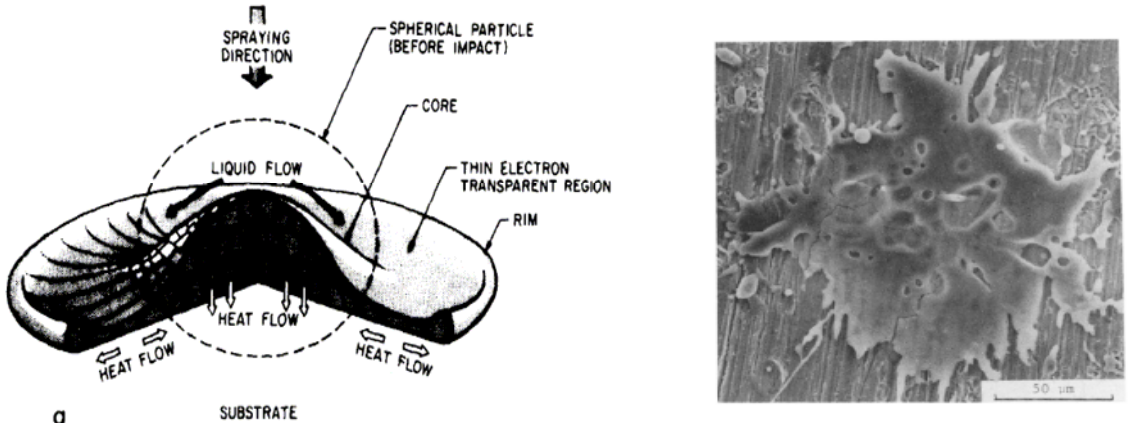


(a) (b)

**Figure 2.6 (a)** Schematic diagram of a particle after impinging onto a flat surface. **(b)** Impact pattern of a single $Al_2O_3$ particle on metallic substrate.

contact may be due to entrapped gases and other asperities between the impinging droplet and the substrate [34]. Hence surface cleaning and grit blasting of the substrates is necessary for better bonding between coating and the substrate [35] (as discussed above).

## 2.6 INDUSTRIAL APPLICATIONS OF PLASMA SPRAYING

There has been a steady growth in the number of applications of thermally sprayed coatings. Availability of hardware and adaptability of the technique are the most important factors for this growth. Plasma spraying has been successfully applied to a wide range of industrial technologies. Automotive industry, aerospace industry, nuclear industry, textile industry, paper industry and iron and steel industry are some of the sectors that have successfully exploited thermal plasma spray technology [36].

**Textile industry:**

Plasma spraying was for the first time employed in textile industry in Czechoslovakia. Plasma spraying has replaced the classical technologies of chrome plating, anodization and chemical surface hardening. Advantages of this technique are a lot, all of which add to the quality and quantity of textile production.

- Critical machinery parts**:** Different thread guiding & distribution rollers, ridge thread brakes, distribution plates, driving & driven rollers, gallets, tension rollers, thread brake caps,lead-in bars etc.
- Coatings and advantages**:** High wear resistance coatings are required on textile machinery parts, which are in contact with synthetic fibers. For this purpose especially Al2O3+ 3% TiO2, Al2O3 + 13% TiO2, Cr2O3, WC + Co are applied. These coatings with hardness ranging from 1800 to 2600 HRV are extraordinarily dense, have high wear resistance and provide excellent bonding with the substrate. Plasma spraying has following advantages in textile industries:
    - Replacement of worn out parts is minimized and hence reduces the idle times.
    - Physical and mechanical properties of fibers are improved.
    - Revolution speed of these lighter parts can be increased.
    - Shelf life of the textile machinery parts with plasma sprayed coating last 5 to 20 times longer than parts coated by chrome plating or another classical technique.
    - Economic savings are realized considerably by substituting heavy steel or cast iron parts with aluminum or durable ones with wear-resistant coatings.

**Paper and printing industry:**

The machinery in the paper and printing industry is usually quite large and is subjected to considerable wear from the sliding and friction contact with the paper products.

- Critical machinery parts**:** Paper drying rolls, sieves, filters, roll pins etc.in paper machines, printing rolls, tension rolls and other parts of printing machines.
- Coatings and advantages**:** Spraying of oxide layers is an available economical solution.

which can be employed right in place in the production shop. Here again oxide layers composed of $Al_2O_3$ with 3 to 13 % additions of $TiO_2$, $Cr_2O_3$or $MnO_2$ are applied. Cast iron

rolls are typically first sprayed with NiCr 80/20, 50 μm thick and then over it 0.2mm thick $Al_2O_3$ + 13% $TiO_2$ layer is coated. The special advantages are mentioned below:

- Ensures corrosion resistance of rolls i.e. the base metal
- Resistance of oxide layers against printing inks extends the life of machine parts
- Production cost is reduced considerably
- Coating resulted to the so-called "orange peel" phenomena, surface finishing obtainable that prevents paper foil, dyes etc. from sticking and allows their proper stretching.

**Automotive industry and the production of combustion engines:**

Plasma sprayed coatings used, in automotive industries of many industrially advanced countries, endure higher working pressure and temperature to improve wear resistance, good friction properties, resistance against burn-off and corrosion due to hot combustion products and resistance against thermal loading. Some of the several applications developed for the automotive industry at the Slovak Academy of Sciences (SAV) in Bratislava are spraying torsion bars with aluminium coatings against corrosion. The plasma spraying technology is introduced in the production of gearshift forks for gearboxes in fiat car factory and on the critical parts of big Diesel engines.

**Glass industry:**

Molten glass quickly wears the surface of metal that comes in contact with it. In order to protect the metal tools, plasma sprayed coatings are made on to it.

**Electrochemical industry:**

In the electromechanical and computer industries the electrically conductive Cu, Al, W and the semi-conductive and insulating ceramic layers are widely used. Some contacts of electrodes, e.g. the spark gaps of nuclear research equipment, are produced of massive tungsten. Modern electrodes can replace such electrodes with a sprayed tungsten coating about 0.5mm thick. This electrode ensures short- time passages of 300,000A current with a life of several hundred switching.

**Hydraulic machines and mechanisms:**

The range of possible applications in this field is very extensive, mainly in water power plants, in production and work of pumps, where many parts are subjected to combined effects of wear, corrosion, erosion and cavitations.

**Rolling mills and foundry:**

In Rolling mills and pressing shops the wear resistant coatings are used to renovate the heavy parts of heavy-duty machines whose replacement would be very costly. Several applications in this field are presented herewith:

- Rolling strand journals being repaired by giving a coating layer of stainless steel. Blooming roll mill journal renovated with a NiCrBSi layer.
- Gears of rolling mill gearbox being renovated by a wear resistance coating.
- To repair a rolling mill slide and the plungers of a forging press a hard wear resistance is applied.
- Heat resistant plasma coating is widely used for foundry and metallurgical equipment where molten metal or very high temperatures are encountered. This equipment includes the sliding plugs of steel ladles with alumina or zirconia coatings.
- Conveyer rollers in plate production with zirconia based refractory coatings.
- Oxygen tubes, cast iron moulds in continuous casting of metals, with Al2O3+ TiO2, ZrSiO4+ ZrO2 +MgO.

**High temperature wear resistant coatings on slide gate plates:**

In steel plants severe erosion of refractory teeming plates (slide gate plates) and generation of macro-micro cracks during teeming of steel is observed, rendering the plates unstable for reuse. Plasma sprayed ceramic coatings on refractory plates is made to minimize the damage and hence increase the life of slide gate plate. $Al_2O_3$, $MgZrO_3$, $ZrO_2$, $TiO_2$, $Y_2O_3$ and calcia stabilized. Zirconia can also be coated.

**Chemical plants:**

The base metal of machine parts is subjected to different kind of wear in chemical plants. In such cases plasma sprayed coatings are applied to protect the base metal. They can be used for various blades, shafts, bearing surfaces, tubes, burners, parts of cooling equipments etc.

**Aircraft jet engines:**

The working parts of Aircraft jet engines are subjected to serve mechanical, chemical and thermal stresses. A jet engine has a number of construction nodes where plasma coating is employed with much success in order to protect them. There are for example, face of the blower box, compressor box and disc, guide bearing, fuel nozzles, blades, combustion chambers.

## 2.7 WEAR

Wear may be defined as damage to the solid surface caused by the removal or displacement of material by the mechanical action of a contacting solid, liquid or gas. It occurs as a natural consequence when two surfaces in relative motion interact with each other. Wear may cause significant surface damage and the damage is usually thought of gradual deterioration. Scientists have developed various wear theories in which the Physico-Mechanical characteristics of the materials and the physical conditions (e.g. the resistance of the rubbing body and the stress state at the contact area) are taken in to consideration. In 1940 Holm [37] starting from the atomic mechanism of wear, calculated the volume of substance worn over unit sliding path.

Wear of materials is probably the most important yet at least understood aspects of tribology as the mechanism of wear is very complex. It is certainly the youngest of the tri of topics, friction, lubrication and wear, to attract scientific attention, although its practical significance has been recognized throughout the ages. It should be understood that the real area of contact between two solid surfaces compared with the apparent area of contact is invariably very small, being limited to points of contact between surface asperities. The load applied to the surfaces will be transferred through these points of contact and the localized forces can be very large. Thus, wear is not an intrinsic material property but characteristics of the engineering system which depend on load, speed, temperature, hardness, presence of foreign material and the environmental conditions [38]. Widely varied wearing conditions causes wear of materials. It may be due to surface damage or removal of material from one or both of two solid surfaces in a sliding, rolling or impact motion relative to one another. In most cases wear occurs through surface interactions at asperities. During relative motion, material on contacting surface may be removed from a surface, may result in the transfer to the mating surface, or may break loose as a wear particle. The wear resistance of materials is related to its microstructure may take place during the wear process and hence, it seems that in wear research emphasis is placed on microstructure [39]. Wear of metals depends on

many variables, so wear research programs must be planned systematically. Therefore researchers have normalized some of the data to make them more useful. The wear map proposed by Lim and Ashby [38] is very much useful in this regard to understand the wear mechanism in sliding wear, with or without lubrication.

## 2.8 TYPES OF WEAR

In most basic wear studies where the problems of wear have been a primary concern, the so-called dry friction has been investigated to avoid the influences of fluid lubricants. Dry friction' is defined as friction under not intentionally lubricated conditions but it is well known that it is friction under lubrication by atmospheric gases, especially by oxygen [40]. A fundamental scheme to classify wear was first outlined by Burwell and Strang [41]. Later, Burwell [42] modified the classification to include five distinct types of wear, namely (1) Abrasive (2) Adhesive (3) Erosive (4) Surface fatigue (5) Corrosive.

### 2.8.1 Abrasive Wear

Abrasive wear or abrasion, is generally defined as the wear that is caused by the displacement of material from a solid surface due to hard particles or protuberances sliding along the surface and cutting grooves on the softer surfaces. It accounts for most failures in practice. This hard material may originate from one of the two rubbing surfaces, rubbing against each other. In sliding mechanisms, abrasion can arise from the existing asperities on one surface (if it is harder than the other), from the generation of wear fragments which are repeatedly deformed and hence get work hardened for oxidized until they became harder than either or both of the sliding surfaces, or from the adventitious entry of hard particles, such as dirt from outside the system. Two body abrasive wear as shown in Fig. 2.7 occurs when one surface (usually harder than the second) cuts material away from the second, although this mechanism very often changes to three body abrasion as the wear debris then acts as an abrasive between the two surfaces. Abrasives can act as in grinding where the abrasive is fixed relative to one surface or as in lapping where the abrasive tumbles producing a series of indentations as opposed to a scratch. According to the recent tribological survey, abrasive wear is responsible for the largest amount of material loss in industrial practice [43].

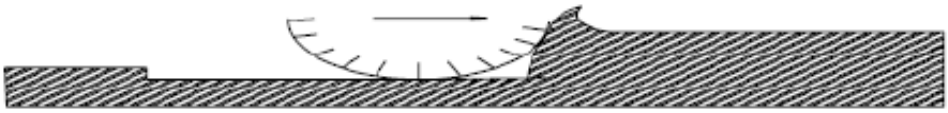

**Figure 2.7** Schematic representations of the abrasion wear mechanism.

### 2.8.2 Adhesive Wear

Adhesive wear can be defined as wear due to localized bonding between contacting solid surfaces leading to material transfer between the two surfaces or the loss from either surface. For adhesive wear as shown in Fig. 2.8 to occur it is necessary for the surfaces to be in intimate contact with each other. Surfaces, which are held apart by lubricating films, oxide films etc. reduce the tendency for adhesion to occur.

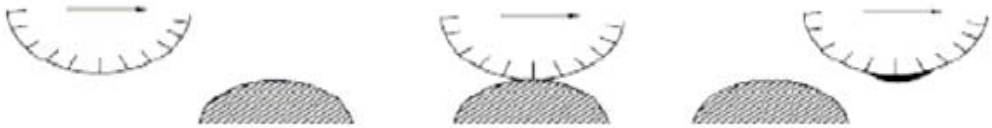

**Figure 2.8** Schematic representation of adhesive wear mechanism.

### 2.8.3 Erosive Wear

In tribology, erosive wear can be defined as the progressive loss of original material from a solid surface due to mechanical interaction between that surface and a fluid, a multi-component fluid, or impinging liquid or solid particles [ASTM G40-99]. As all kinds of wear, erosion causes costly damage in many machine parts. When the angle of impingement is small, the wear produced is closely analogous to abrasion. When the angle of impingement is normal to the surface, material is displaced by plastic flow or is dislodged by brittle failure. The schematic representation of the erosive wear mechanism is shown in Fig.2.9.

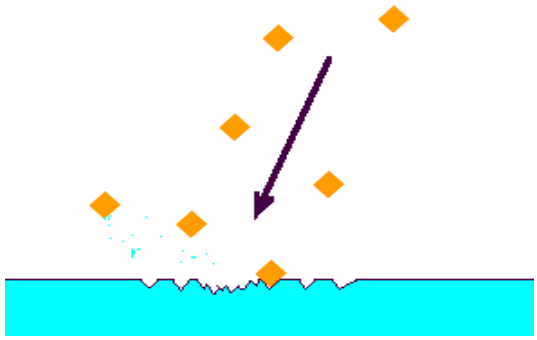

**Figure 2.9** Schematic representations of erosive wear mechanism.

The erosion mechanism depends on the material and is different for brittle and ductile materials and therefore erosion has been divided into brittle and ductile erosion. Ductile materials fail as a result of impacting particles causing localized plastic flow that exceeds the critical strain to failure in the local areas. When the erodent particles in either gas or liquid carrier fluid strikes the surface of a ductile material, they initially extrude thin microplatelates of the base material from craters which are formed at the sites of impacts. The platelates are then further flattened, i.e. pancake forged, by subsequent particles striking the initially deformed material. After a small number of particles have impacted the same localized area, the extruded platelates would have been strained to their critical strain and fracture of portions of the platelate will occur [44]. The mechanism of erosion of brittle materials i.e. ceramic type materials is considerably different. Brittle materials are removed by a cracking and chipping mechanism. Here erosion occurs by the propagation and intersection of cracks produced by the impacting particles. The dense, columnar grain, outer scale cracks are chipped away, while the small equiaxed grains of the inner scale initially form hertzian cone cracks or ring cracks. Subsequently, at latter times, increased loading leads to increasing number of ring cracks leading to chipping away of the inner scales [44, 45].

Erosion modes can be subdivided according to the erosive medium as:

- **Liquid impingement erosion:** It occurs when small drops of liquid are striking on the surface of a solid at a high speed (1000m/s) and very high pressures are experienced, exceeding the yield strength of most materials. Thus plastic deformation or fracture may result from a single impact and repeated impacts may lead to pitting and erosive wear. Liquids need not contain particles to damage to a solid surface [46].
- **Cavitation erosion:** Cavitation is defined as the formation and subsequent collapse of cavities or bubbles within liquid and cavitation erosion is the mechanical damage of a solid surface caused by these cavities or bubbles collapsing either at or near the surface [47].

- **Solid particle erosion:** It is the loss of material that results from repeated impact of small solid particles in gaseous or liquid medium [48]. In solid particle erosion, a series of particles strike and rebound from the surface and cause a force on the material due to their deceleration. This is different from abrasion in the way that, here abrasive particles slide on the surface under an external force.

- **Slurry erosion:** Slurry erosion is defined as the type of wear or loss of mass that is experienced by material exposed to a high velocity stream of slurry i.e. a mixture of solid particles in a liquid [49].

- **Erosion/Corrosion:** This is basically erosion enhanced/inhibited by corrosion mechanism. Corrosion may enhance the erosion rate through preferential dissolution or it may inhibit erosion through the formation of a passive film. Erosion-corrosion interaction is the potential synergy between the two processes. When metal alloys are exposed to the combined degradation mechanisms of corrosion and small solid particle erosion, combinations of the loss mechanisms of ductile and brittle materials occur, but primarily the brittle behavior [44].

### 2.8.4 Surface Fatigue Wear

Wear of a solid surface can be caused by fracture arising from material fatigue. The term 'fatigue' is broadly applied to the failure phenomenon where a solid is subjected to cyclic loading involving tension and compression above a certain critical stress. Repeated loading causes the generation of micro cracks, usually below the surface, at the site of a pre-existing point of weakness. On subsequent loading and unloading, the micro crack propagates. Once the crack reaches the critical size, it changes its direction to emerge at the surface, and thus flat sheet like particles is detached during wearing. The number of stress cycles required to cause such failure decreases as the corresponding magnitude of stress increases. Vibration is a common cause of fatigue wear. The schematic representation of the surface fatigue wear mechanism is shown in Fig. 2.10.

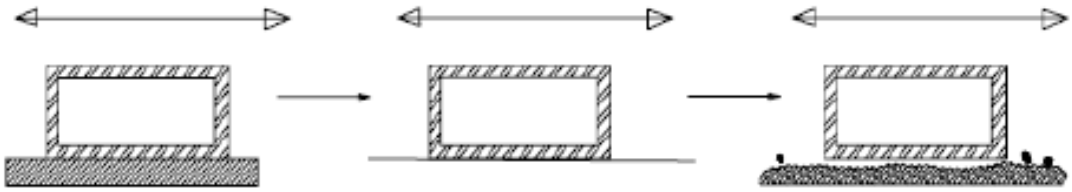

**Figure 2.10** Schematic representations of surface fatigue wear mechanism.

### 2.8.5 Corrosive Wear

Most metals are thermodynamically unstable in air and react with oxygen to form an oxide, which usually develop layer or scales on the surface of metal or alloys when their interfacial bonds are poor. Corrosion wear is the gradual eating away or deterioration of unprotected metal surfaces by the effects of the atmosphere, acids, gases, alkalis, etc. This type of wear creates pits and perforations and may eventually dissolve metal parts.

## 2.9 SYMPTOMS OF WEAR

Wear is a characteristic of the system and is influenced by many parameters. Thus a clear and deeper understanding of the wear mechanism is required if an improvement in wear resistance of the coatings is to be achieved. Laboratory scale investigation if designed properly allows careful control of such tribo systems where by the effects of different variables on wear behaviour of the coating can be isolated and determined. The data generated through such investigation under controlled conditions may help in correct interpretation of the results. A summary of the appearance and symptoms of different wear mechanism is indicated in Table 2.2 [50] and the same is a systematic approach to diagnose the wear mechanisms.

## 2.10 RECENT TRENDS IN MATERIAL WEAR RESEARCH

Much of the wear researches carried out in the 1940's and 1950's were conducted by mechanical engineers and metallurgists to generate data for the construction of motor drive, trains, brakes, bearings, bushings and other types of moving mechanical assemblies [51].

It became apparent during the survey that wear of metals was a prominent topic in a large number of the responses regarding some future priorities for research in tribology. Some 22 experienced technologists in this field, who attended the 1985 'Wear of Materials Conference' in Canada, prepared a ranking list [52]. Their proposals with top priority were further investigations of the mechanism of wear and this no doubt reflects the judgments that particular effects of wear should be studied against a background of the basic physical and chemical processes involved in surface interactions. The list proposed is shown in Table 2.3 [52].

Peterson [53] reviewed the development and use of tribo-materials and concluded that metals and their alloys are the most common engineering materials used in wear applications. Grey cast iron for example has been used as early as 1388. Much of the wear research conducted over the past 50 years is in ceramics, polymers, composite materials and coatings [54].

Wear of metals encountered in industrial situations can be grouped into categories shown in Table 2.4 [29] though there are situations where one type changes to another or where two or more mechanism play together.

**Table 2.2** Symptoms and appearance of different types of wear.

| Types of wear | Symptoms | Appearance of worn out surface |
|---|---|---|
| Abrasive | Presence of clean furrows cut out by abrasive particles. | Grooves. |
| Adhesive | Metal transfer is the prime symptoms. | Seizure, catering rough and torn-out surfaces. |
| Erosion | Presence of abrasives in the fast moving fluid and short abrasion furrows. | Waves and troughs. |
| Corrosion | Presence of metal corrosion products. | Rough pits or depressions. |
| Fatigue | Presence of surface or subsurface cracks accompanied by pits and spalls. | Sharp and angular edges around pits. |
| Impacts | Surface fatigue, small sub micron particles or formation of spalls. | Fragmentation, peeling and pitting. |
| Delamination | Presence of subsurface cracks parallel to the surface with semi-dislodged or loose flakes. | Loose, long and thin sheet like particles. |
| Fretting | Production of voluminous amount of loose debris. | Roughening, seizure and development of oxide ridges. |
| Electric attack | Presence of micro craters or a track with evidence of smooth molten metal | Smooth holes. |

**Table 2.3** Priority in wear research.

| Ranking | Topics |
|---|---|
| 1. | Mechanism of Wear |
| 2. | Surface Coatings and treatments |
| 3. | Abrasive Wear |
| 4. | Materials |
| 5. | Ceramic Wear |
| 6. | Metallic Wear |
| 7. | Polymer Wear |
| 8. | Wear with Lubrication |
| 9. | Piston ring-cylinder liner Wear |
| 10. | Corrosive Wear |
| 11. | Wear in other Internal Combustion Machine Components |

**Table 2.4** Types of wear in industry.

| Type of wear in Industry | Approximate percentage involved |
|---|---|
| Abrasive | 50 |
| Adhesive | 15 |
| Erosion | 8 |
| Fretting | 8 |
| Chemical | 5 |

## 2.11 WEAR RESISTANT COATINGS

Today a variety of materials, e.g., carbides, oxides, metallic, etc., belonging to the above category are available commercially. The wear resistant coatings can be classified into the following categories: [12]

(i) Carbides: WC, TiC, SiC, ZrC, $Cr_2C_3$ etc.

(ii) Oxides: $Al_2O_3$, $Cr_2O_3$, $TiO_2$, $ZrO_2$ etc.

(iii) Metallic: NiCrAlY, Triballoy etc.

(iv) Diamond

The choice of a material depends on the application. However, the ceramic coatings are very hard and hence on an average offer more abrasion resistance than their metallic counterparts.

### 2.11.1 Carbide Coatings

Amongst carbides, WC is very popular for wear and corrosion applications [55]. The WC powders are clad with a cobalt layer. During spraying the cobalt layer undergoes melting and upon solidification form a metallic matrix in which the hard WC particles remain embedded. Spraying of WC-Co involves a close control of the process parameters such that only the cobalt phase melts without degrading the WC particles. Such degradation may occur in two ways:

- Oxidation of WC leading to the formation of $CoWO_4$ and $WC_2$ [56].
- Dissolution of WC in the cobalt matrix leading to a formation of brittle phases like $CoW_3C$, which embrittles the coating [57].

An increase in the spraying distance and associated increase of time in flight leads to a loss of carbon and a pickup of oxygen. As a result the hardness of the coating decreases [58]. An increase in plasma gas flow rate reduces the dwell time and hence can control the oxidation to some extent. However, it increases the possibility of cobalt dissolution in the matrix [59]. The other option to improve the quality of such coating is to conduct the spraying procedure in vacuum [57].

Often carbides like TiC, TaC and NbC are provided along with WC in the cermet to improve upon the oxidation resistance, hardness, and hot strength. Similarly the binder phase is also modified by adding chromium and nickel with cobalt. The wear mechanism of plasma sprayed WC-Co coatings depends on a number of factors, e.g., mechanical properties, cobalt content, experimental conditions, mating surfaces, etc. The wear mode can be abrasive [60,61,62] adhesive or surface fatigue [63,64]. The coefficient of friction of WC-Co (in self mated condition) increases with increasing cobalt content [63]. A WC-Co coating when tested at a temperature of 450°C exhibits signs of melting [65]. The wear resistance of these coatings also depends on porosity [61]. Pores can also act as source from where the cracks may grow. Thermal diffusivity of the coatings is another important factor. In narrow contact regions, an excessive heat generation may occur owing to rubbing. If the thermal diffusivity of the coating is low the heat cannot escape from a narrow region easily resulting a rise in temperature and thus failure occurs owing to thermal stress [61, 65]. The wear mechanism of WC-Co nanocomposite coating on mild steel substrates has been

studied in details by Stuart and Shipway [66]. The wear rates of such coatings are found to be much greater than that of commercial WC-Co composite coating, presumably owing to an enhanced decomposition of nanoparticles during spraying. Wear has been found to occur by subsurface cracking along the preferred crack paths provided by the binder phase or failure at the inter-splat boundary. Coatings of TiC or TiC+ TaC with a nickel cladding are alternative solutions for wear and corrosion problems. High temperature stability, low coefficient of thermal expansion, high hardness and low specific gravity of these coatings may outperform other materials, especially in steam environment. Instead of nickel, nickel chromium alloy can serve as the matrix material [67, 68]. The mode of wear can be adhesive, abrasive, surface fatigue or micro-fracture depending on operating conditions [64, 68].

A coating of $Cr_3C_2$ (with Ni-Cr alloy cladding) is known for its excellent sliding wear resistance and superior oxidation and erosion resistance, though its hardness is lower than that of WC. After spraying in air, $Cr_3C_2$ loses carbon and transforms to $Cr_7C_3$. Such transformation generally improves hardness and erosion resistance of the coating [69]. The sliding wear behaviour of the $Cr_3C_2$ -Ni -Cr composite has been studied by several authors against various metals and ceramics [61, 64, 70]. It is felt that at lower loads the wear is owing to the detachment of splats from the surface. As the load increases, melting, plastic deformation and shear failure come into play.

### 2.11.2 Oxide Coatings

Metallic coatings and metal containing carbide coatings sometime are not suitable in high temperature environments in both wear and corrosion applications. Often they fail owing to oxidation or decarburization. In such case the material of choice can be an oxide ceramic coating, e.g., $Al_2O_3.Cr_2O_3$, $TiO_2$, $ZrO_2$ or their combinations. However, a high wear resistance, and chemical and thermal stability of these materials are counterbalanced by the disadvantages of low values of thermal expansion coefficient, thermal conductivity, mechanical strength, fracture toughness and somewhat weaker adhesion to substrate material. The thickness of these coatings is also limited by the residual stress that grows with thickness. Therefore, to obtain a good quality coating it is essential to exercise proper choice of bond coat, spray parameters and reinforcing additives.

### 2.11.3 Metallic Coatings

Metallic coatings can be easily applied by flame spraying or welding techniques making the process very economical. Moreover plasma sprayable metallic consumables are also available in abundant quantity. Metallic wear resistant materials are classified into three categories:

(i) cobalt based alloys

(ii) nickel based alloys

(iii) iron based alloys

The common alloying elements in a cobalt-based alloy are Cr, Mo, W and Si. The microstructure is constituted by dispersed carbides of $M_7C_3$ type in a cobalt rich FCC matrix. The carbides provide the necessary abrasion resistance and corrosion resistance. Hardness at elevated temperatures is retained by the matrix [71, 72]. Sometimes a closed packed intermetallic compound is formed in the matrix, which is known as the Laves phase. This phase is relatively soft but offers significant wear resistance [73]. The principal alloying elements in Ni-based alloys are Si, B, C and Cr. The abrasion resistance can be attributed to the formation of extremely hard chromium borides. Besides carbides, Laves phase is also present in the matrix [71].

Iron based alloys are classified into pearlitic steels, austenitic steels, martensitic steels and high alloy irons. The principal alloying elements used are Mo, Ni, Cr and C. The softer materials, e.g., ferritic, are for rebuilding purpose. The harder materials, e.g., martensitic, on the other hand provide wear resistance. Such alloys do not posses much corrosion, oxidation or creep resistance [71, 74, 75]. Nickel aluminide is another example of coating material for wear purpose. The prealloyed Ni-Al powders, when sprayed, react exothermically to form nickel aluminide. This reaction improves the coating substrate adhesion. In addition to wear application, it is also used as bond coat for ceramic materials [24].

NiCoCrAlY is an example of plasma sprayable superalloy. It shows an excellent high temperature corrosion resistance and hence finds application in gas turbine blades. The compositional flexibility of such coatings permits tailoring of such coating composition for both property improvement and coating substrate compatibility. In addition, it serves as a bond coat for zirconia based thermal barrier coatings [76].

### 2.11.4 Diamond Coatings

Thin diamond films for industrial applications are commonly produced by CVD, plasma assisted CVD, ion beam deposition, and laser ablation technique [77, 78]. Such coatings are used in electronic devices and ultra wear resistant overlays. The limitation of the aforesaid methods is their slow deposition rates. The DIA-JET process involving DC $Ar/H_2$ plasma with methane gas supplied at the plasma jet is capable of depositing diamond films at a high rate [79]. However, the process is extremely sensitive to the process parameters. Deposition of diamond film is also possible using an oxy-acetylene torch [80]. One significant limitation of a diamond coating is that it cannot be rubbed against ferrous materials, owing to a phase transformation leading to the formation of other carbon allotropes [81]. Diamond films are tested for the sliding wear against abrasive papers, where wear progresses by micro fracturing of protruding diamond grits. The process continues till the surfaces becomes flat and thereafter wear progresses by an interfacial spalling. Therefore, the life of the coating is limited by its thickness [82].

## 2.12 UTILIZATION OF FLY ASH AS WEAR RESISTANT COATINGS

Fly ash emerges as a by-product from the combustion of raw coal in thermal power plants. This industrial waste presents serious problems of storing and environmental pollution by posing a serious threat to health is set to touch the 100 million tones per year mark by the turn of the century from the current level of 80 million tones per year in India. Fly ash is a finely divided residue with particle size varying from 0.5 to 100 μm. It is refractory and abrasive in nature. Although the generation of fly ash is very high in India, the utilization is only 6%, posing a serious threat to the environment. Therefore, the effective utilization of waste fly ash not only decreases environmental pollution, but also produces high value-added products [83, 84]. The chemical composition of fly ash is not constant everywhere due to the nature of coal available from different places. However, its main constituents are silicon dioxide (SiO2), aluminium oxide ($Al_2O_3$) and iron oxide ($Fe_2O_3$), and are hence a suitable source of aluminum and silicon. For a long time, silica and alumino-silicate bricks have been preferred as refractory materials in many industrial applications due to their high wear resistance and high load bearing capacity at high temperatures. During the last decade, although a large number of investigations have been carried out for development of plasma spray ceramic coatings, not much effort has been made to use low-grade raw materials for plasma spray purposes [4]. Recently, attempts have been made to develop the plasma spray deposition of alumino-silicate composite coatings

onto metal substrates using industrial waste. The properties of fly ash has been studied by Tiwari and Saxena and coatings that were developed have shown improved corrosion and abrasion resistance and also better resistance to chemicals (5% $Na_2CO_3$ , 1% NaOH, and 2% $H_2SO_4$ ) and organic solvents (toluene and mineral spirit). Fly ash can be a cost effective substitute for conventional extenders in high performance industrial coatings [85]. It can be utilized to develop ceramic coatings on metal substrate. Good quality coating and homogeneously distributed phases are observed in the coatings made at power levels between 12 to 20 kW [86]. Fly ash with aluminium additions can be used to provide plasma spray ceramic composite coating on metal substrates and it is found that the coating quality and properties are improved with higher aluminium content in the feed material and are affected by the operating power level of the plasma [6]. Buta singh et.al have investigated the fly ash coating obtained by shrouded plasma spray process on carbon steel and found it to be effective to increase the oxidation and salt corrosion resistance of the given carbon steel [4]. The work done by Mishra et al established Redmud-Flyash mixture as a potential coating material, suitable for plasma spraying and for wear resistant applications and also opened up a new pathway for value added utilization of these industrial wastes [87]. In the recent past, efforts were also made to deposit fly ash premixed titania bearing ore i.e. illmenite on metal substrates [7].

## 2.13 EROSION WEAR OF CERAMIC COATINGS

Surface damage can result in changes in surface condition and dimension of a mechanical component, and this may sometimes cause disastrous failure of an entire mechanical system. One of cost-effective approaches against surface failure is coating. Various coating techniques have been successfully applied in industry to protect machinery and equipment from surface damage respectively caused by corrosion, oxidation and wear. However, when used in a harsh environment involving two or more damage modes, such as corrosion-wear or corrosion-erosion, many coatings perform poorly due to the synergistic action of wear and corrosion. Considerable efforts have been continuously made to develop high-performance coatings that can resist corrosive wear encountered in various industries such as mining, oil, sand, petroleum and chemical industries [88]. It has been reported that the thermal spray is a technique that produces a wide range of coatings for diverse applications [89]. Coatings of a wide variety of materials are commonly applied to substrates for many purposes. Often, coatings are applied to improve tribological performance. These may include the enhancement of mechanical properties, visual

appearance or corrosion resistance or may provide special magnetic and optical properties [90]. Plasma sprayed coatings are used today as thermal barriers and abrasion, erosion or corrosion resistant coatings in a wide variety of applications owing to their high hardness and high temperature performance. With the applications of these coatings to such as coal and biomass fired boiler tubes, vanes operated in sandy environment, study of their particle erosion behaviour is of particular interest. This is because of the erosion by impact of solid particles entrained in a moving fluid stream is a major life-limiting constraint in many industrial environments [91, 92]. Plasma spraying is the most flexible and versatile thermal spray process with respect to the sprayed materials. Almost any material can be used for plasma spraying on almost any type of substrate. The high temperatures of plasma spray processes permit the deposition of coatings for applications in areas of liquid and high temperature corrosion and wear protection and also special applications for thermal, electrical and biomedical purposes [93, 94]. The loss of material caused by the impingement of tiny, solid particles, which have a high velocity and impact on the material surface at defined angles, is called erosive wear [95]. Particulates ingested into the engine or formed as a result of incomplete combustion are known to cause erosion problems in gas turbines [96, 97]. Erosion is a serious problem in many engineering systems, including steam and jet turbines, pipelines and valves used in slurry transportation of matter, and fluidized bed combustion systems [48]. Gas and steam turbines operate in environments where the ingestion of solid particles is inevitable. In industrial applications and power generation, such as coal-burning boilers, fluidized beds, and gas turbines, solid particles are produced during the combustion of heavy oils, synthetic fuels, and pulverized coal and causes erosion of materials. In such environments, protective coatings on the surface of superalloys are frequently used [98, 99]. Erosion tests on coatings have been widely reported. However, the mechanisms of coating damage in this type of test depend on the coating material and its thickness, the properties of the interface, the substrate material and the test conditions [100].

Liquid impact erosion is a well-known phenomenon in hydro and low-pressure steam turbine blades, and also in aircraft or missiles traveling at high speed through rain [101-103]. The material damage is caused mainly by the high pressure caused by the impact of liquid droplets and the micro-jetting action due to the asymmetrical collapse of bubbles on or near the surface. The surface damage can be minimized by heat treatment or surface modification and substantial advances have been made in this field. Lee et al. [104] investigated the liquid impact erosion resistance of 12Cr steel and stellite 6B coated with TiN by reactive magnetron sputter ion plating. The stresses generated by droplet impact

were stated to have been decreased by the TiN as a result of stress attenuation and stress wave interactions.

Solid Particle Erosion (SPE) is a wear process where particles strike against surfaces and promote material loss. During flight a particle carries momentum and kinetic energy, which can be dissipated during impact, due to its interaction with a target surface. Different models have been proposed that allow estimations of the stresses that a moving particle will impose on target [105]. It has been experimentally observed by many investigators that during the impact the target can be locally scratched, extruded, melted and/or cracked in different ways. The imposed surface damage will vary with the target material, erodent particle, impact angle, erosion time, particle velocity, temperature and atmosphere.

Plasma sprayed coatings are used today as erosion or abrasion resistant coatings in a wide variety of applications. Extensive research shows that the deposition parameters like energy input in the plasma and powder properties affect the porosity, splat size, phase composition, hardness etc. of plasma sprayed coatings [106]. These in turn, have an influence on the erosion wear resistance of the coatings. Quantitative studies of the combined erosive effect of repeated impacts are very useful in predicting component lifetimes, in comparing the performance of materials and also in understanding the underlying damage mechanisms involved.

Resistance of engineering components encountering the attack of erosive environments during operation can be improved by applying ceramic coatings on their surfaces. Alonso et.al. experimented with the production of plasma sprayed erosion resistant coatings on carbon fiber-epoxy composites and the studied of their erosion behaviour [107]. The heat sensitivity of the composite substrate requires a specific spraying procedure in order to avoid its degradation. In addition, several bonding layers were tried to allow spraying of the protective coatings. Two different functional coatings; a cermet (WC-12 Co) and a ceramic oxide (Al2O3) were sprayed onto an aluminium-glass bonding layer. The microstructure and properties of these coatings were studied and their erosion behaviour determined experimentally in an erosion-testing device. Tabakoff and Shanov [108]. designed a high temperature erosion test facility to provide erosion data in the range of operating temperatures experienced in compressors and turbines. In addition to the high temperatures, the facility properly simulates all the erosion parameters important from the aerodynamics point of view. These include particle velocity, angle of impact, particle size, particle concentration and sample size. They reported the erosion behavior of titanium carbide coating exposed to fly ash and chromite particles. Chemical vapor deposition

technique (CVD) was used to apply a ceramic coating on nickel and cobalt based super-alloys (M246 and X40). The test specimens were exposed to particle-laden flow at velocities of 305 and 366 m/s and temperatures of 550°C and 815°C.

A good number of reports are available on erosion behaviour of alumina coatings. The resistance to erosion of such coatings depends upon intersplat cohesion, shape, size, and hardness of erodent particles, particle velocity, angle of impact and the presence of cracks and pores [109]. The slurry (SiC and $SiO_2$) and airborne particle ($Al_2O_3$ and $SiO_2$) erosions of flame sprayed alumina coatings have also been reported in the literature. SiC and Al2O3 are found to cause significant amount of erosion in slurry and airborne erosion testing respectively. High particle velocity enhances the erosion rate and the erosion rate is maximum for an impact angle of $90^o$. The failure is by the progressive removal of splats and can be attributed to the presence of defects and pores in the inter-splat regions. Similar observation has been made for the plasma sprayed alumina coatings subjected to an erosive wear caused by the $SiO_2$ particles [110]. A typical model, exemplifying the rate of erosion depending on size and velocity of particle on impacting the substrate is shown in Fig.2.11. It is based on the assumptions that the effective parameters for erosion damage include impact velocity, angle, size and shape of the particles (particle property) and material hardness as one of mechanical properties of the target material. Thus a predictive equation for erosion at $90^0$ is given as:

$$\mathbf{E_{90} = K\,(Hv)^{k1}\,(v)^{k2}\,(D)^{k3}} \qquad \text{------ (2.1)}$$

where k1, k2 and k3 are exponent factors for material hardness, velocity and particle diameter, which are affected by other parameters respectively. K denotes a particle property factor such as particle shape (angularity) and hardness.

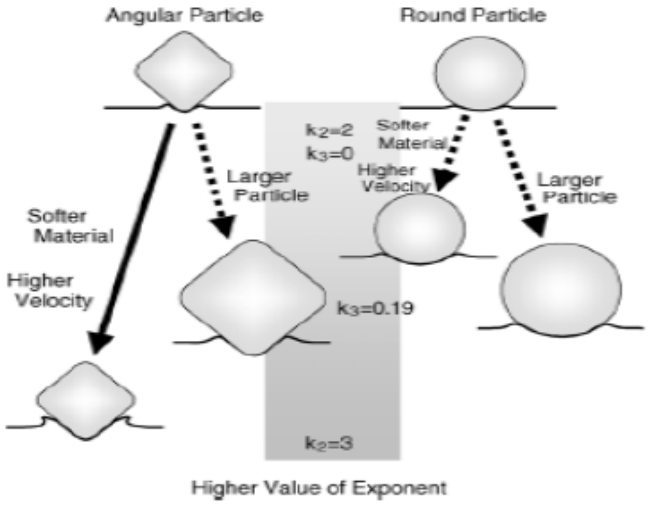


**Figure 2.11** Model of the effects of impact parameters on exponents k2 and k3.

The increase in impact velocity or particle diameter clearly accelerates erosion damage. From the fact that an increase in particle velocity or size leads to larger or deeper indentations as schematically shown in Fig. 2.9, deviations in k2 and k3 values from the theoretical ones (k2 =2, k3= 0) indicate the true effects of impact velocity and particle diameter which are connected with the relative aggressiveness of indentation. The larger or deeper is the indentation the greater amount of material is removed from the rim of the indentation [111].

Branco et al. [112] examined room temperature solid particle erosion of zirconia and alumina-based ceramic coatings, with different levels of porosity and varying microstructure and mechanical properties. The erosion tests were carried out by a stream of alumina particles with an average size of 50μm at 70 m/s, carried by an air jet with impingement angle of $90^{o}$. The results indicate that there is a strong relationship between the erosion rate and the coating porosity.

The erosion wear behaviour and mechanism of several kinds of middle temperature seal coatings were investigated by Yi Maozhong et al. [113]. The results show that the relationship between the erosion mass loss and the erosion time is linear, the coatings hold a maximum erosion rate at $60^{o}$ impact angle, and the relation between the erosion rate and the impact speed is an exponential function. The speed exponent increases with the increase of the impact angle. At $90^{0}$ impact, the abrasive particles impinging on the coating surface produce indentations and extruded lips, and then the lips are work-hardened and fall off; and flattened metal phase grains are impacted repeatedly, loosed and debonded. At $30^{o}$ impact, the micro cutting, plowing and tunneling via pores and non-metal phase are involved. The model of the erosion mechanism is advanced on the basis of the above-mentioned erosion wear behaviour, as shown in Fig 2.12.

Against these few backgrounds, the present research work has been undertaken, with an objective to explore the coating potential of fly ash-quartz.

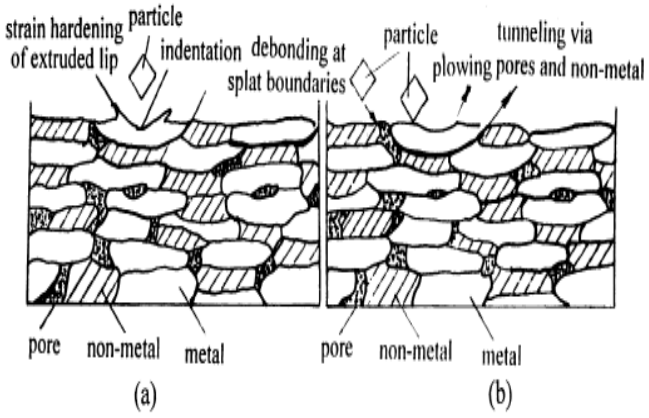


**Figure 2.12** Schematic diagram of Model of erosion wear **(a)** at $90^{0}$ **(b)** at $30^{0}$

# Chapter 3

# Experimental set up and Methodology

- Introduction
- Development of coatings
- Characterization of powder
- Characterization of coatings
- Erosion wear of coatings

# CHAPTER 3
# EXPERIMENTAL SET UP AND METHODOLOGY

## 3.1 INTRODUCTION

This chapter deals with the details of the experimental procedures followed in this study. The coating procedure itself requires some basic preparation, i.e., shot blasting and cleaning. After plasma spraying, the coated materials have been subjected to a series of tests, e.g., microstuctural characterization of the surfaces and cross sections, micro hardness measurement, X - ray diffraction studies, adhesion test, erosion wear test etc. The details of each process are described here.

## 3.2 DEVELOPMENT OF COATINGS

### 3.2.1 Preparation of Powder

In this study, fly ash and quartz powders (fly ash with 40 wt% quartz) are mechanically milled in a FRITSCH-Planetary ball mill for 3 hours to get a homogeneous mixture. The planetary ball mill has 4 numbers of zirconia balls (20g) and 20 numbers of zirconia balls (2g) for milling. The powders obtained were sieved to proper particle size range with the help of a roto-tap sieve shaker machine by using Laboratory test sieves (ISO R565).

### 3.2.2 Preparation of Substrate

Commercially available copper and mild steel have been chosen as different substrate materials. The specimens were circular discs of diameter 1 inch having thickness 3mm. The specimens were grit blasted at a pressure of 3 $kg/cm^2$ using alumina grits having a grit size of 60. The standoff distance in shot blasting was kept between 120-150 mm. The average roughness of the substrates was ~ 6.8 μm. The grit blasted specimens were cleaned with acetone in an ultrasonic cleaning unit. Spraying was carried out immediately after cleaning.

### 3.2.3 Plasma Spray Coating Deposition

The plasma spraying was done at the Laser and Plasma Technology Division, Bhaba Atomic Research Center, Mumbai. Conventional 40kW atmospheric plasma spraying (APS) set up was used. The plasma input power was varied from 11 to 21 kW by controlling the gas flow rate, voltage and the arc current. The powder feed rate was kept constant at 15 gm/min, using a turntable type volumetric powder feeder. The general arrangement of the plasma spraying equipment and schematic diagram of the plasma spraying process are shown in Fig.3.1 and 3.2 respectively. The equipment consists of the following units:

1. Plasma spraying equipment
2. Control console
3. Powder feeder
4. Power supply
5. Torch cooling system (water)
6. Hoses, cables, gas cylinders and accessories

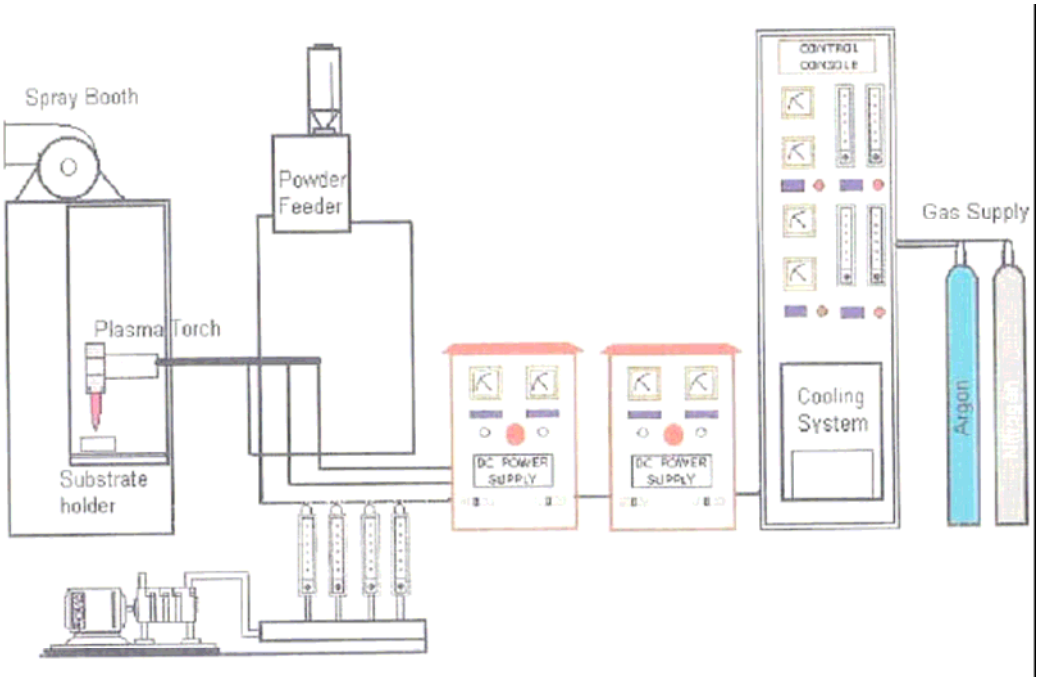


**Figure 3.1** General arrangement of plasma spraying equipment

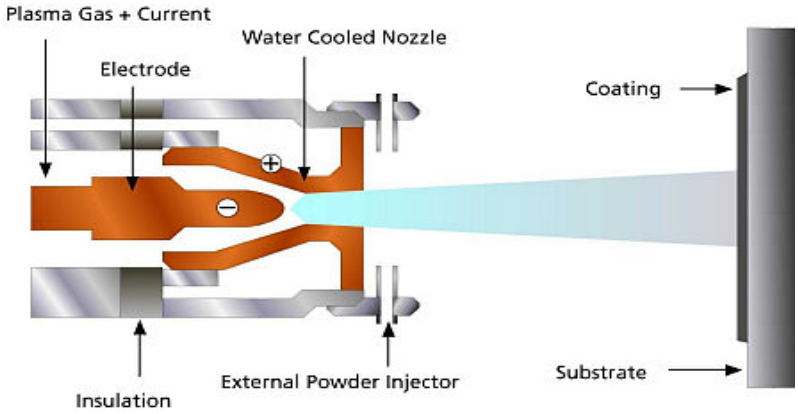


**Figure 3.2** Schematic diagram of plasma spraying process

Argon is used as the primary plasmagen gas and nitrogen as the secondary gas. The powders are deposited at spraying angle of 90°. The powder feeding is external to the gun. The properties of the coatings are dependent on the spray process parameters. The operating parameters during coating deposition are listed in Table 3.1.

**Table 3.1** Operating parameters during coating deposition

| **Operating parameters** | **Values** |
|---|---|
| Plasma arc current (amp) | 260, 360, 425, 500 |
| Arc voltage (volts) | 40, 40, 44, 44 |
| Torch input power (kW) | 11, 15, 18, 21 |
| Plasma gas (Argon) flow rate (lpm) | 28 |
| Secondary gas ($N_2$) flow rate (lpm) | 3 |
| Carrier gas (Argon) flow rate (lpm) | 12 |
| Powder feed rate (gm/min) | 15 |
| Torch to base distance TBD (mm) | 100 |

## 3.3 CHARACTERIZATION OF FEEDSTOCK

### 3.3.1 Particle Size Analysis

The particle sizes of the raw materials used for coating (fly ash-quartz powder) were characterized using Laser particle size analyzer of Malvern Instruments make.

### 3.3.2 Compositional Analysis

The compositional analysis of fly ash was done by wet chemical analysis method.

## 3.4 CHARACTERIZATION OF COATINGS

### 3.4.1 Evaluation of Coating Deposition Efficiency

Deposition efficiency is defined as the ratio of the weight of coating deposited on the substrate to the weight of the expended feedstock. Weighing method is accepted widely to measure this. Each specimen is weighed before and after coating deposition. The difference is the weight ($G_c$) of coating deposited on the substrate. From the powder feed rate and time of deposition the weight of expended feedstock ($G_p$) is determined. The deposition efficiency ($\eta$) is then calculated using the equation $\eta = (G_c / G_p \times 100)$ % Weighing of samples was done using a precision electronic balance with $\pm$ 0.1 mg accuracy [114].

### 3.4.2 Coating Thickness Measurement

Thickness of the fly ash-quartz coatings on different substrates was measured on the polished cross-sections of the samples, using an optical microscope. Five readings were taken on each specimen and the average value is reported as the mean coating thickness.

### 3.4.3 Hardness Measurement

Small specimens were sliced from the coated samples. Samples containing coating cross-sections were mounted and polished for the hardness measurement. Microscopic observation under optical microscope of the polished section of the coatings exhibited three distinctly different regions/ phases namely white, dull and spotted/mixed. Vickers hardness measurement was made using Leitz Micro hardness Tester equipped with a monitor and a microprocessor based controller, with a load of 50 Pa (0.419N) and a loading time of 20

seconds. About twelve or more readings were taken on each sample and the average value is reported as the data point.

### 3.4.4 Porosity Measurement

Measurement of porosity was done using the image analysis technique. The porosity of the coatings was measured by putting polished cross sections of the coating sample under a microscope (Neomate) equipped with a CCD camera (JVC, TK 870E). This system is used to obtain a digitized image of the object. The digitized image is transmitted to a computer equipped with VOIS image analysis software. The total area captured by the objective of the microscope or a fraction thereof can be accurately measured by the software. Hence the total area and the area covered by the pores are separately measured and the porosity of the surface under examination is determined.

### 3.4.5 Evaluation of Coating Interface Bond Strength

To evaluate the coating adhesion strength, a special type jig (Fig.3.3) was fabricated. Cylindrical mild steel dummy samples (length 25 mm, top and bottom diameter 12 mm) were prepared. The surfaces of the dummies were roughened by punching. These dummies were then fixed on top of the coating with the help of a polymeric adhesive and pulled with tension after being mounted on the jig (Fig.3.4). The coating pullout test was carried out using the set up Instron 1195 at a crosshead speed of 1 mm/minute. The moment coating got torn off from the specimen, the reading (of the load), which corresponds to the adhesive strength of the coating, was recorded. A typical test set up (during testing) is shown in Fig.3.5. The test was performed as per ASTM C-633.

**Figure 3.3** Jig under the test

**Figure 3.4** Specimen under tension

**Figure 3.5** Adhesion test with Instron 1195 UTM

### 3.4.6 X-Ray Diffraction Studies

X-ray diffraction technique was used to identify the different (crystalline) phases present in the coatings. XRD analysis was done using Ni-filtered Cu-Kα radiation in a Philips X-ray diffractometer. The characteristic d-spacing of all possible values are taken from JCPDS cards and were compared with d-values obtained from XRD patterns to identify the various X-ray peaks obtained.

### 3.4.7 Scanning Electron Microscopic Studies

Microstructure of plasma sprayed coated specimens and plasma processed powders were studied by JEOL JSM-6480 LV scanning electron microscope mostly using the secondary electron imaging. The surface as well as the interface morphology of all coatings was observed under the microscope. Small specimens were sliced from the coated samples and were mounted using thermosetting molding powders. Coating cross-sections was polished in three stages using SiC abrasive papers of reducing grit sizes and then with diamond pastes on a wheel for coating interface analysis under SEM. These specimens were also utilized for the hardness measurement.

## 3.5 EROSION WEAR BEHAVIOUR OF COATINGS

Solid particle erosion (SPE) is usually simulated in laboratory by one of two methods. The ‘sand blast’ method, where particles are carried in an air flow and impacted onto a stationary target; and the ‘whirling arm’ method, where the target is spun through a chamber of falling particles.

In the present investigation, an erosion apparatus (fabricated in laboratory) of the 'sand blast' type is used (Fig.3.6). It is capable of creating highly reproducible erosive situations over a wide range of particle sizes, velocities, particles fluxes and incidence angles, in order to generate quantitative data on materials and to study the mechanisms of damage. The test is conducted as per ASTM G76 standards.

(a) (b)

**Figure 3.6** Erosion test set up

The jet erosion test rig used in this work (schematic diagram shown in Fig. 3.7) employs a 300 mm long nozzle of 3 mm bore and 300 mm long. This nozzle size permits a wider range of particle types to be used in the course of testing, allowing better simulations of real erosion conditions. The mass flow rate was measured by conventional method. Particles were fed from a simple hopper under gravity into the groove. Velocity of impact is measured using double disc method [115].

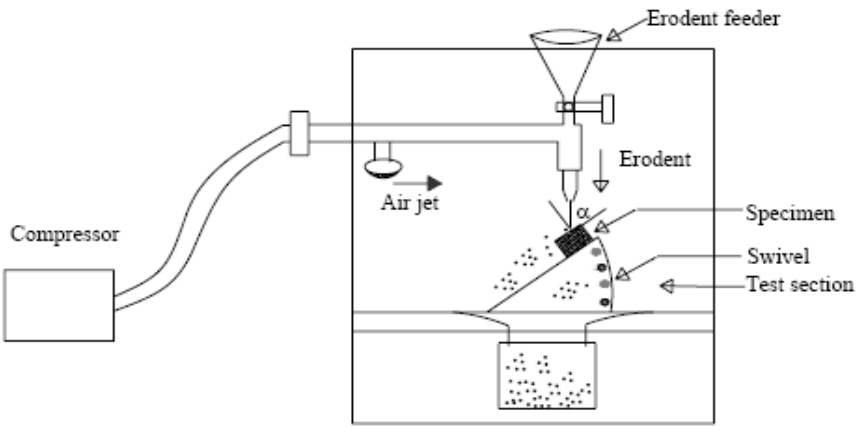


**Figure 3.7** Schematic diagram of erosion test rig

Some of the features of this test set up are:

- Vertical traverse for the nozzle: provides variable nozzle to target standoff distance, which influences the size of the eroded area.
- Different nozzles may be accommodated: provides stability to change the particle plume dimensions and velocity range.
- Large test chamber with sample mount (typical sample size 25mm X 25mm) that can be angled to the flow direction: by tilting the sample stage, the angle of impact of the particles can be changed in the range of $0^0 – 90^0$ and this will influence the erosion process.

The erosion wear rates were obtained by carrying out experiments as per conditions of a standard Taguchi experimental plan with notation **L9,** for fly ash-quartz coatings of 18 kW power level. Based on the results, the coatings were eroded at different impact angles (i.e. at $30^0$, $60^0$, $90^0$), which proved to be the dominant factor in erosion, at standoff distance of 100 mm; and at a pressure of 5.5 kgf/cm$^2$ (i.e. at a velocity of 58m/sec) with dry silica sand and silicon carbide erodent of 150 μm size. Amount of wear is determined on 'mass loss' basis [116,90]. It was done by measuring the weight change of the samples at regular time intervals during the test duration. A precision electronic balance with 0.001 mg accuracy was used for weighing. Erosion rate, defined as the coating mass loss per unit erodent mass (mg/kg) was calculated.

# Chapter 4

# Results and Discussion

- Introduction
- Characterization of feedstock
- Characterization of coatings
- Coating performance
- Discussion

# CHAPTER 4
# RESULTS AND DISCUSSION

## 4.1 INTRODUCTION

Plasma sprayed coatings of fly ash-quartz were developed on two different metal substrates (i.e. copper and mild steel), using a 40 kW atmospheric plasma spray system, at different input power levels to the plasma torch (in the range from 11 kW to 21 kW). Characterizations of the coatings were done and the tribological performances of the coating were evaluated. The results of various tests are presented and discussed in this chapter.

## 4.2 CHARACTERIZATION OF COATING MATERIAL:

### 4.2.1 Particle Size Analysis

The particle size distribution of fly ash-quartz powder (after mixing in ball mill and before plasma spraying) was characterized using Laser particle size analyzer of Malvern Instruments make. Fig 4.1 shows the particle size distribution of the feedstock. It can be seen that, majority of particles are in the range of 40 to 100 micron. Maximum volume fractions of the particles are in the range of 50 micron.

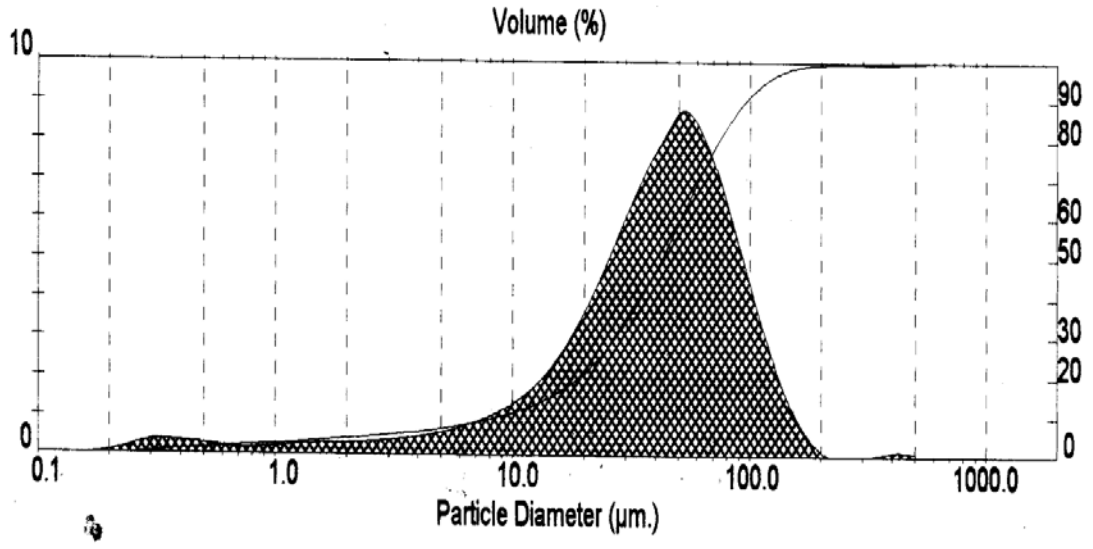


**Figure 4.1** Particle size analysis of fly ash – quartz feedstock.

### 4.2.2 Composition Analysis

The chemical composition analysis of major constituents of fly ash is given in Table 4.1. To this material, quartz powder ($SiO_2$) has been added at the rate of 40 wt% to prepare the feedstock.

**Table 4.1** Chemical analysis of fly ash used for coating

| $Al_2O_3$ | $SiO_2$ | $Fe_2O_3$ | $TiO_2$ |
|---|---|---|---|
| 29.33% | 58.00% | 5.60% | 1.7% |

Along with these major compounds some other compounds like CaO, MgO, $K_2O$ and $Na_2O$ are present in traces. The LOI of the feedstock is found to be 3.6%.

### 4.2.3 Powder Morphology

SEM micrographs of fly ash – quartz feedstock prior to coating are shown in Fig. 4.2.

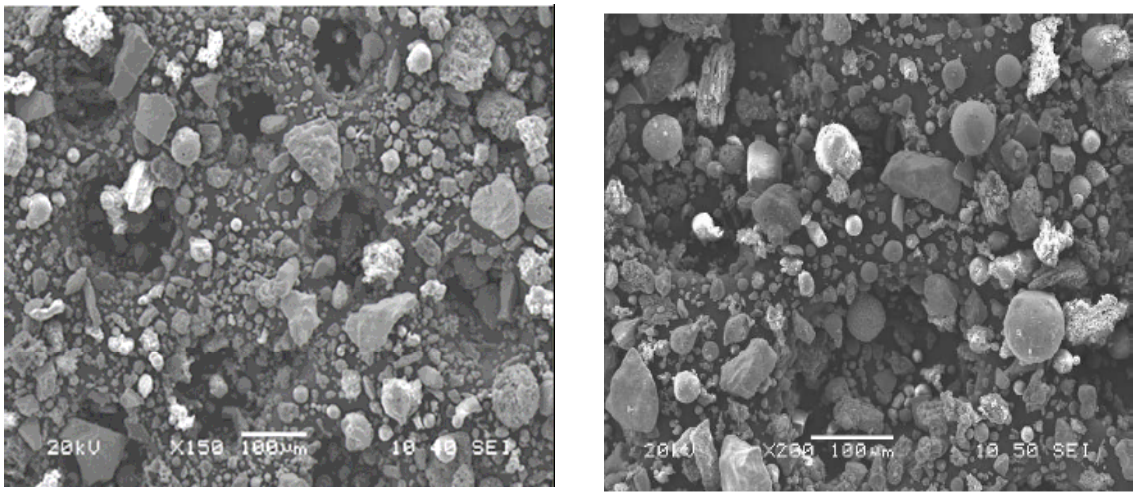


**Figure 4.2** SEM micrographs of fly ash – quartz raw powder prior to coating (i.e. feedstock)

It is observed that the Particles are of varied sizes, irregular in shape. Some particles are elongated type and some are multifaceted.

## 4.3 CHARACTERIZATION OF COATINGS

The coatings are deposited with APS and the following characterizations are carried out.

### 4.3.1 Coating Deposition Efficiency

Deposition efficiency is an important factor that determines the techno-economics of the process. Deposition efficiency of coatings made within the scope of this investigation is evaluated. Coating deposition efficiency is defined as the ratio of the weight of coating deposited on the substrate to the weight of the expended feedstock. Weighing method is accepted widely to measure this [114]. It can be described by the following equation

$$\eta = (G_c / G_p) \times 100\ \% \qquad \text{------ (4.1)}$$

Where, η is the deposition efficiency.

Gc is the weight of coating deposited on the substrate.

Gp is the weight-expended feedstock.

Deposition efficiency depends on many factors that include the input power to the plasma torch, material properties, such as melting point, particle size range, heat capacity of the powder being sprayed and standoff distance (torch to substrate distance) etc. For a given standoff distance and given material with specific particle size, torch input power appears to be an important factor for the deposition efficiency. The deposition efficiency is a measure of the fraction of the powder that is deposited on the substrate. Deposition efficiency values of fly ash-quartz coating made at different operating power levels (on mild steel substrate) are given in Table 4.2.

**Table 4.2** Deposition efficiency of fly ash-quartz coatings.

| Sl no. | Specimen | Power level (kW) | Deposition efficiency (%) |
|---|---|---|---|
| 1. | Fly ash – quartz coating | 11 | 20 |
| 2. | -do- | 15 | 25 |
| 3. | -do- | 18 | 32 |
| 4. | -do- | 21 | 35 |

The variation of deposition efficiency of fly ash-quartz coatings with operating power level on mild steel substrate is shown in Fig. 4.3. It is interesting to note that the deposition efficiency is increased in a sigmoidal fashion with the torch input power. It reveals that efficiency of coating deposition is significantly influenced by the input power to the torch. Plasma spray deposition efficiency of a given material depends on its melting point, thermal heat capacity, rate of dissipation of heat at substrate and particle size of the sprayed powder etc. At lower power level, the plasma jet temperature is not high enough to melt the entire feed powder (particles) that enters the plasma jet. As the power level is increased, plasma

temperature and enthalpy increases, thus melting a larger fraction of the feed powder. The spray efficiency therefore increases with increase in input power to the plasma torch. However, beyond a certain power level of the torch, temperature of the plasma becomes high enough leading to vaporization/dissociation of the feedstock. Thus there is not much increase in deposition efficiency. This tendency is generally observed in deposition of plasma spray coatings. However, the operating power above which the efficiency decrease depends on the chemical nature of the feed material i.e. powder and its particle size, thermal conductivity, in-situ phase transformations etc.

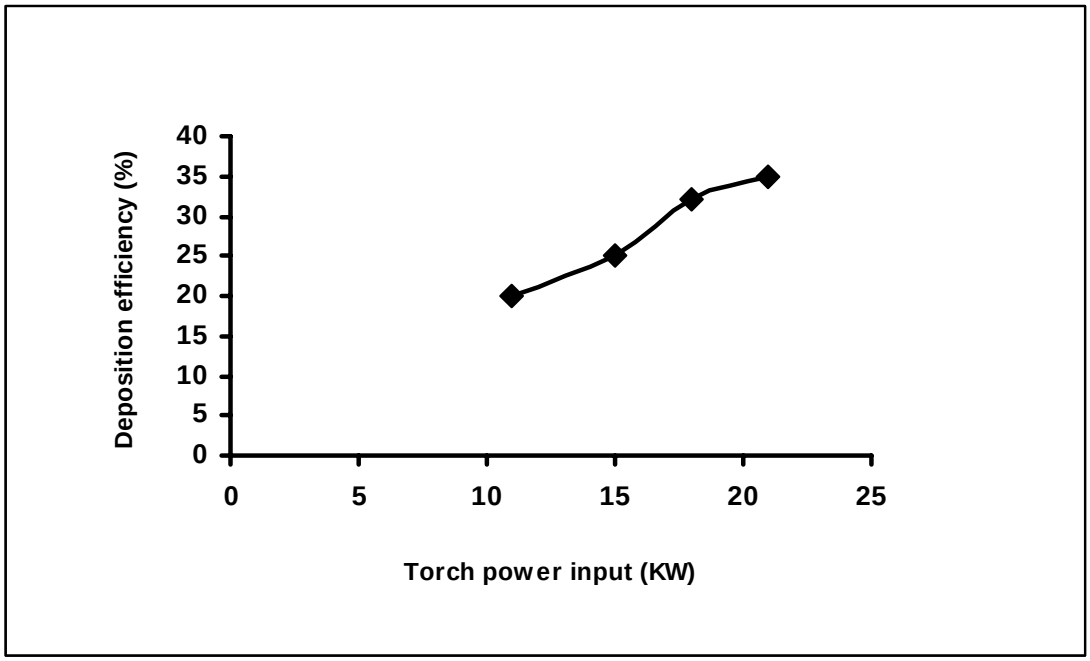


**Figure 4.3** Variation of deposition efficiency of fly ash-quartz coatings at different power levels.

### 4.3.2 Coating Thickness

To ensure the coating of fly ash-quartz on different substrates, coating thickness was measured on the polished cross-sections of the samples, using an optical microscope. The thickness values obtained for coatings deposited at different power levels for Mild steel substrates are presented in Table 4.3. Each data point on the curves is the average of at least five readings/measurements. The variation of thickness values with torch input power for Mild steel substrate is presented in Fig.4.4.

**Table 4.3** Thickness values of fly ash – quartz coatings on mild steel substrates.

| Sl no. | Specimen | Power level (kW) | Coating thickness (microns) |
|---|---|---|---|
| 1. | Fly ash – quartz coatings | 11 | 161.1 |
| 2. | -do- | 15 | 235 |
| 3. | -do- | 18 | 209.2 |
| 4. | -do- | 21 | 197.4 |

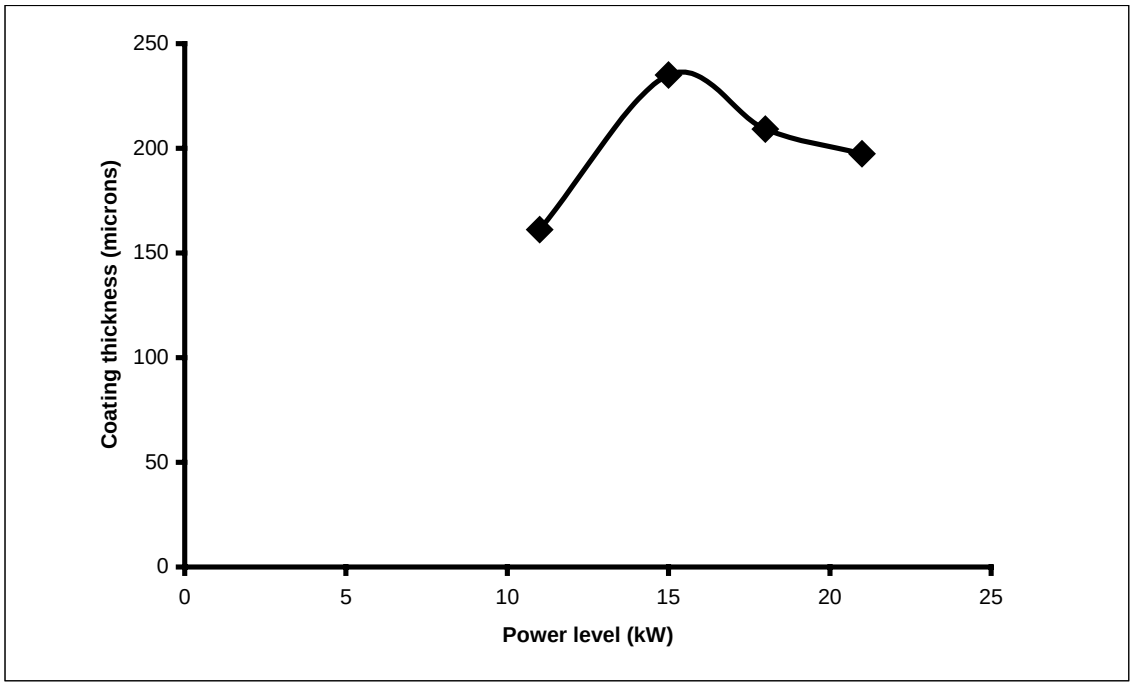


**Figure 4.4** Variation of coating thickness of fly ash-quartz coatings at different power levels.

From the above figure it is observed that maximum coating thickness of ~ 235 microns is obtained at 15 kW power level on mild steel substrates which decreases gradually with the increase in input power to the plasma torch. In case of thermal spray of oxide coatings developed by APS technique, particle deposition is influenced by the input power to the plasma torch. With the increase in power level, the plasma density increases leading to rise in enthalpy and thereby the particle temperature. Hence more number of particles gets melted during in- flight traverse through the plasma jet. When these molten species hit the substrate, get flattened and adhere to the surface forming big splats. If the inter-lamellar bonding between these splats is strong and the area of contact between the

lamellae is more, leads to less amount of porosity. Hence, although there is decrease in coating thickness but a dense coating is formed. The increase of coating thickness with porosity and vice versa was observed by Sarikaya in case of alumina coatings [117]. Maximum coating thickness in case of 15 kW plasma power level may be due to more amount of porosity.

### 4.3.3 Hardness of the Coatings

Microscopic observation of the polished cross section of the coatings under optical microscope revealed three distinct different visible regions/ phases namely white, dull and mixed/spotted. Coating hardness measurement is carried out with Leitz Micro-Hardness Tester using 50Pa (0.419N) load, are summarized in Table 4.4. Each data point is the average of twelve observations.

**Table 4.4** Hardness on the coating cross section for the coatings deposited at different power levels.

| Sl no. | Specimen | Power level (kW) | Hardness (HV) |
|---|---|---|---|
| 1. | Fly ash – quartz coating | 11 | 588.0 |
| 2. | -do- | 15 | 597.12 |
| 3. | -do- | 18 | 655.0 |
| 4. | -do- | 21 | 775.0 |

From the above table, it is observed that there is an increase in coating hardness with the increase in plasma power level. This may be due to the formation/transformation of compounds viz. silica and alumina etc. to their allotropic forms and their compositional variations during spray deposition with the increase in input power to the plasma torch.

### 4.3.4 Coating Porosity

Porosity measurement of the coatings was done using the image analysis technique. The polished interfaces of various coatings are studied under optical microscope (Neomate) equipped with a CCD camera (JVC, TK 870E). From the digitized image obtained by this system, coating porosity was determined using VOIS image analysis software. The results are tabulated in Table 4.5.

**Table 4.5** Porosity of coatings for different power levels

| Sl no. | Specimen | Power level (kW) | Porosity (Vol %) |
|---|---|---|---|
| 1. | Fly ash – quartz coating | 11 | 19.76 |
| 2. | -do- | 15 | 18.54 |
| 3. | -do- | 18 | 15 |
| 4. | -do- | 21 | 16.56 |

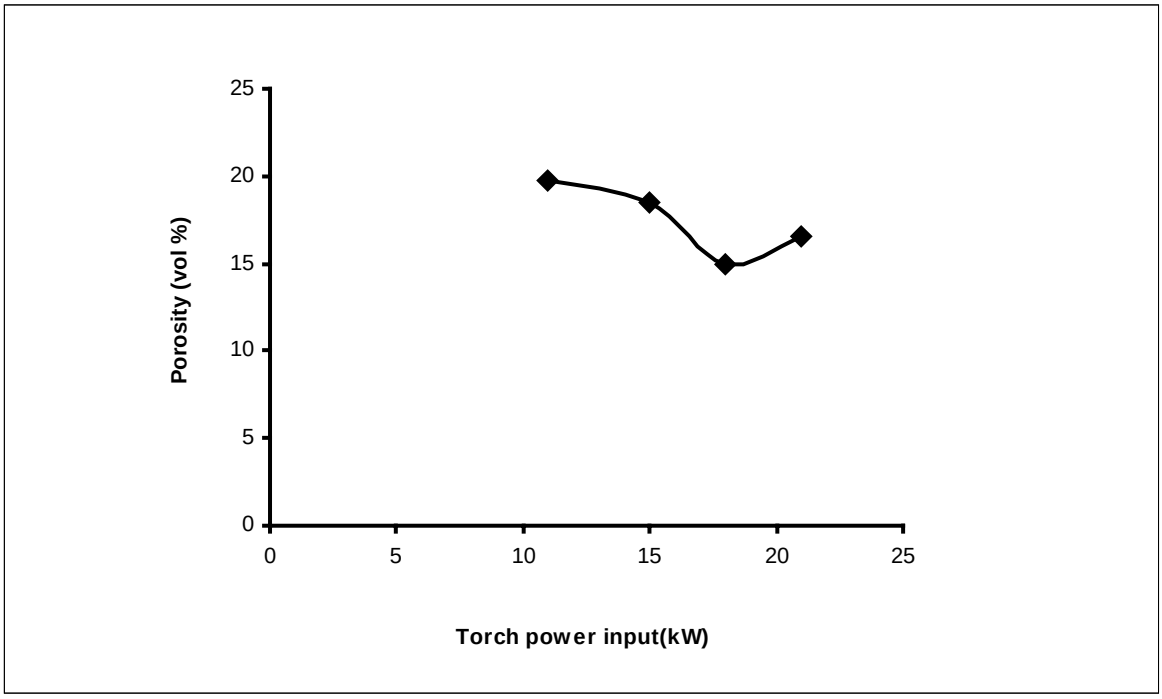


**Figure 4.5** Variation of coating porosity with plasma torch input power

Variation of coating porosity of fly ash - quartz with torch input power is shown in Fig.4.5. It is observed that porosity volume fraction of these coatings lie in the range of from ~16 % to ~20%. The amount of porosity is more in the case of coatings made at lower (11kW) and at higher (21kW) power levels. However porosity is minimum at 18kW for the coatings under this study. The increased value of porosity may be the reason for low adhesion strength and higher thickness [117] of the coatings deposited at low and at high power levels.

### 4.3.5 Coating Adhesion Strength

Coating adhesion tests have been carried out by many investigators with various coatings. It has been stated that, the fracture mode is adhesive if it takes place at the coating-substrate interface and that the measured adhesion value is the value of practical adhesion, which is strictly an interface property, depending exclusively on the surface characteristics of the adhering phase and the substrate surface condition [6, 118]. From the microscopic point of view, adhesion is due to physico-chemical surface forces (Vander-walls, Covalent, ionic etc.), which are established at the coating-substrate interface [119], and corresponds to the work of adhesion. From the mechanical point of view, adherence can be estimated by the force corresponding to interfacial fracture and is macroscopic in nature.

In the present investigation, evaluation of coating interface bond strength is done using coating pull out method confirming to ASTM C-633. It is found that, in all the samples fracture occurred at the coating-substrate interface. The results are tabulated in Table 4.6. The low values of adhesion strength may be due to difference in coefficient of thermal expansion coefficient of substrate and coating material and/or formation of pores, cracks, voids in the coating and along coating-substrate interfaces.

**Table 4.6** Adhesion strength values of fly ash-quartz coating at different power levels

| Sl no. | Specimen | Power level (kW) | Substrate | Adhesion strength (MPa) |
|---|---|---|---|---|
| 1. | Fly ash – quartz | 11 | Mild steel | 3.3 |
| 2. | -do- | 15 | -do- | 4.26 |
| 3. | -do- | 18 | -do- | 5.923 |
| 4. | -do- | 21 | -do- | 6.120 |
| 5. | -do- | 11 | Copper | 2.98 |
| 6. | -do- | 15 | -do- | 3.62 |
| 7. | -do- | 18 | -do- | 5.691 |
| 8. | -do- | 21 | -do- | 5.802 |

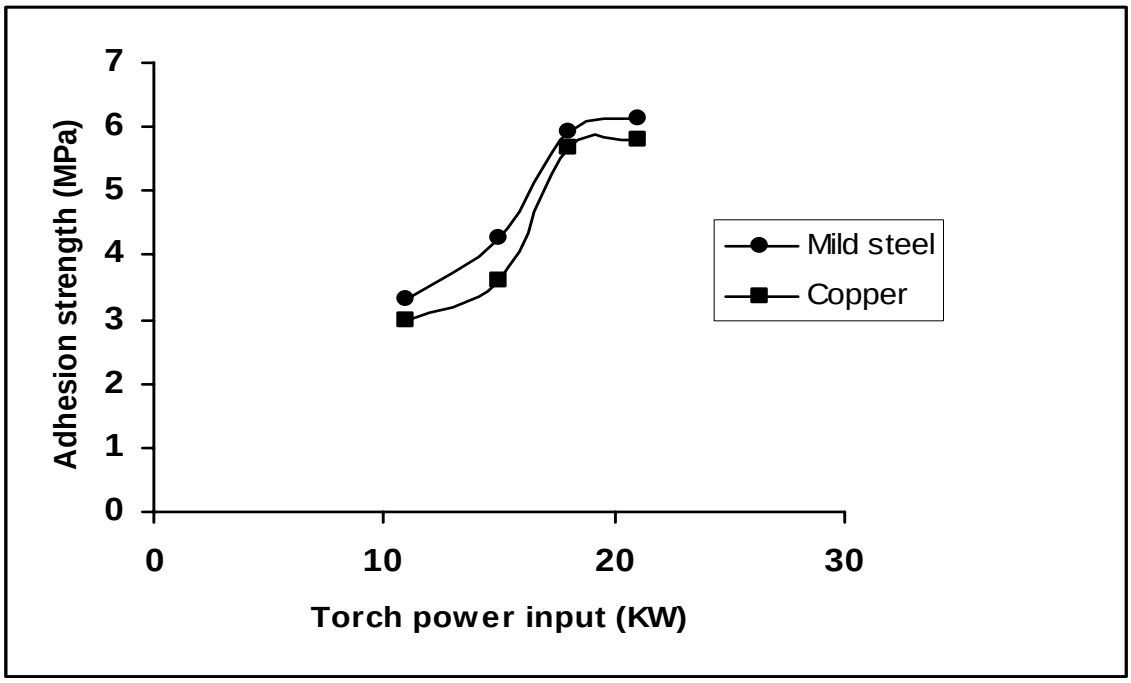


**Figure 4.6** Adhesion strength of fly ash-quartz coatings on different substrates

The variation of adhesion strength of fly ash-quartz coating at different power levels is shown in Fig.4.6. Each data point is the average of five test runs. From the figure, it is clear that the adhesion strength varies with operating power of the plasma torch. Maximum adhesion strength of 6.12 MPa on mild steel and of 5.802 MPa on copper substrate is recorded. It can be visualized that, the interface bond strength increases with increase in input power to the torch up to a certain power level and then shows a very little or nominal variation in coating adhesion irrespective of the substrate material. This might be due to the fact that, when the operating power level is increased, larger fraction of particles attain molten state as well as the velocity of the particles also increase. Therefore there is better probability for splat formation i.e. forms a lamellar structure and hence better mechanical inter-locking of molten particles/splats on the substrate leading to increase in adhesion strength [46]. But with increase in torch input power, fragmentation and vaporization of the particles increases. There is also a greater chance to fly off of smaller particles and results almost no increase in adhesion strength of the coatings. Coating adhesion strength is higher in case of mild steel substrate than that of copper substrate may be due to (I) the dependence of thermal conductivity for melted particle, dissipation of heat at substrate interface and also may be due to (II) the thermal expansion coefficient mismatch of the coating and the substrate [120].

### 4.3.6 ANN Prediction of Adhesion Strength (Neural Computation)

Plasma spraying is considered as a non-linear problem with respect to its variables: either materials or operating conditions. To obtain functional coatings exhibiting selected in-service properties, combinations of processing parameters have to be planned. These combinations differ by their influence on the coating properties and characteristics. In order to control the spraying process, one of the challenges nowadays is to recognize parameter interdependencies, correlations and individual effects on coating characteristics. Therefore a robust methodology is needed to study these interrelated effects. In this work, a statistical method, responding to the previous constraints, is implemented to correlate the processing parameters to the coating properties. This methodology is based on artificial neural networks (ANN), which is a technique that involves database training to predict property-parameter evolutions. This section presents the database construction, implementation protocol and a set of predicted results related to the coating erosion wear. ANNs are excellent tools for complex processes that have many variables and complex interactions. It is a computational system that simulates the microstructure (neurons) of biological nervous system. The most basic components of ANN are modeled after the structure of brain. Inspired by these biological neurons, ANN is composed of simple elements operating in parallel. It is the simple clustering of the primitive artificial neurons. This clustering occurs by creating layers, which are then connected to one another. The multilayered neural network which has been utilized in the most of the research works for material science, reviewed by Zhang and Friedrich [121]. The analysis is made here taking into account training and test procedure to predict the dependence of coating adhesion strength on different operating plasma input power levels and on different substrates. This technique helps in saving time and resources for experimental trials. The details of this methodology are described by Rajasekaran and Pai [122]. Each of these parameters is characterized by one neuron and consequently the input layer in the ANN structure has three neurons. The database is built considering experiments at the limit ranges of each parameter. Experimental result sets are used to train the ANN in order to understand the input-output correlations. The database is then divided into three categories, namely: (i) a validation category, which is required to define the ANN architecture and adjust the number of neurons for each layer. (ii) a training category, which is exclusively used to adjust the network weights and (iii) a test category , which corresponds to the set that validates the results of the training protocol. The input variables are normalized so as to lie in the same range group of 0-1. To train the neural network used for this work, about 24 data sets

obtained during erosion trials are considered. Different ANN structures (I-H-O) with varying number of neurons in the hidden layer are tested at constant cycles, learning rate, error tolerance, momentum parameter, noise factor and slope parameter. Based on least error criterion, one structure, shown in Table 4.7, is selected for training of the input-output data. The learning rate is varied in the range of 0.001-0.100 during the training of the input-output data. Neuron number in the hidden layer is varied and in the optimized structure of the network, this number is found to be 9. The number of cycles selected during training is high enough so that the ANN models could be rigorously trained.

**Table 4.7** Input parameters selected for training (Coating adhesion strength)

| **Input Parameters for Training** | **Values** |
|---|---|
| Error tolerance | 0.0001 |
| Learning rate (ß) | 0.1 |
| Momentum parameter(α) | 0.1 |
| Noise factor **(NF)** | 0.3 |
| Number of epochs | 5000000 |
| Slope parameter (£) | 0.6 |
| Number of hidden layer | 9 |
| Number of input layer neuron **(I)** | 4 |
| Number of output layer neuron **(O)** | 1 |

A software package NEURALNET for neural computing developed by Rao and Rao [123] using back propagation algorithm is used as the prediction tool for adhesion strength of coatings under various test conditions. The three-layer neural network having an input layer (I) with three input nodes, a hidden layer (H) with nine neurons and an output layer (O) with one output node employed for this work is shown in Fig. 4.7.

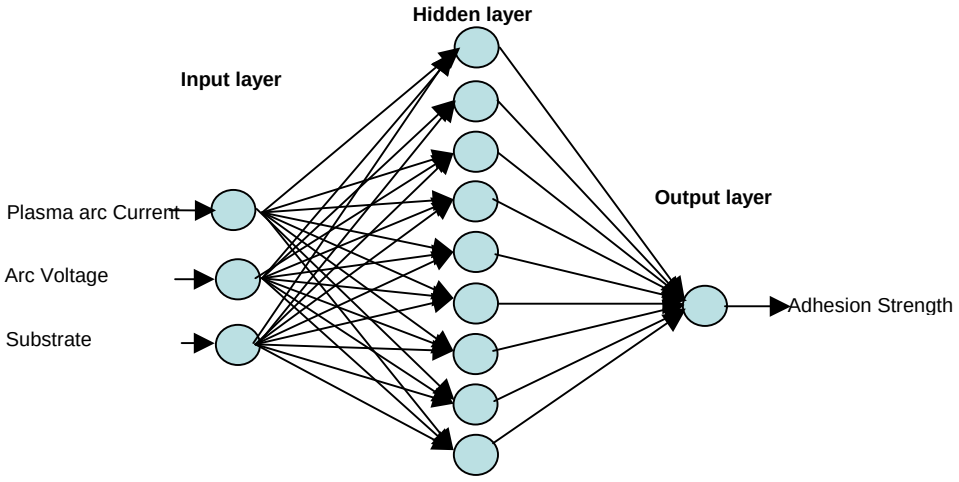


**Figure 4.7** The three layer neural network for adhesion strength

Seventy five percent of data collected from erosion test is used for training whereas twenty five percent data is used for testing. The parameters of three layer architecture of ANN model are set as input nodes = 3, output node = 1, hidden nodes = 9, learning rate = 0.1, momentum parameter = 0.1, number of epochs = 5000000 and a set of predicted output is obtained. A comparison between the experimental and the ANN predicted results for adhesion strength of coatings deposited at different plasma input power levels on mild steel and copper substrates are presented Fig. 4.8. It is observed that maximum error between ANN prediction and experimental adhesion strength is between 0 - 5 %. The error in case of ANN model can further be reduced if number of test patterns is increased.

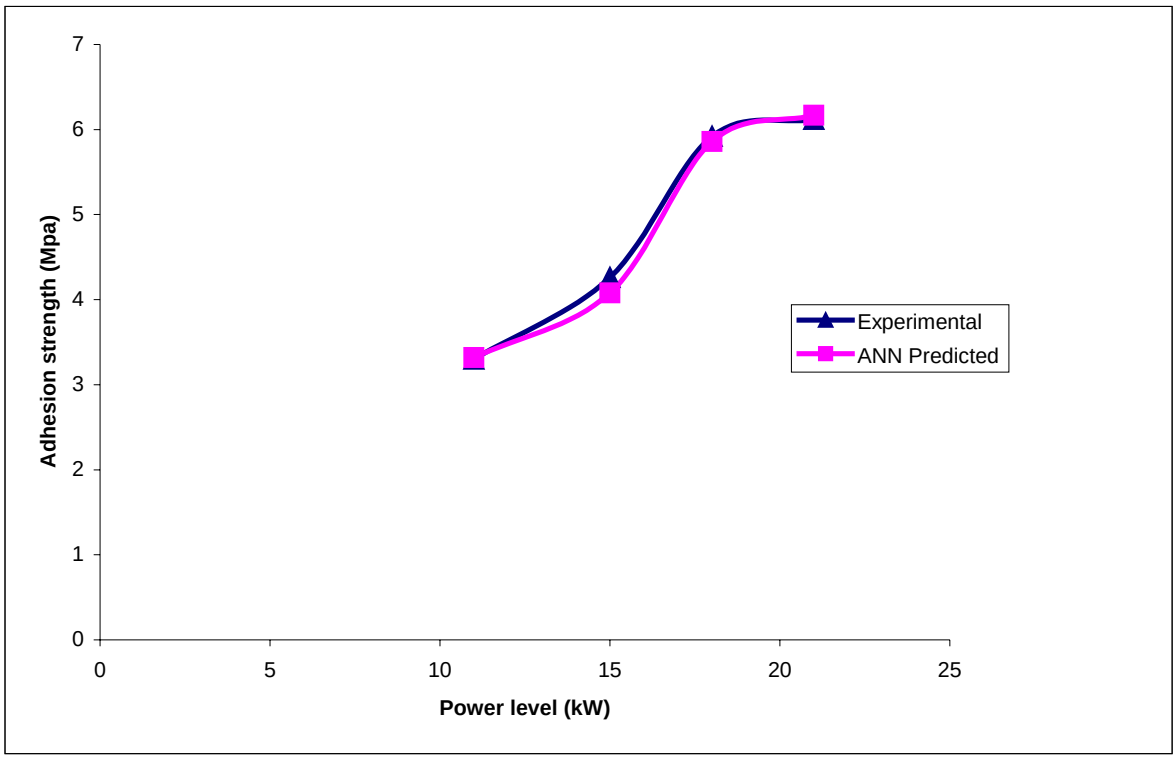


**Figure 4.8 (a)** Comparison plot for ANN predicted and experimental values of coating adhesion strength with different torch input power on mild steel substrates.

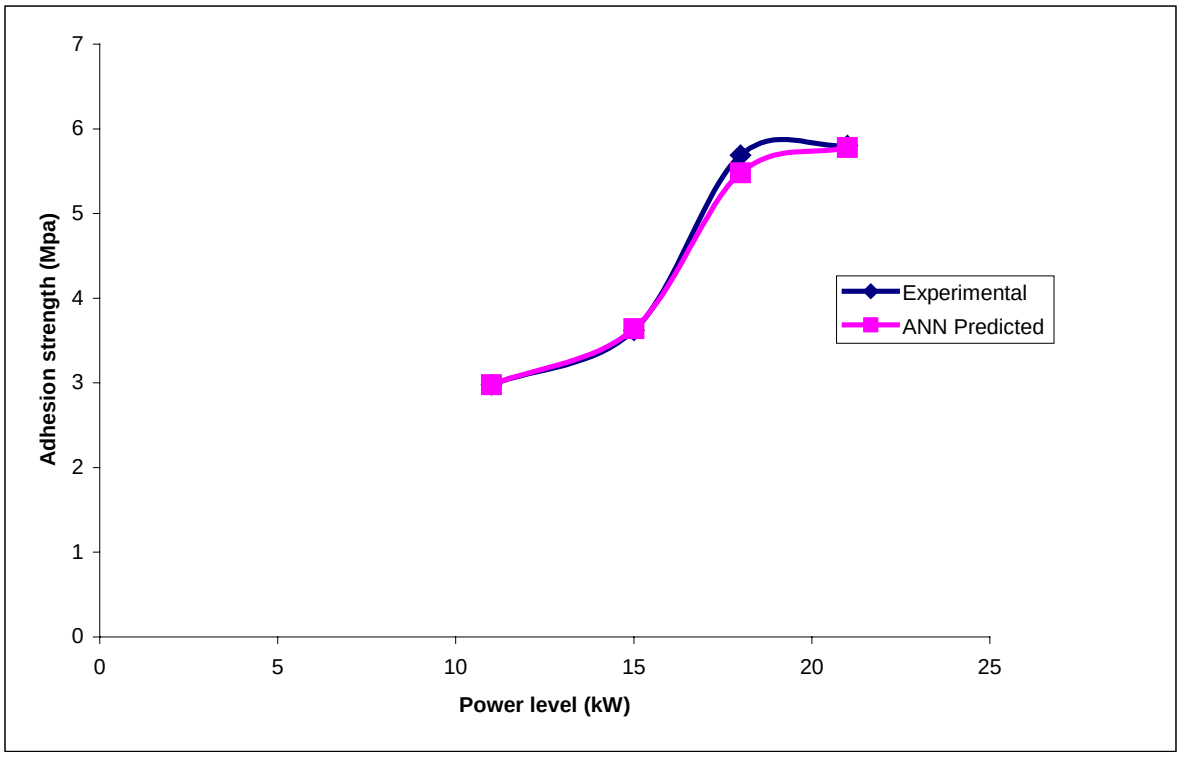


**Figure 4.8 (b)** Comparison plot for ANNpredicted and experimental values of coating adhesion strength with different torch input power on copper substrates.

It is interesting to note that the predictive results show good agreement with experimental sets realized after having generalizing the ANN structures. The optimized ANN structure further permits to study quantitatively the effect of the considered input power. The range of the chosen parameter can be larger than the actual experimental limits, thus offering the possibility to use the generalization property of ANN in a large parameter space. In the present investigation, this possibility was explored by selecting the torch input power in a range from 6 kW to 30 kW, and a set of prediction for coating adhesion strength is evolved. Fig.4.9 illustrates the predicted evolution of coating adhesion strength of fly ash - quartz coatings on copper and mild steel substrates with torch input power.

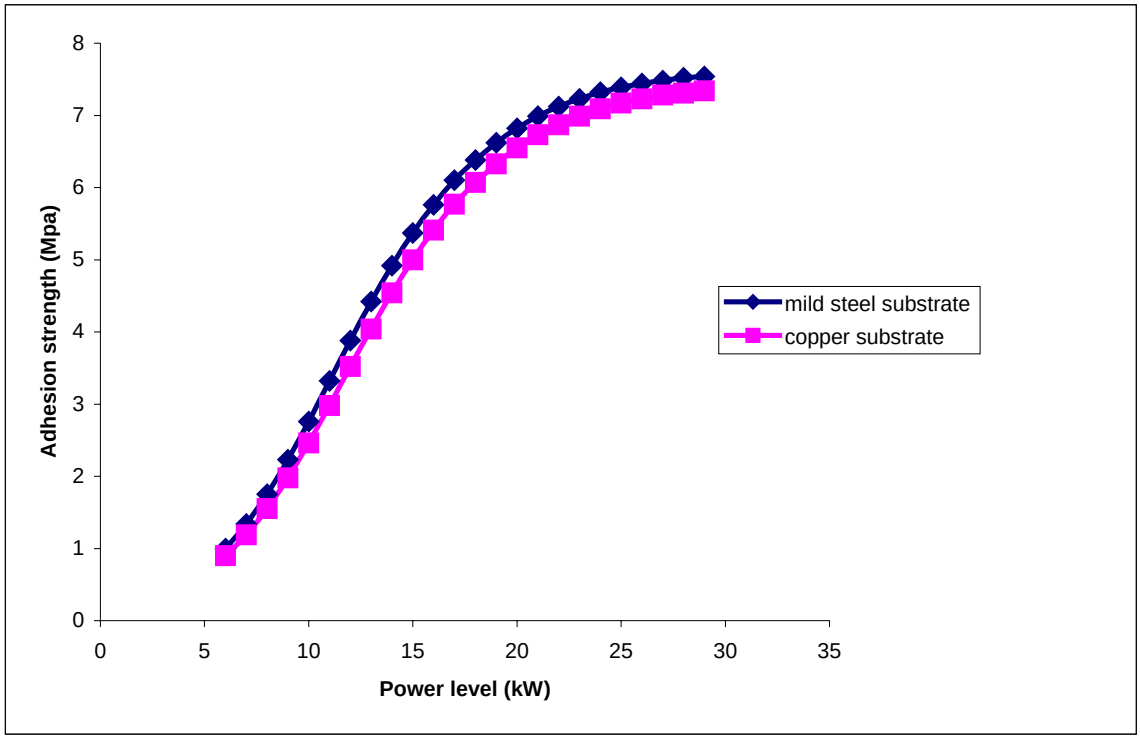


**Figure 4.9** ANN Predicted values of coating adhesion strength of fly ash - quartz coatings on copper and mild steel substrates at different torch input power.

### 4.3.7 XRD ANALYSIS

Micro structural observation of the interface under an optical microscope shows optically different regions on the coating cross sections. Therefore, to ascertain the phases present and phase changes / transformations taking place during plasma spraying, X-ray diffractograms are taken on the raw material and on coatings using a Philips X Ray Diffractometer with CuKα radiation. The XRD results are shown in Fig 4.10.

XRD of the feed material shows the presence of quartz, alumina, wustite etc. phases. With increase in coating power level, appearance of some new phases such as mullite, tridymite, cristobolite, γ-alumina, etc. are found. Especially the percentage of mullite and tridamite (high temperature phase of silica) are found to increase with increase in torch input power for coating deposition. It may be due to the availability of high temperature and high enthalpy, that has accelerated the phase transformations; and different phase are formed depending on enthalpy/environment and transformation conditions [124]. As these coatings is consists of mixture of hard oxides, it is expected that a ceramic composite coating from low grade materials could be made which can have better wear resistance properties.

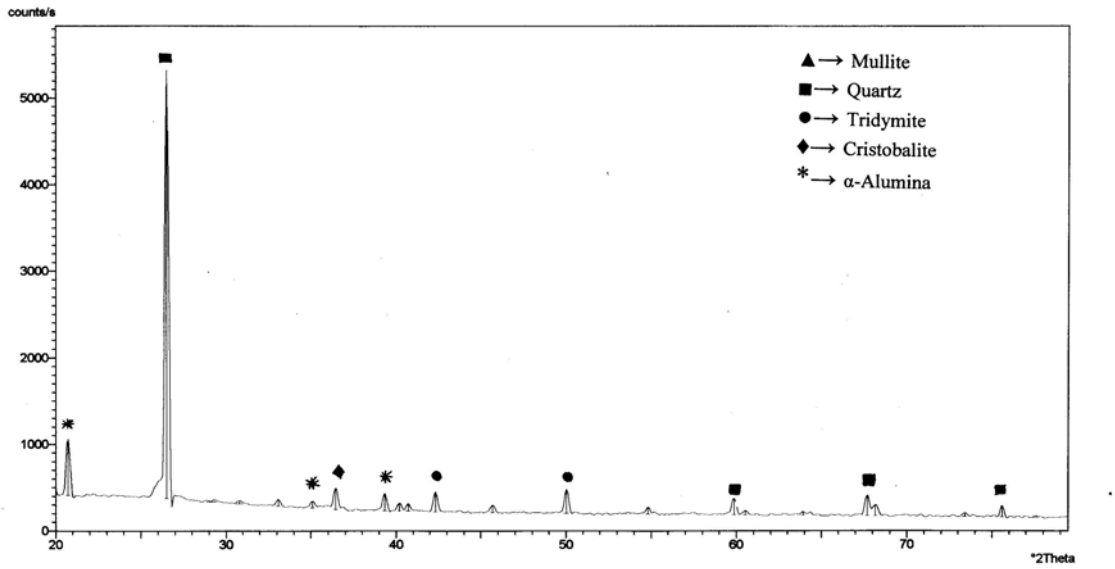


**Figure 4.10 (a)** X-Ray diffractogram of fly ash – quartz feedstock.

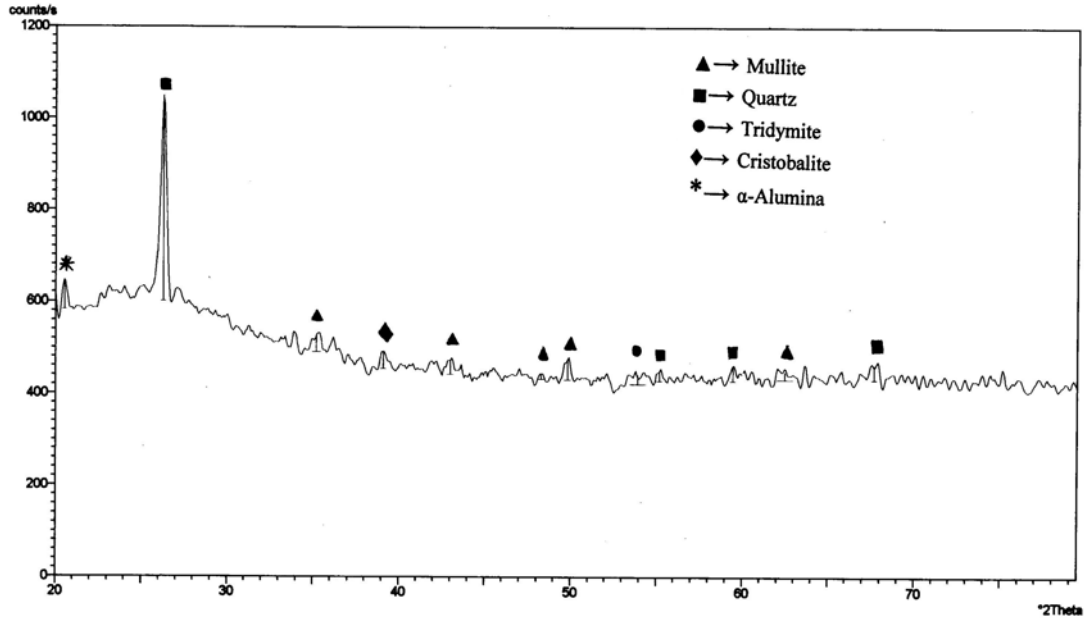


**Figure 4.10 (b)** X-Ray diffractogram of fly ash – quartz coating deposited at 11kW.

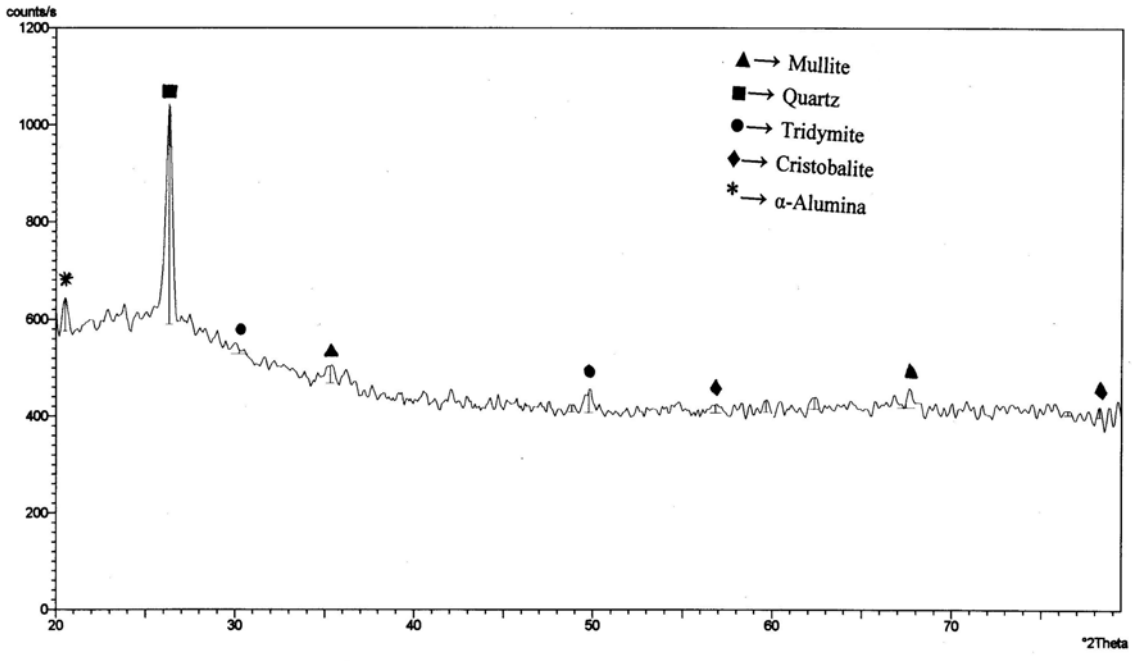


**Figure 4.10 (c)** X-Ray diffractogram of fly ash – quartz coating deposited at 15kW

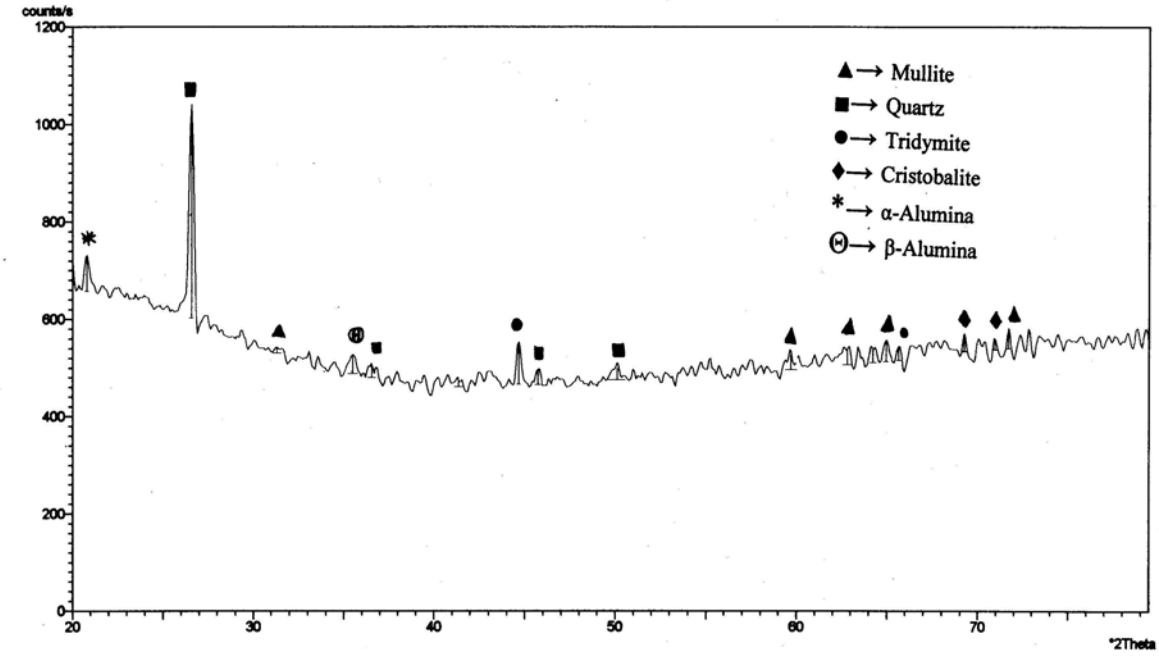


**Figure 4.10 (d)** X-Ray diffractogram of fly ash – quartz coating deposited at 18kW.

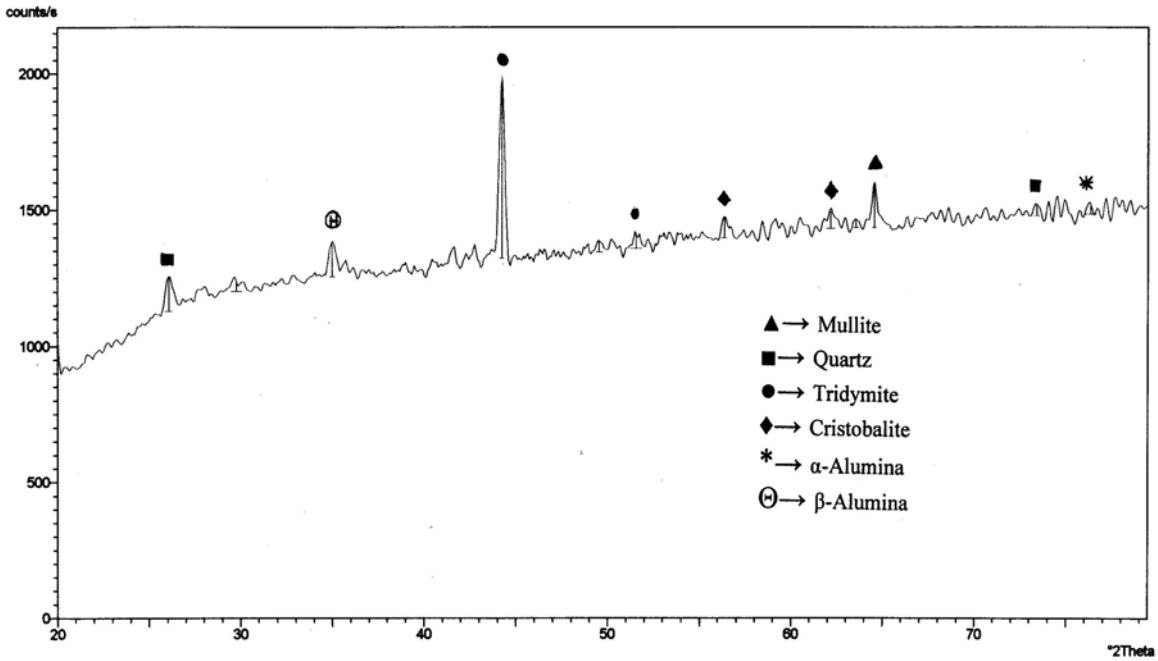


**Figure 4.10 (e)** X-Ray diffractogram of fly ash – quartz coating deposited at 21kW.

### 4.3.8 MICROSTRUCTURAL INVESTIGATION OF THE COATINGS

**Surface Morphology**

The interface adhesion of the coatings depends on the coating morphology and inter-particle bonding of the sprayed powders. SEM micrographs of fly ash-quartz coating surfaces are shown in Fig 4.11.

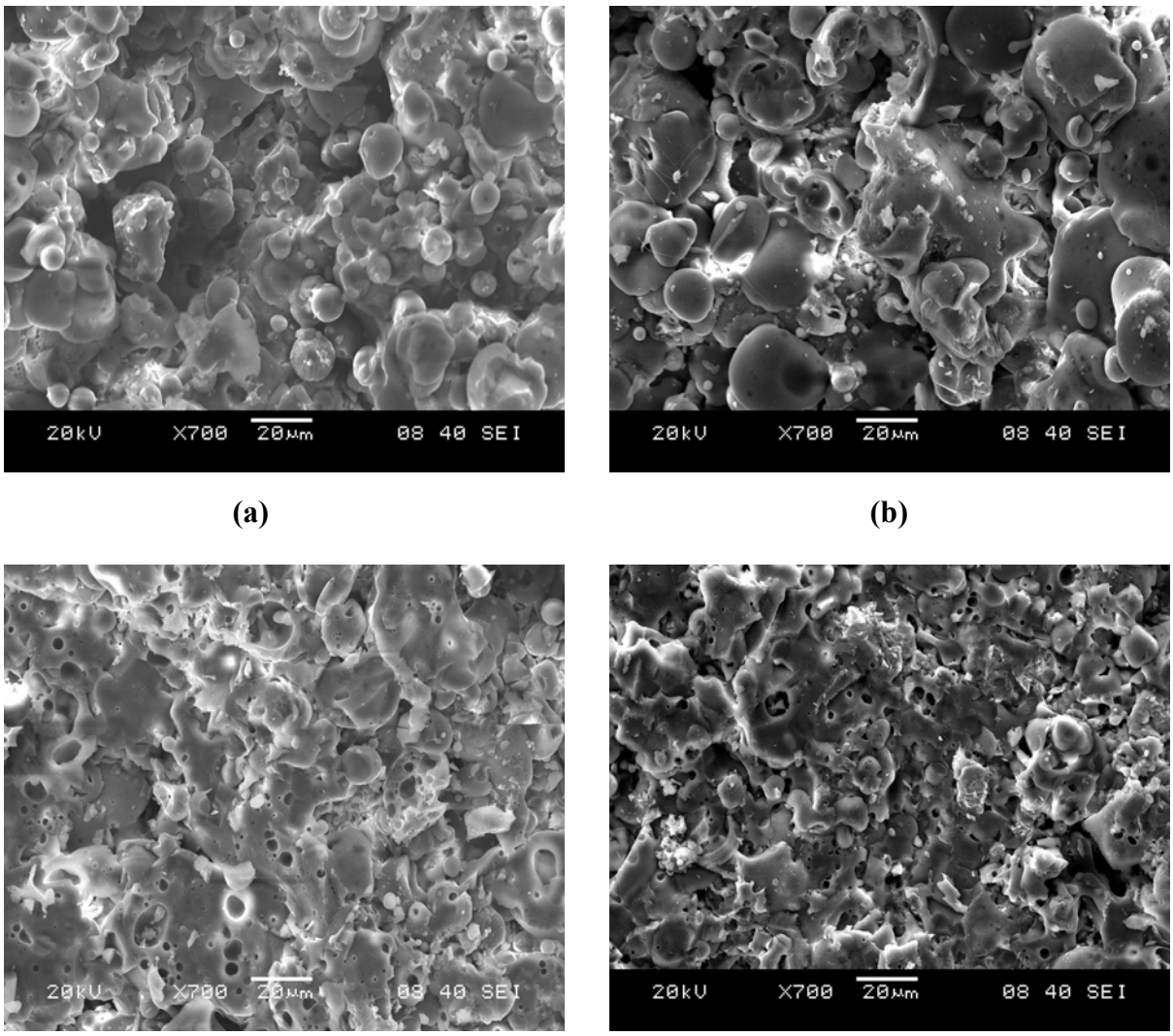


**(a)** **(b)**

**(c)** **(d)**

**Figure 4.12** Surface morphology of fly ash-quartz coatings deposited on mild steel Substrates, at **(a)** 11kW **(b)** 15kW **(c)** 18 kW **(d)** 21kW power level.

The coating deposited at 11 kW power level (Fig. 4.11(a)) on mild steel substrate, shows a uniform distribution of molten/semi molten particles, which have agglomerated to form laths. More amount of cavitation are observed. Some (open) large pores are found on the inter particle boundaries and at triple particle/grain junctions. These may have originated

due to the inadequate flow of molten particles during their solidification [125]. Coating made at 15kW (Fig. 4.11 (b)) bears a different morphology. Some spheroidal splats are found, indicative of complete melting of particles during in-flight traverse through plasma jet. Deep pores are found but the amount of cavitations is less. In case of coatings made at 18 kW (Fig. 4.11 (c)), the particles get more thermal energy. So during solidification from molten state, they agglomerate to form splats i.e. flattened regions. Less cavitation is observed at inter-granular boundaries. This may be the reason for better interface adhesion of the coating onto the substrate, leading to increase of adhesion strength. At still higher power level i.e. 21kW (Fig. 4.11 (d)), much smaller particles are found which are formed by breaking / fragmentation of bigger particles during their in-flight traverse through the plasma jet and then have solidified in the form of spheres due to fast rate of quenching (of the order of $10^{-6}$ degree/sec), and some of them are fused together in lumps to form flattened regions. The amount of porosity appears to have slightly increased i.e. cavitation is more as compared to the previous case (i.e. Fig.4.11 (c)). This might be the cause for the improper inter-particle bonding and poor stacking to the substrate, which have resulted in lowering the interface bond strength.

## Interface Morphology

The coating substrate interface plays the most important role in the adhesion of coatings. The surface morphology of the coatings cannot predict the interior (layer deposition) structures and their importance / acceptability. The polished cross sections of the samples are examined under SEM and are shown in Fig. 4.12.

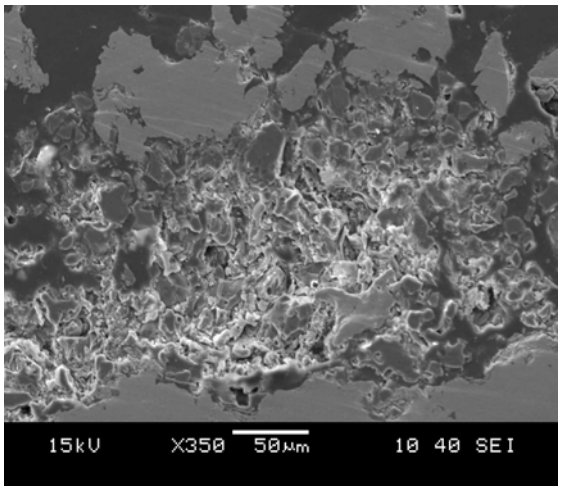


**(a)**

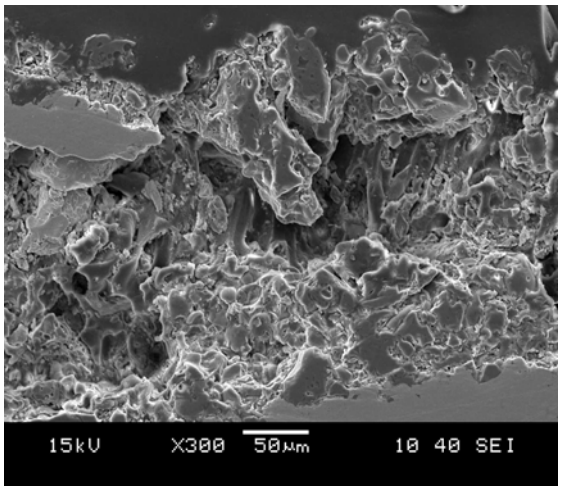


**(b)**

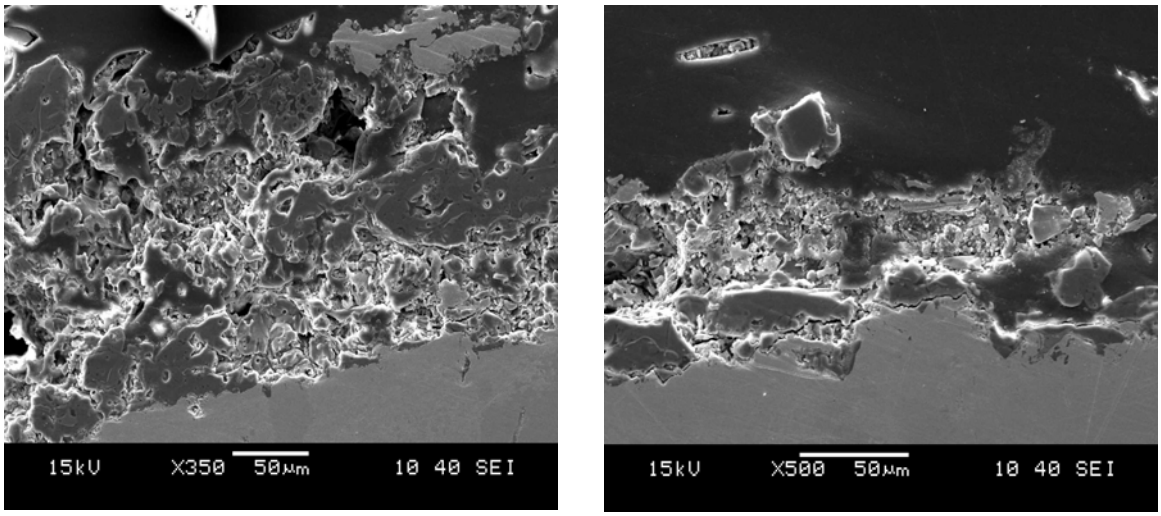


**(c)** **(d)**

**Figure 4.12** Interface morphology of fly ash-quartz coatings deposited on mild steel Substrates, at **(a)** 11kW **(b)** 15kW **(c)** 18 kW **(d)** 21kW power level.

From the micrographs, it is evident that, for the coating deposited at 11kW (Fig. 4.12 (a)) shows a lamellar structure with some amount of cavitations at the interface between the lamellas. Presence of some open pores along the direction of heat flow i.e. towards the surface due to shrinkage of particles parallel to the surface of the substrate. Such type of observations is also been made by Johner et al. [126]. Poor mechanical bonding of the coating onto the substrate (in micro level) is also observed at some places, leading to minimum adhesion strength. Interface of the coating made at 15 kW (Fig. 4.12 (b)) shows improved mechanical bonding at the coating substrate interface. Splats/coating layers are globular, larger in dimension and equi-axed type. Better inter-particle boundary match leading to better adhesion between them and also less amount of cavitations are observed. Coating made at 18 kW (Fig. 4.12 (c)) shows a homogeneous nature throughout the length of the coating with good interface bonding at metal-ceramic contact. Some spheroidal particles are also observed at some places. Porosity seems to have decreased in this case. At 21 kW (Fig. 4.12 (d)) plasma input power level, larger fractions of the coating shows particles of smaller dimensions which might have been formed due to simultaneous melting and fragmentation of particles during their in flight traverse through the plasma torch. Some regions exhibit splats of larger dimensions. Other than the mechanical interlocking of the

sprayed coating with the metal substrate, some metallurgical bonding might have occurred at the interface which is evident from the presence of some inter-diffusion zones. Amount of cavitations is found to have increased, leading to a slight decrease in adhesion strength.

## 4.4 EVALUATION OF COATING PERFORMANCE

### 4.4.1 Erosion Wear Behaviour of Coatings

Statistical methods are commonly used to improve the quality of a product or process. Such methods enable the user to define and study the effect of every single condition possible in an experiment where numerous factors are involved. Solid particle erosion is a dynamic process that leads to progressive loss of material from the target surface due to impingement of fast moving solid particles [127]. During flight, a particle carries momentum and kinetic energy, which are dissipated during impact on a target surface. In case of plasma spray coatings encountering such situations, no specific model has been developed and thus the study of their erosion behavior has been mostly based on experimental data [112]. Erosion is a nonlinear process with respect to its variables: that are materials and operating conditions. To obtain the best functional output of coatings exhibiting selected in-service properties, the right combinations of operating parameters are to be known. These combinations normally differ by their influence on the erosion wear rate i.e. coating mass loss. The less erosion wear rate is one the main requirements of the coatings developed by plasma spraying. In order to achieve certain values of erosion rate accurately and repeatedly, the influence parameters of the process have to be controlled accordingly. Since the number of such parameters in plasma spraying is too large and the parameter-property correlations are not always known, statistical methods can be employed for precise identification of significant control parameters for process optimization.

Hence, in the present work a statistical technique called Taguchi method is used to optimize the process parameters leading to minimum erosion of the coatings under study. That is why in recent years, Taguchi method has become a widely accepted methodology for improving productivity with minimum input/trials. The Taguchi method consists of a plan of experiments with the objective of acquiring data in a controlled way, executing these experiments and analyzing data, in order to obtain information about the behavior of a given process. One of the advantages of the Taguchi method over the conventional experiment design methods is that it minimizes the variability around the target when bringing the performance value to the target value in addition keeping the experimental cost at the

minimum level. Another advantage is that, optimum working conditions determined from the laboratory work can also be reproduced in the real production environment [128-132].

### 4.4.2 Taguchi Experimental Design

Four parameters viz., impact velocity, standoff distance, impingement angle and erodent size, each at three levels, are considered in this study. In Table 4.8, each column represents a test parameter and a row gives a test condition that is nothing but combination of parameter levels. Four parameters each at three levels would require $3^4 = 81$ runs in a full factorial experiment. Whereas, Taguchi's factorial experiment approach reduces it to 9 runs only offering a great advantage.

**Table 4.8** Levels of variables used in the experiment

| | **Levels** | | | |
|---|---|---|---|---|
| **Control factors** | **I** | **II** | **III** | **Units** |
| A: Erodant size | 150 | 260 | 360 | μm |
| B: Impingement angle | 30 | 60 | 90 | Degrees |
| C: Velocity of impact | 32 | 44 | 58 | m/sec |
| D: Stand off distance | 100 | 140 | 180 | mm |

The erosion wear rates of fly ash - quartz coatings under various test conditions are given in Table 4.9.

**Table 4.9** S/N ratios for coating erosion wear rate at 18kW

| Test runs | A | B | C | D | Erosion wear rate (mg/kg) | S/N Ratio |
|---|---|---|---|---|---|---|
| 1 | 150 | 30 | 32 | 100 | 238.095 | -47.5350 |
| 2 | 150 | 60 | 44 | 140 | 243.055 | -47.7141 |
| 3 | 150 | 90 | 58 | 180 | 317.460 | -50.0338 |
| 4 | 260 | 30 | 44 | 180 | 166.667 | -44.4370 |
| 5 | 260 | 60 | 58 | 100 | 283.018 | -49.0363 |
| 6 | 260 | 90 | 32 | 140 | 238.095 | -47.5350 |
| 7 | 360 | 30 | 58 | 140 | 172.413 | -44.7314 |
| 8 | 360 | 60 | 32 | 180 | 185.185 | -45.3521 |
| 9 | 360 | 90 | 44 | 100 | 253.396 | -48.0760 |

The experimental observations are transformed into a signal-to-noise (S/N) ratio. There are several S/N ratios available depending on the type of characteristics. The S/N ratio for minimum erosion rate coming under *smaller-is-better* characteristic, which can be calculated as logarithmic transformation of the loss function as shown below.

Smaller is the better characteristic:

$$\frac{S}{N} = -10 \log \frac{1}{n}\left(\sum y^2\right) \qquad \text{------ (4.2)}$$

where "n" the number of observations, and "y" the observed data. "Lower is better" (LB) characteristic, with the above S/N ratio transformation, is suitable for minimization of erosion rate. In Table 4.8, the last column represents S/N ratio of the erosion rate that is in fact the average of three replications. The overall mean for the S/N ratio of the erosion rate is found to be -45.674 db.

The analysis is made using the popular software specifically used for design of experiment applications known as MINITAB 14. The effects of individual control factors are shown in Fig. 4.13. The S/N ratio response are given in Table 4.10, from which it can be concluded that among all the factors, impact angle is the most significant factor followed by erodent size and standoff distance while the impact velocity has the least or almost no significance on erosion of the coatings. It also leads to the conclusion that factor combination of $A_3$, $B_1$, and $D_3$ gives minimum erosion rate.

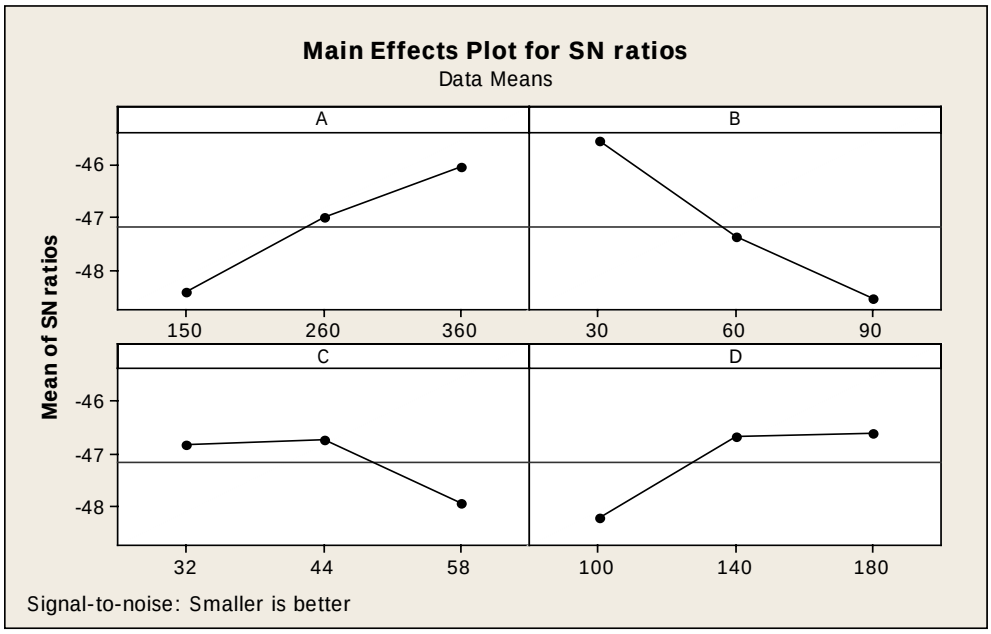


**Figure 4.13** Relative effects of control factors on erosion rate of the coatings made at 18kW.

**Table 4.10** Signal to noise ratio (S/N) response table for erosion rate.

| Level | A | B | C | D |
|---|---|---|---|---|
| I | -48.43 | -45.57 | -46.81 | -48.22 |
| II | -47.00 | -47.37 | -46.74 | -46.66 |
| III | -46.05 | -48.55 | -47.93 | -46.61 |
| Delta | 2.37 | 2.98 | 1.19 | 1.61 |
| Rank | 2 | 1 | 4 | 3 |

Based on the above findings, erosion tests were carried out, on plasma sprayed fly ash-quartz coatings by a stream of dry silica sand and silicon carbide particles of average size of ~ 150 μm; at different impact angles ($30^o$, $60^o$, $90^o$) with stand of distance of 100 mm (i.e. exit point of the erodent form the nozzle to the specimen/substrate) and at a velocity of 58 m/sec.

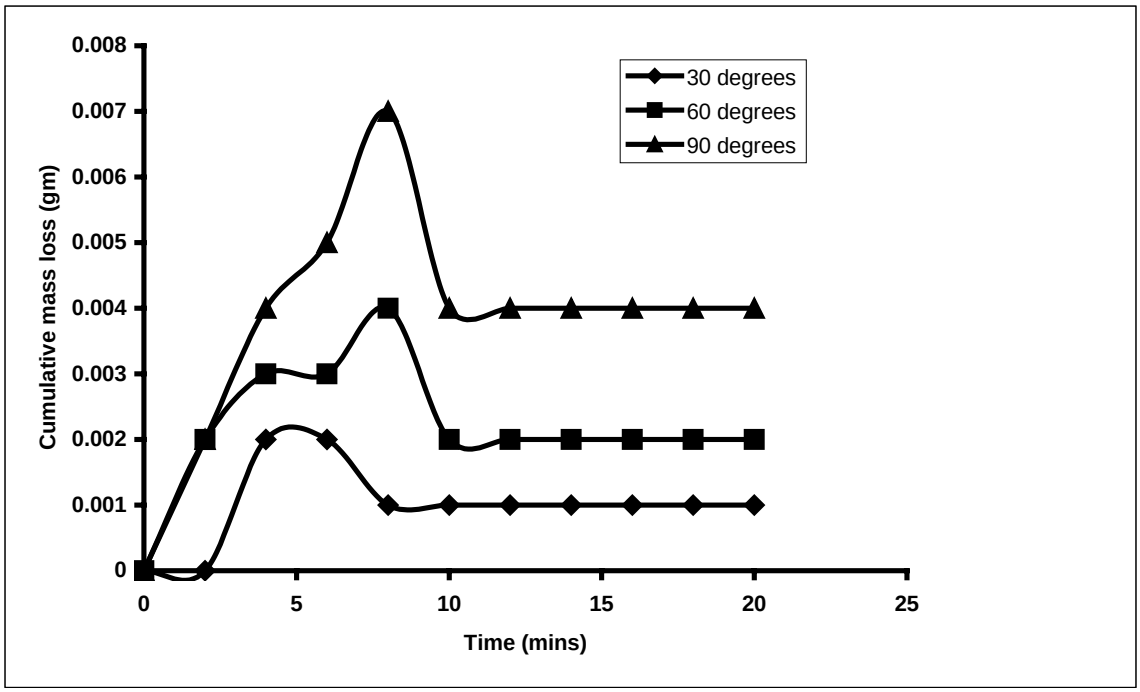


**Figure 4.14** Variation of coating mass loss with time for 150 μm dry silica sand erodant.

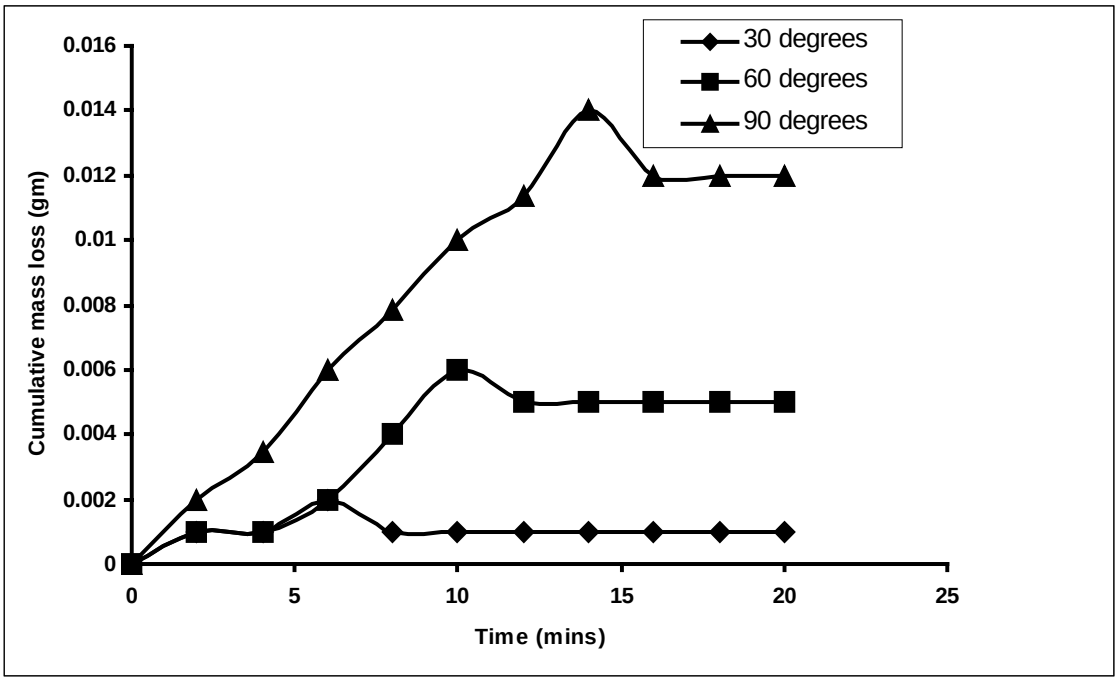


**Figure 4.15** Variation of coating mass loss with time for 150 μm SiC erodent.

The variation of cumulative mass loss with time, in case of the coating eroded by sand is illustrated in Fig 4.14 and in case of the coating eroded by SiC is illustrated in Fig 4.15. From the figures, it is seen that, the coating mass loss increases with increasing the time of attack initially irrespective of the angle of impact. This can be attributed to the fact that, the fine protrusions on the top layer of the coatings may be relatively loose i.e. having lesser contact area with the neighborhood particles, due to first rate of heat transfer to the surrounding (air atmosphere) and hence removed with less energy than what would be necessary to remove a similar portion/layer from the inner layers of the coating at further time length of impact/erosion. Consequently, the initial mass loss is high but it follows a steady state after certain time of exposure. Finnie [45] has explained that the drastic drop of erosion rates is due to transition of type of fracture mechanism i.e. from brittle to ductile mechanism/behaviour. Sparks and Hucthings [133] have also discussed this type of transition in detail using models based on Hertzian fracture and lateral fracture. And such mechanisms are explained in the book edited by Ritter [134] also. So in our observation, sharp change/decrement in cumulative mass loss of the coatings may be due to brittle to ductile transition behaviour, with increment in attack time.

The variation of erosion rate of coatings with time at impact angles of 30°, 60° and 90°, eroded with 150 μm size silica sand and silicon carbide erodent are shown in Fig.4.16 and Fig.4.17.

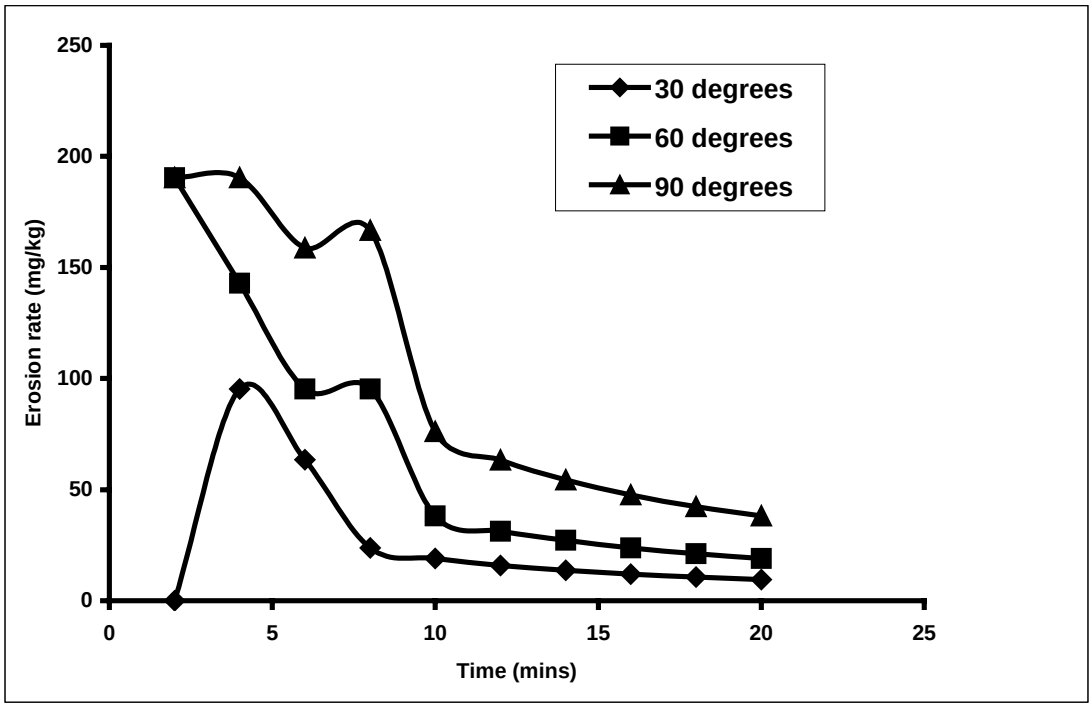


**Figure 4.16** Variation of erosion rate with time for coatings eroded with 150 μm sand erodent.

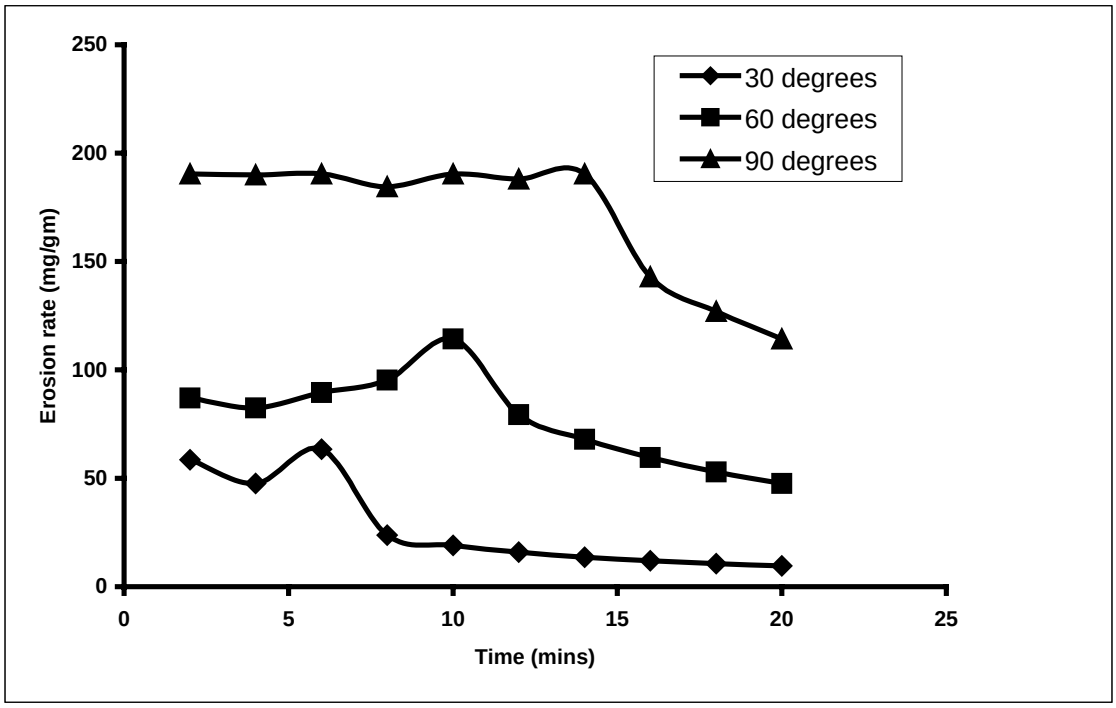


**Figure 4.17** Variation of erosion rate with time for coatings eroded with 150 μm SiC erodent.

From the above figures, it is evident that the initial wear rate is high irrespective of the angle of impact. With increasing exposure time the rate of wear starts decreasing and in the transient regime, a steady state is attended. It is also found that, maximum erosion occurs at normal impact angle ($\alpha = 90^0$) for both the erodants (dry silica sand and SiC). This behaviour is observed in case of brittle materials where the erosion rate continuously increases with increasing the impact angle and attains a maximum at $90^0$ (normal impact), in addition under brittle erosion conditions the magnitude of erosion rate is determined only by normal component of impact velocity [135], where as in case of ductile materials; major amount of material removal is by plastic deformation and high rate of material removal is at shallow impact angles. According to the common rule of the erosion rate with the change of impact angle $\alpha$, the erosion wear can be divided into ductile/plastic material wear and brittle material wear. The relationship between erosion rate and impact angle as predicted by Lishizhou [136] is as follows:

$$E = A\cos^2 \alpha \sin(m\alpha) + B \sin^2 \alpha \qquad \text{------ (4.3)}$$

Where m, A, B are constants.

For typical brittle material, $A$ is equal to zero and the erosion rate is largest at $90^o$ impact angle. For typical plastic material, $B$ is equal to zero and the erosion rate is largest at about $20^o$–$30^o$ impact angle. Further, it is also observed that the mass loss and thus in turn the erosion wear rate is higher in case of SiC erodent than that of dry silica sand of same particle size. It may be due to higher hardness of SiC as compared to dry silica sand. Studies on effect of erodent hardness on erosion rate also suggest an increase of erosion rate with increase in hardness of the impinging particles. Srinivasan and Scattergood [137] have observed such behaviour while comparing the erosion rates using SiC and $Al_2O_3$ erodants and found that the wear rate was higher in case of SiC than $Al_2O_3$. The variation of erosion wear (Fig.4.16, 4.17) thus confirms that the angle at which the stream of solid particles impinges the coating surface influences the rate of material removal i.e. the degree of erosion. It further suggests that, this dependency is also influenced by the hardness of the erodent particles.

### 4.4.3 Neural Computational Analysis for Erosion Wear Rate

To obtain minimum wear rate, combinations of operating parameters have to be planned. Therefore to study these interrelated effect, ANN statistical method, responding to the constraints, is implemented to correlate the operating parameters. In the present analysis

the velocity of impact, standoff distance, impingement angle and erodent size are taken as the four input parameters for training. Each of these parameters is characterized by one neuron and consequently the input layer in the ANN structure has four neurons. The input variables are normalized so as to lie in the same range group of 0-1. To train the neural network used for this work, about 45 data sets obtained during erosion trials are considered. Different ANN structures (I-H-O) with varying number of neurons in the hidden layer are tested at constant cycles, learning rate, error tolerance, momentum parameter, noise factor and slope parameter. Based on least error criterion, one structure, shown in Table 4.11, is selected for training of the input-output data. The learning rate is varied in the range of 0.001-0.100 during the training of the input-output data. Neuron number in the hidden layer is varied and in the optimized structure of the network, this number is 12. The number of cycles selected during training is high enough so that the ANN models could be rigorously trained.

**Table 4.11** Input parameters selected for training (coating wear rate)

| **Input Parameters for Training** | **Values** |
|---|---|
| Error tolerance | 0.00001 |
| Learning rate (ß) | 0.1 |
| Momentum parameter(α) | 0.3 |
| Noise factor **(NF)** | 0.5 |
| Number of epochs | 10000000 |
| Slope parameter ( ) | 0.6 |
| Number of hidden layer | 12 |
| Number of input layer neuron **(I)** | 4 |
| Number of output layer neuron **(O)** | 1 |

A software package NEURALNET for neural computing developed by Rao and Rao [122] using back propagation algorithm is used as the prediction tool for erosion wear rate of different coatings under various test conditions. The three-layer neural network having an input layer (I) with four input nodes, a hidden layer (H) with twelve neurons and an output layer (O) with one output node employed for this work is shown in Fig. 4.18.

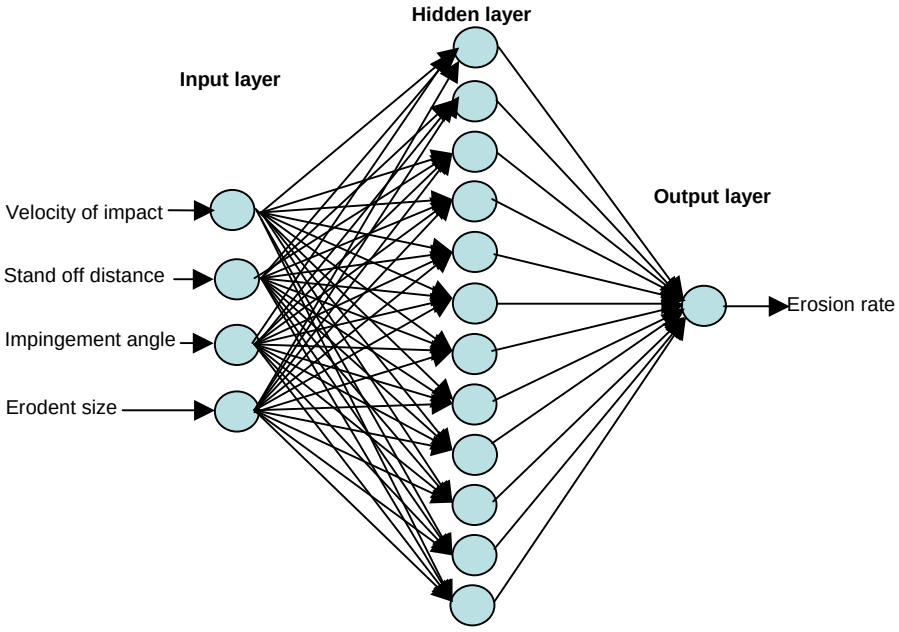


**Figure 4.18** The three layer neural network (for erosion wear rate)

Seventy five percent of data collected from erosion test is used for training whereas twenty five percent data is used for testing. The parameters of three layer architecture of ANN model are set as input nodes = 4, output node = 1, hidden nodes = 12, learning rate = 0.1, momentum parameter = 0.3, number of epochs = 10000000 and a set of predicted output ($E_{ANN}$) is obtained. A comparison among the experimental and the ANN predicted results are presented in Table 4.12 and Fig. 4.19. The errors calculated with respect to the experimental results are also given. It is observed that maximum error between ANN prediction and experimental wear rate is between 0 - 8 %. The error in case of ANN model can further be reduced if number of test patterns is increased. However, present study demonstrates successful implementation of ANN for prediction of wear rate in a complex process of solid particle erosion of coatings.

**Table 4.12** Comparison between the experimental and the ANN predicted results

| Test runs | Erosion wear rate Experimental (mg/kg) | Erosion wear rate ANN Predicted (mg/kg) | Error (%) |
|---|---|---|---|
| 1 | 238.095 | 238.086 | 0.003 |
| 2 | 243.055 | 262.40 | 7.95 |
| 3 | 317.460 | 317.47 | 0.003 |
| 4 | 166.667 | 166.66 | 0.005 |
| 5 | 283.018 | 283.009 | 0.003 |
| 6 | 238.095 | 238.104 | 1.58 |
| 7 | 172.413 | 167.766 | 2.69 |
| 8 | 185.185 | 185.199 | 0.007 |
| 9 | 253.396 | 253.386 | 0.003 |

### 4.4.4 Predictive Equation for Determination of Erosion Rate

In this study, an attempt is made to derive a predictive equation in terms of the significant control factors for determination of erosion rate. The single-objective function requires quantitative determination of the relationship between erosion rates with combination of control factors. In order to express, erosion rate in the form of a mathematical model in the following correlation is suggested.

$$E = K_0 + K_1 \times A + K_2 \times B + K_3 \times C + K\,4 \times D \quad \text{------ (4.4)}$$

Here, $E$ is the performance output terms and $K_i$ (i = 0, 1…3) are the model constants. The constant are calculated using non-linear regression analysis with the help of SYSTAT 7 software and the following relations are obtained.

$$E = 228.43 - 0.298 \times A + 1.288 \times B + 1.462 \times C - 0.438 \times D \quad \text{------ (4.5)}$$

The correctness of the calculated constants is confirmed as high correlation coefficients ($r^2$) in the tune of 0.997 are obtained for Eq. (4.5).

A comparison between experimental values and values predicted by the predictive equation for erosion rate are given in Table 4.13 and their comparison plot with ANN

predicted erosion rate is given in Fig. 4.19. It is observed that maximum error between predictive equation and experimental wear rate is between 0 - 10 %.

**Table 4.13** Comparison between the experimental and the predictive equation results

| Test runs | Erosion wear rate Experimental values (mg/kg) | Erosion wear rate Predictive equation values (mg/kg) | Error (%) |
|---|---|---|---|
| 1 | 238.095 | 225.354 | 5.35 |
| 2 | 243.055 | 264.018 | 8.62 |
| 3 | 317.460 | 305.606 | 3.73 |
| 4 | 166.667 | 175.078 | 5.04 |
| 5 | 283.018 | 269.226 | 4.86 |
| 6 | 238.095 | 252.338 | 5.98 |
| 7 | 172.413 | 183.266 | 6.29 |
| 8 | 185.185 | 166.374 | 10.00 |
| 9 | 253.396 | 257.598 | 1.65 |

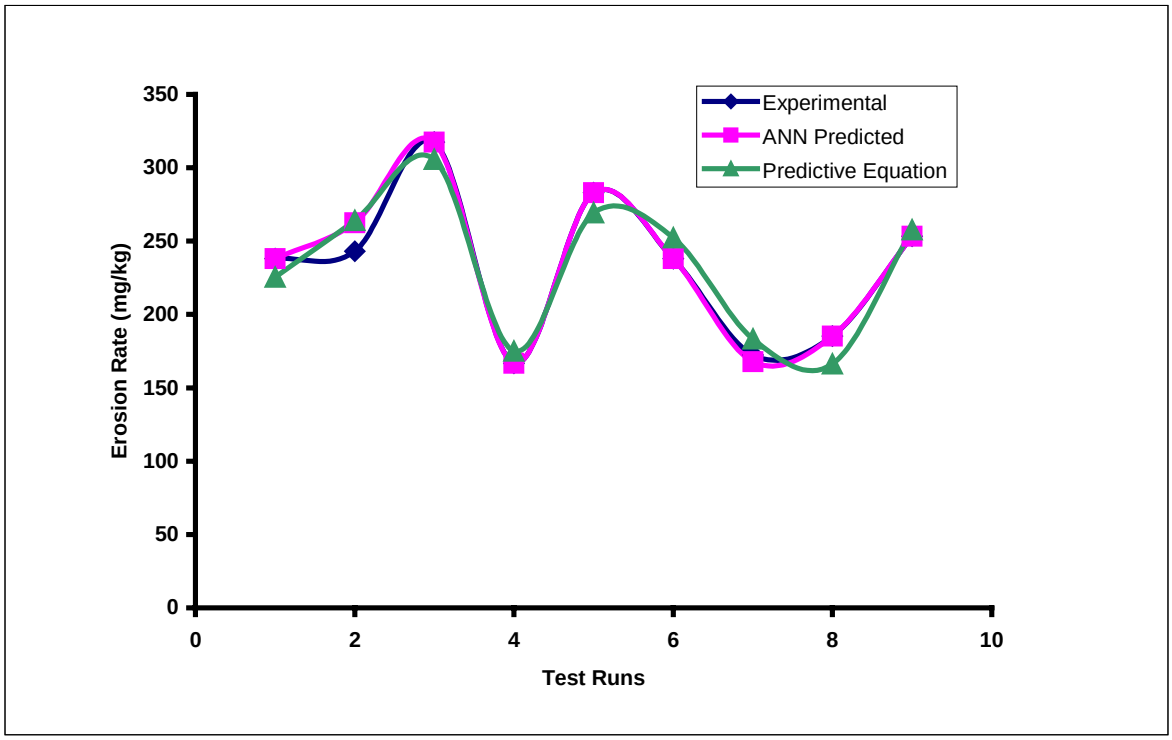


**Figure 4.19** A comparison plot for experimental, ANN predicted and predictive equation values for erosion rate of fly ash – quartz coatings.

### 4.4.5 Microstructural Investigation of Erodants and Eroded Surfaces

**Morphology of the Erodants**

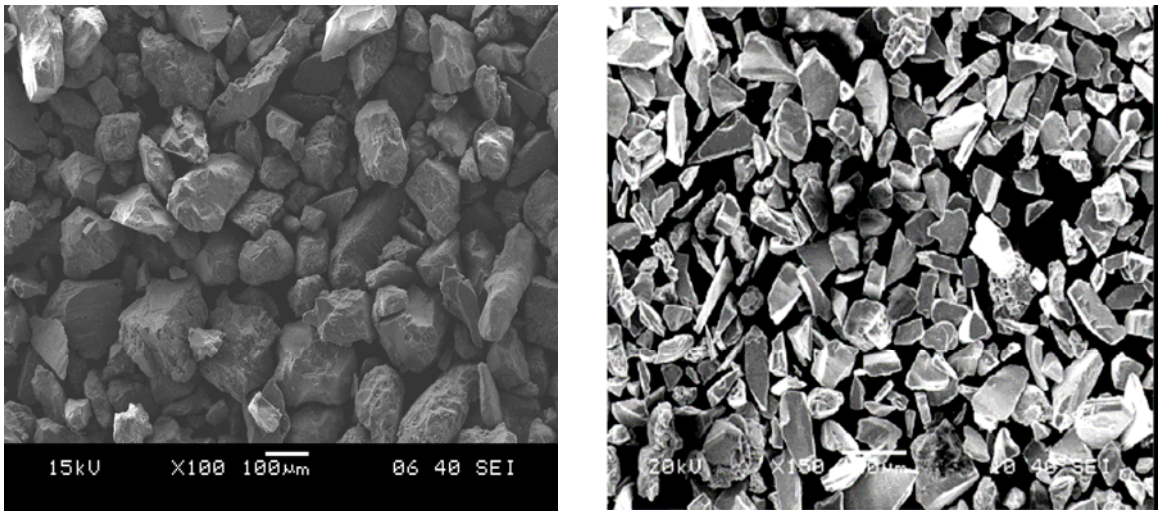


**(a)** **(b)**

**Figure 4.20** Surface morphology of **(a)** dry silica sand and **(b)** SiC particles

The morphology of the erodents (i.e. Sand and SiC) are shown in Fig. 4.20. It can be visualized that, the sand particles are mostly spherical or rounded / equiaxed in shape with cleavage/quasi-cleavage edges, as observed in Fig.4.20 (a), while silicon carbide particles are having multiple angular facets and sharp edges, as seen in Fig.4.20 (b). This might be the cause of fast rate of removal of material through chipping/plowing of the surface when silicon carbide is used as erodent, thereby leading to higher amount of material loss (i.e. cumulative mass loss). Hence erosion rate is higher when SiC is used. So there is negligible crack initiation/formation and minor chipping portions are observed on the eroded surfaces.

**Morphology of Eroded Surfaces**

Surface morphology of fly ash-quartz coating eroded with dry silica sand and SiC erodent at different impact angles are shown in Fig.4.21 and Fig. 4.22 respectively.

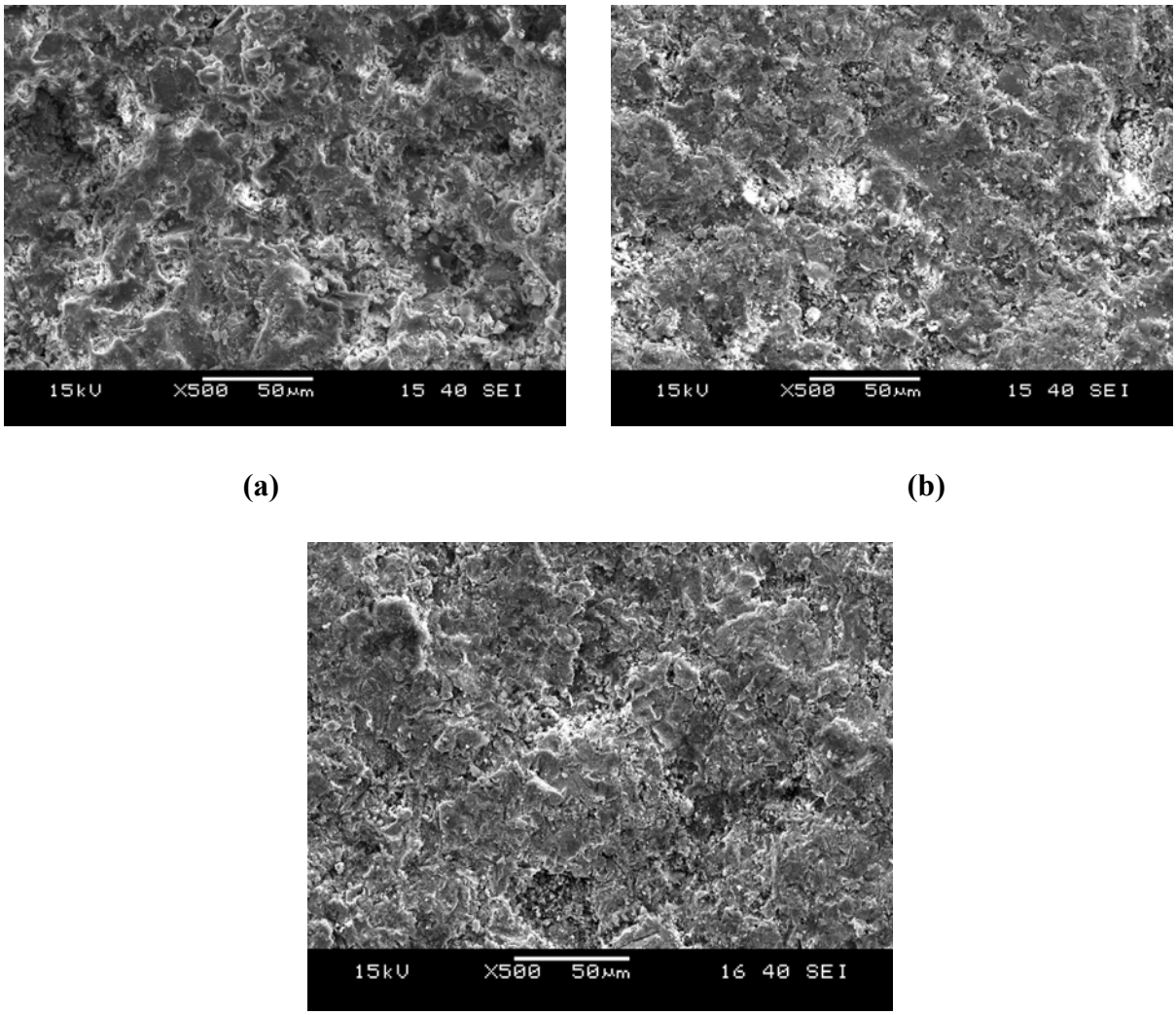


**(a)** **(b)**

**(c)**

**Figure 4.21** SEM micrographs of eroded surfaces of coatings deposited at 18 kW at angle of impact **(a)** $30^0$ **(b)** $60^0$ **(c)** $90^0$ using sand as the erodent.

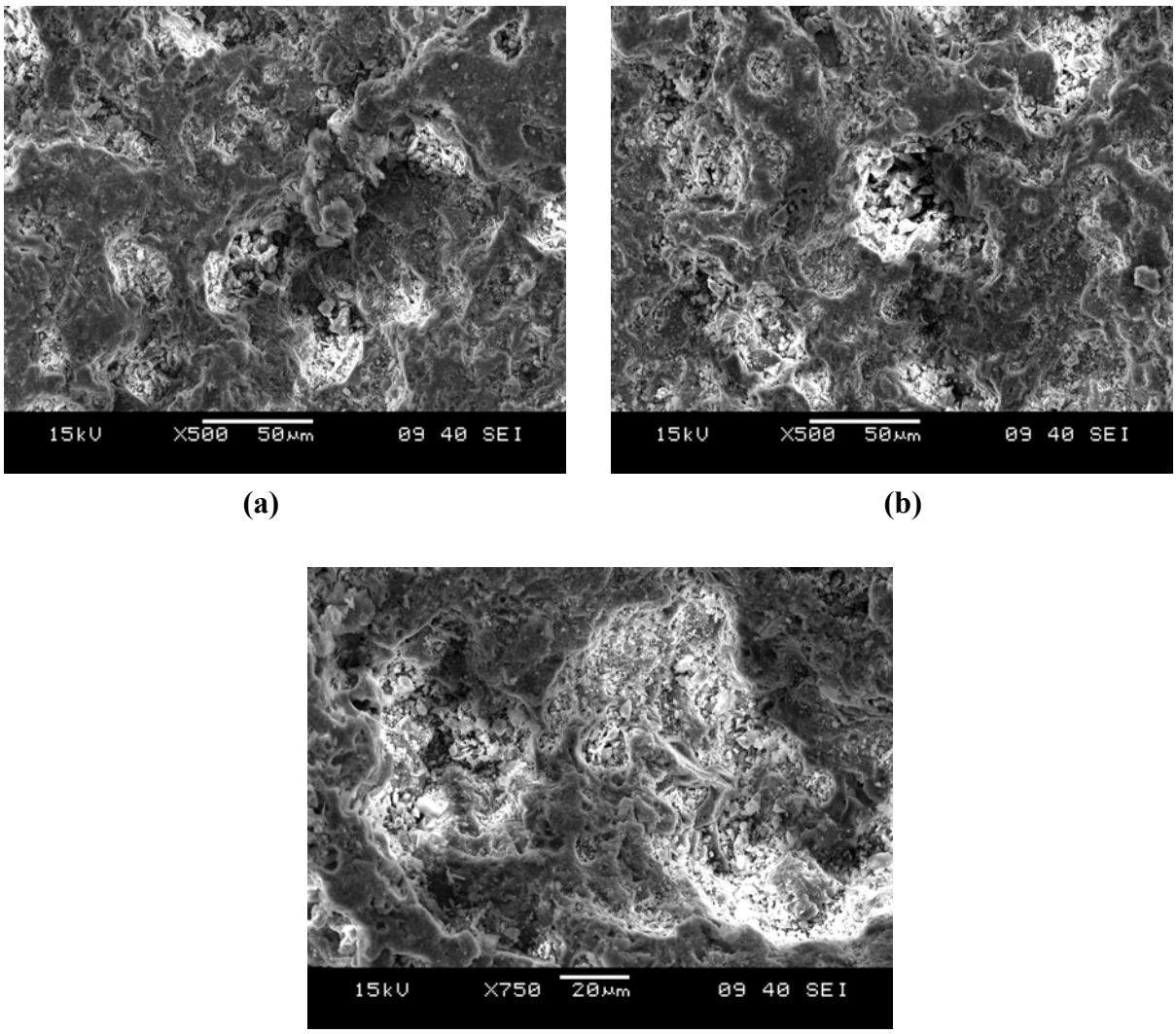


**(a)** **(b)**

**(c)**

**Figure 4.22** SEM micrographs of eroded surfaces of coatings deposited at 18 kW at angle of impact **(a)** $30^0$ **(b)** $60^0$ **(c)** $90^0$ using SiC as the erodent.

Fig. 4.21 (a) and Fig 4.22 (a), show the surface morphology of worn surfaces, when the erodent is impacted at $30^0$. Chipping away of layers/plowing caused by dominancy of the shear component of erodent particles, might be playing the principal role and hence more cavities are formed. Some small cracks are observed and spread along grains/splats boundaries. At $90^0$ angle of impact, (Fig.4.21 (c) and Fig 4.22 (c)), sharp deep groves are seen which is due to dominating effect of perpendicular component of the force of impingement of the erodent. As described by Maozhong [113], during normal impacting of the erodent particles, the surface of the coating endures Hertz force; partial plastic deformation takes place and cracks initiate. The cracks propagate through the grain boundaries, which is more prominent when sand is used as the erodent (Fig. 4.21 (c)) than

that of the SiC erodent (Fig. 4.22 (c)). And then the flattened grains on the coating surface get loosen and eventually fall off by repeated impact. Fig. 4.21 (b) and Fig 4.22 (b) exhibit the morphology of worn surface when erodent is impacted at $60^0$. It is clearly seen that the traces of chipping/plowing are not as shallow and flat as was at $30^0$ and/or $90^0$ impact angle. So, erosion at $60^0$ is somewhere in between that at $30^0$ and $90^0$ impingement angles. In general it can be stated that the when hard and multifaceted erodent i.e. SiC is used, deeper groves are produced and plastically flow regions are found and also limit the surface crack propagation.

## 4.5 DISCUSSION

From this study, it is found that deposition efficiency has increased with increase in input power to the plasma torch. But after 18 kW, power input, the increase is not significant. This is a measure of the amount of material deposited per unit surface area. It is observed that the coating thickness acquires a maximum of 235 μm at 15 kW input power and then decreases. The porosity in the coatings is also found to be maximum at the same input power level. This indicates that though the deposition efficiency is not maximum at 15 kW, but higher thickness of the coatings may be due to presence of more amount of porosity. The adherence of the coatings to the substrate is of major concern. Analysis of the adhesion strength of the coatings envisages that the adhesion strength increases with increase in input power and attains a maximum at 18 kW, and decreases thereafter. The increased amount of porosity in case of low and high power levels may be the cause of low adhesion strength. Variation of coating hardness with power level reveals that, there might be formation/transformation of allotropic forms (of silica and alumina) and their compositional variations during spray deposition, which is evident from the XRD compositional analysis.

To assess the suitability of these coatings for tribological applications, solid particle erosion wear behaviour is studied. Taguchi statistical technique is used to identify the significant parameter affecting the wear rate of the coatings made at 18 kW power level (as maximum adhesion strength is observed in this case). Impingement angle followed by erodent size is identified as the important process parameter affecting the erosion of the coatings. With the increase in impact angle erosion wear increases and attains maximum at $90^0$. The angle of impact determines the relative magnitude of the two components of the impact velocity namely, the component normal to the surface and parallel to the surface. The normal component determines/is responsible for the lasting time of impact (i.e. contact

time) and the load. The product of this contact time and the tangential (parallel) velocity component determines the amount of sliding that takes place. The tangential velocity component also provides a shear loading to the surface in addition to the normal load of the normal velocity component. Hence, as this angle changes the amount of sliding that takes place also changes as does the nature and magnitude of the stress system. Both of these aspects influence the way a coating/material wears. Statistical modeling/analysis techniques viz. ANN, Taguchi method and SYSTAT technique etc. can be very much useful to predict the experimental data with conducting least number of experiments; and also can predict experimental results beyond the parameter domains used in the experimentations.

# Chapter 5

# Conclusions

# CHAPTER 5
# CONCLUSIONS

The conclusions drawn from the present investigation are as follows:

- Fly ash, the waste generated from thermal power plants may be eminently coatable on metal substrates when mixed with quartz, a low grade mineral ore, employing atmospheric plasma spraying technique. Such coatings possibly posses desirable coating characteristics such as good adhesion strength, hardness, etc.

- Adhesion strength of the coatings varied with the plasma power input and the kind of substrate on which coatings are deposited. Maximum adhesion strength of 6.12 Mpa on mild steel substrate and 5.802 Mpa on copper substrate is recorded on the coatings deposited at 18 kW. It is noted that, invariably in all cases, the interface bond strength increases with the input power to the torch up to a certain power level and further increase in input power there is no significant increase in adhesion strength. Coating adhesion is better in case of mild steel substrate than that of copper substrate.

- A maximum deposition efficiency of 35 % could be achieved with mild steel substrates. It is interesting to note that the deposition efficiency has increased in a step up fashion with the increase in torch power input.

- Amount of porosity is more in case of coatings made at (lower) 11 kW and at (higher) 21 kW power levels. However porosity is less for the coatings made 18 kW. More amount of porosity may be the reason for low adhesion strength of the coatings deposited at low and high power levels.

- Operating power level of the plasma torch influences the coating adhesion strength, deposition efficiency and coating hardness to a great extent. The coating morphology is largely affected by the plasma input power.

- The microstructure of the coatings is also dependent on the physical characteristics such as porosity, phase transformations of the raw materials during spraying at different power levels.

- Due to phase transformations and inter-oxide formation during plasma spraying, changes in coating characteristics such as hardness etc. are observed.

- The coatings developed in this work are much harder than substrate metals on which they are deposited. Hence these coatings can be recommended for tribological applications.

- Factors such as erodent size, impact angle of the erodent, velocity of impact and standoff distance and hardness etc. affect the coating erosion wear rate. Taguchi experimental design has proved to be a useful tool for identifying the significant parameters in this case. It has identified impact angle and erodent size as the most significant factors affecting the erosion wear rate of fly ash – quartz coatings.

- Maximum erosion of the coatings took place at an impact angle of $90^0$ irrespective of the type of erodent used i.e. whether dry silica sand or SiC.

- The erosion wear rate is higher in case of coatings eroded by SiC erodent than eroded by dry silica sand. This may be due to the higher hardness and multi faceted structure of the SiC particles as compared to sand, which bears rounded shape appearance and also has lower hardness as compared to SiC.

- Microstructure of the eroded surfaces suggests that when hard and multifaceted erodent i.e. SiC is used, deeper groves are produced and plastically flow regions are found and also less amount of surface crack propagation. While in case of sand erodent, crack propagation through the grain boundaries is prominent.

- Erosion wear behavior is one of the main requirements of the coatings developed by plasma spraying for recommending specific application. In order to achieve tailored erosion wear rate accurately and repeatedly, the influence of the process parameters are to be controlled accordingly. The coating sustains erosion by solid particle

impingement substantially and therefore fly ash-quartz can be considered as a potential coating material suitable for various tribological applications.

## SCOPE FOR FUTURE WORK

The present work opens up a wide area for future investigators to explore the possibility of development of ceramic composite coatings using fly ash premixed with other ore minerals. Thermal stability of these coatings is to be evaluated to find its suitability for high temperature applications. Sliding wear behavior under different conditions can be investigated to identify other areas of application. Post heat treatment of these coatings can be made to ascertain further improvement in coating properties.

# References

**1.** Taylor, P.R., Das, A.K., "Thermal Plasma Processing of Materials", Power Beams and Materials Processing PBAMP, Mumbai, India: Allied Publishers Pvt. Ltd., (2002), pp.13-20.

**2.** Bandopadhyaya, P.P., "Processing and Characterization of Plasma sprayed Ceramic Coatings on Steel Substrate", Ph.D.Thesis, IIT, Kharagpur, India, (2000).

**3.** Pawlowski, L., "The Science and Engineering of Thermal Spray Coatings", New York, USA: Wiley, (1995), pp. 432.

**4.** Sidhu, Buta Singh, Singh, Harpreet, Puri D., Prakash, S., "Wear and Oxidation Behavior of Shrouded Plasma Sprayed Fly ash Coatings", Tribology International, Volume 40, (2007), pp.800-808.

**5.** Sampath, S., Herman, H., In:Yazici, R.M., (ed)., "Protective Coatings Processing and Characterization", USA, The Minerals, Metals and Material Society, (1990), pp.145.

**6.** Mishra, S.C., Rout, K.C., Padmanavan, P.V.A., Mills, B., "Plasma Spray Coating of Flyash Premixed with Aluminium Powder Deposited on Metal Substrates", Journal of Materials Processing Technology, Volume 102, No1-3, (2000), pp.9-13.

**7.** Mishra, S.C., Satpathy, Alok, Das, Satyabati, Sarkar, S., Ananthapadmanavan, P.V., Sreekumar, K.P., "Plasma Spray Composite Coating on Metals using Flyash and Illmenite", Journal of Manufacturing Engineering, Volume 3, No 2, (2008), pp.118-123.

**8.** Mishra, S.C., "Mineral Processing Recent Advances and Future Trends", New Delhi, India, Allied Publications, (1995), pp. 837.

**9.** Cotell, C.M. and Sprague, J.A., Preface, Surface Engineering, ASM Handbook, ASM International, Volume 5, (1994), pp.5.

**10.** Heiman, R.B., "Plasma Spray Coating: Principle and Application", VCH, Weinheim, Germany, (1996).

**11.** Edwards, R., Cutting Tools, The Institute of Materials, UK, (1993).

**12.** Budinski, K. G., Surface Engg. for Wear Resistance, N.J., USA, (1988).

**13.** Metco Plasma Spraying Manual, Metco, USA, (1993).

**14.** Thorpe, M.L., "Thermal Spray. Industry in Transition", Adv.Mater.Process., Volume 143, No. 5, (1993), pp. 50-61.

**15.** Herman, H., "Plasma Spray Deposition Processes", MRSBull., Volume 12, (1988), pp. 60-67.

**16.** Longo, L. F., Thermal Spray Coatings, ASM, USA, (1985).

**17.** Meringolo, V., Thermal Spray Coating, Tappi Press, Atlanta, USA, (1983).

**18.** Satpathy, Alok, Mishra, S.C., Padmanabhan, P.V.A, Sree Kumar, K.P., "Development of Ceramic Coatings Using Red Mud – A Solid Waste of Alumina Plants", Journal of Solid Waste Technology and Management, Volume 33, No 2, (2007), pp.48-53.

**19.** Fauchais, P., Verdelle, M., Verdelle, A., Bianchi, L., "Plasma Spray: Study of Coating Generation", Ceramic International, Volume 22, (1996), pp.295-303.

**20.** Wrigren, J., Surf. Coat. Tech. Volume 45, (1991), pp. 263.

**21.** Nicholas, M. G. and Scott, K. T., "Characterization of Grit Blasted Surfaces", Surfacing Journal, Volume 12, (1981), pp.5.

**22.** Funk, W., Goebe, F., "Bond Strength Optimization of Plasma-Sprayed $Cr_2O_3$ Layers by Factorial Two-Level Experiments." Thin Solid Film, Volume128, (1985), pp. 45.

**23.** Wielage, B., Hofmann, U., Steinhauser A., Zimmerman G., " Improving Wear and Corrosion Resistance of Thermal Spray Coatings", Surface Engineering, Volume 14, No.2, (1998), pp.136-138.

**24.** Lee, N. Y., Stinton, D. P., Brandt, C. C., Erdogan, F., Lee, Y. D. and Mutasim, Z., "Concept of Functionally Graded Materials for Advanced Thermal Barrier Coating Applications", J.Am. Cer. Soc., Volume 79, No.12, (1996), pp. 3003-3012.

**25.** Nash, A.R., Weare, N. E. and Walker, D. L., J. Metals., (1961), pp. 473.

**26.** Ramchandran, K. and Selvarajan, P. A., "Microstructure, Adhesion, Microhardness, Abrasive Wear Resistance and Electrical Resistivity of Plasma Sprayed Alumina and Alumina-Titania Coatings", Thin Solid Film, Volume 315, (1998), pp. 149-152.

**27.** Ingham, H. S. and Fabel, A. J., Welding Journal, (1975)**,** pp. 101.

**28.** Hennaut, J., Othmezouri, J. and Charlier, J., Mat. Sc and Tech., Volume11, (1995), pp. 174.

**29.** Elvers, B., Hawkins S. and Schultz G., Ulhmann's Encyclopedia of Industrial Chemistry, Volume 1/16, VCH, (1990), pp. 433.

**30.** Mc Pherson, R., "A Review of Microstructure and Properties of Plasma Sprayed Ceramic Coatings", Surface and Coatings Technology, Volume 39, No. 40, (1989), pp.173-181.

**31.** Mc Pherson, R., "The Relationship Between the Mechanism of Formation, Microstructure and Properties of Plasma Sprayed Coatings", Thin Solid Films, Volume 83, (1981), pp.297-310.

**32.** Ault, N.N., "Characteristics of Refractory Oxide Coatings Produced by Flame Spraying", J.Am.Ceram.Soc., Volume 40, (1957), pp. 69-74.

**33.** McPherson, R., "Formation of Metastable Phases in Flame and Plasma Sprayed Coatings", J.Mater.Sci., Volume 8, (1973), pp. 851.

**34.** McPherson, R. and Shafer, B.V., "Interlamellar Contact Within Plasma Sprayed Coatings", Thin Solid Films, Volume 97, (1982), pp.201-204.

**35.** Safai, Saed, Herman, Herbert, "Microstructural Investigation of Plasma Sprayed Aluminium Coatings", Thin Solid Films, Volume 45, (1977), pp.295-307.

**36.** Tape, N. A., Baker, E. A. and Jackson B. C., Plating and Surface finishing, (1976), pp. 30.

**37.** Holm, R., "The Frictional Force Over the Real Area of Contact", Wiss. Vereoff. Siemens Werken, Volume 17, No. 4, (1938), pp. 38-42.

**38.** Ashby, M. F. and Lim, S. C., "Wear - Mechanism Maps" Scripta Metallurgical et Materialia, Volume 24, (1990), pp. 805-810.

**39.** Wang, Y., Lei, T.C. and Gao, C.Q. "Influence of Isothermal Hardening on the Sliding Wear Behaviour of 52100 Bearing Steel", Tribology International, Volume 23, No.1, (1990), pp.47-63.

**40.** Soda, N., "Wear of Some F.F.C metals During Unlubricated Sliding Part-1, Effects of Load, Velocity and Atmospheric Pressure on Wear", Wear, Volume 33, (1975), pp. 1-16.

**41.** Burwell, J.T. and Strang, C.D., Metallic Wear, Proc. Soc (London), 212A, (1953), pp. 470-477.

**42.** Burwell, J.T., "Survey of Possible Wear Mechanisms", Wear, Volume 1, (1957/58), pp.119-141.

**43.** Zumgahr, K.H., Microstructure and Wear of Materials, Elsevier , Amsterdam , (1987).

**44.** Levy, A.V., "The Erosion-Corrosion Behaviour of Protective Coatings", Surface and Coatings technology, Volume 36, (1988), pp. 381-406.

**45.** Finnie, Iain., "Some Reflections on the Past and Future of Erosion", Wear, Volume 186, No. 187, (1995), pp. 1-10.

**46.** Hallings, J., Principles of Tribology, London and Basingstoke, The Macmillan Press Ltd., (1975), pp. 401.

**47.** Hansson, C.M., "Cavitation Erosion", In: ASM Handbook, Friction, Lubrication and Wear Technology, ASM International, USA, Volume 18, (1992), pp.214-220.

**48.** Kosel, T.H., "Solid Particle Erosion", In: ASM Handbook, Friction, Lubrication and Wear Technology, ASM International, USA, Volume 18, (1992), pp.199-213.

**49.** Miller J.E., "Slurry Erosion", In: ASM Handbook, Friction, Lubrication and Wear Technology, ASM International, USA, Volume 18, (1992), pp.233-235.

**50.** Ko, P.L., "Metallic Wear-A Review with Special References to Vibration-Induced Wear in Power Plant Components", Tribology International, Volume 20, No. 1, (1987), pp.66-78.

**51.** Eyre, L.S., "Wear Characteristics of Metals", Tribology International, (1976), pp. 203-212.

**52.** Dowson, "Wear Oh Where" International Conference on Wear of Materials, Vancouver Canada, April 14-18, (1985).

**53.** Peterson, M. B., "Advances in Tribo-Materials I: Achievements in Tribology", Amer. Soc. Mech. Eng., Volume 1, New York, (1990), pp. 91-109.

**54.** Blau, J., "Fifty Years of Research on the Wear of Metals." Tribology International, Volume 30, No. 5, (1997), pp. 321-331.

**55.** Cadenas, M., Vijendra, R., Montes, H.J. and Sierra, J.M., "Wear Behaviour of Laser Cladded and Plasma Sprayed WC-Co Coatings", Wear, Volume 212, (1997), pp. 244-253.

**56.** Nolan, Mercer, P. and Samadi, M., Surf. Engg., Volume 21, (1998), pp.124.

**57.** Naerheim, Coddet, C. and Droit, P., Surf. Engg., Volume 11, ( 1995), pp. 66.

**58.** Hojmrle, K., and Dorfman, M., Mod. Dev. Powder. Met., Volume 15, No.15, (1985), pp. 609.

**59.** Knotek, O., Lugschedar, E., Reiman, H., J. Vac. Sc. Tech. A, Volume 12, No. 4, (1975), pp.75.

**60.** Roy, M., Rao, C.V.S., Rao, D.S., Sundarajan, G., "Abrasion Wear Behaviour of Detonation Sprayed WC-Co Coatings on Mild Steel", Surf. Engg., Volume 15, No. 2, (1999), pp.129-136.

**61.** Chuanxian, Bingtang, H., Huiling, L., "Plasma Sprayed Wear Resistant Ceramic and Cermet Coating Materials", Thin Solid Films, Volume 118, (1984), pp.485-493.

**62.** Guilemey, J.M., De Pacco, J.M., Surf. Engg., Volume 11, No. 2, (1998), pp.129.

**63.** Wang, Y., "Friction and Wear Performances of Detonation Gun and Plasma Sprayed Ceramic and Cermet Hard Coatings Under Dry Friction", Wear, Volume 161, (1993), pp.69-78.

**64.** Wang, Y., Yansheng, J., Shizhu, W., "The Analysis of the Friction and Wear Mechanisms of Plasma Sprayed Ceramic Coatings at $450^0$", Wear, Volume 128, (1988), pp.265-276.

**65.** Tronche, A. and Fauchais, P., Wear, Volume 102, (1988), pp.1.

**66.** Stuart, A.A., Shipway, P.H., Mc Cartney, D.G., "Abrasive Wear Behaviour of Conventional and Nanocomposite HVOF Sprayed WC-Co Coatings", Wear, Volume 225-229, (1999), pp.789-798.

**67.** Economou, S., De Bonto, M., Celis, J.P., Roos, J.R., Smith, R.W., Lugscheider, E., Valencic, A., "Tribological Behaviour of TiC/TaC Reinforced Cermet Plasma Sprayed Coatings Tested Under Sapphire", Wear, Volume 185, (1995), pp.93-110.

**68.** Menne, U., Molar, A., Bonner, M., Varpoort, C., Ebert, K., Bauman, R., Proc. Thermal Spraying – 93, (1993), pp.280.

**69.** Mohanty, M., Smith, R.W., De Bonto, M., Celis, J.P., Lugscheder, E., "Sliding Wear Behaviour of Thermally Sprayed 75/25 $Cr_3C_2$/NiCr Wear Resistant Coatings", Wear, Volume 198, (1996), pp.251-266.

**70.** Li, J.F., Ding, C.X., Huang, J.Q., Zhang, P.Y., "Wear Mechanism of Plasma Sprayed $Cr_3C_2$-NiCr Against $TiO_2$ Coatings", Wear, Volume 211, (1997), pp.177-184.

**71.** Metals Handbook, ASM Metals Park, Ohio, USA.

**72.** Atamert, S. and Stekly, J., "Microstructure", Surf. Engg., Volume 9, No. 3, (1993), pp.231.

**73.** Price, M.O., Wolfla, T.A., Tucker, R.C., "Some Comparative Properties of Laves and Carbide Strengthened Coatings Deposited by Plasma or Detonation Gun", Thin Solid Films, Volume 45, (1977), pp.309-319.

**74.** Moore, M.A., "The Relationship Between Abrasive Wear Resistance, Hardness and Microstructure of Ferrite Steels", Wear, Volume 28, (1974), pp.59-61.

**75.** Hurricks, P.L., "Some Aspects of Metallurgy and Wear Resistance of Surface Coatings", Wear, Volume 22, (1972), pp.291-320.

**76.** Habsur, M.G. and Miner, R.V., Mat. Sc. Engg., Volume 83, (1986), pp.239.

**77.** Spear, A.E., "Diamond-Ceramic Coating of the Future", J.Am.Cer.Soc., Volume 72, (1989), pp.171-191.

**78.** Marakawa, A., "Surface Coatings of Super hard Materials for Tool Applications", Mat. Sc. Forum, Volume 246, (1997), pp.1-28.

**79.** Okada, K., Komatsu, S., Matsumoto, S., Moriyoshi, Y., "Morphology of Diamonds Prepared in a Combustion Flame", J. Mat. Sc., Volume 26, (1991), pp.3081-3085.

**80.** Zhu, W., Tan, B.H., Tan, H.S., " Diamond Thin Films Synthesized by a Multinozzle Oxy-Acetylene Chemical Vapor Deposition Method", Thin Solid Films, Volume 236, (1993), pp.106-110.

**81.** Hollman, P., Alhelisteten, A., Bjorke, T., Hogmark, S., "CVD Diamond Coatings in Sliding Contact With Al, Al-17Si and Steel", Wear, Volume 179, (1994), pp.11-16.

**82.** Alhelisten, A., "Abrasion of Hot Flame Deposited Diamond Coatings", Wear, Volume 185, (1995), pp.213.

**83.** Dong, Yingchao, Feng, Xuyong, Feng, Xuefei, Ding, Yanwei, "Preparation of Low-cost Mullite Ceramics from Natural Bauxite and Industrial Waste Fly ash", Journal of Alloys and Compounds, Volume 460, (2008), pp.559-606.

**84.** Satapathy, L.N., "A Study on the Mechanical, Abrasion and Microstructural Properties of Zirconia-Fly ash Material", Ceramics International, Volume 26, (2000), pp. 39-45.

**85.** Tiwari, S., Saxena, M., "Use of Fly ash in High Performance Industrial Coatings", British Corrosion Journal, Volume 34, No. 3, (1999), pp. 184-191.

**86.** Mishra, S.C., Satpathy, Alok, Singh, K.P., Sethy, Sangeeta, Padmanabham, P.V.A., Sreekumar, K.P. and Satpute R., "Plasma Spray Coating of Fly Ash on Metals for Tribological Application", Proceedings of the International Seminar on Mineral Processing Technology, Chennai, India. (2006), pp. 825 - 829.

**87.** Satapathy, Alok, Mishra, S.C., Mohanty, Umaprasad, Mishra, Tapan Kumar and Raulo, Pratyusha P., "Plasma Spraying of Red Mud-Fly ash Mixture on Metals: an Experimental Study", National Conference on Materials and Related Technology, TIET, Patiala, India (2003).

**88.** Zhang, Tiancheng , Luo, Yichun, Li, D.Y., " Erosion Behavior of Aluminide Coating Modified with Yttrium Addition Under Different Erosion Conditions", Surface and Coatings Technology, Volume 126, (2000), pp.102-109.

**89.** Herman, H., Sampath, S., "Thermal Spray Coatings", Metallurgical and Ceramic Protective Coatings, Chapman and Hall, London, UK, (1996) pp. 261.

**90.** Mishra, S.B., Chandra, K., Prakash, S., Venkataraman, B., "Characterisation and Erosion Behaviour of a Plasma Sprayed $Ni_3Al$ Coating on a Fe-Based Superalloy", Materials Letters, Volume 59, (2005), pp.3694 – 3698.

**91.** Westergard, R., Erickson, L.C., Axen, N., Hawthorne, H.M., Hogmark S., "The Erosion Abrasion Characteristics of Alumina Coatings Plasma Sprayed Under Different Spraying Conditions", Tribol. Int., Volume 31, No. 5, (1998), pp. 271-279.

**92.** Li, Chang-Jiu., Yang, Guan-Jun., Ohmori, Akira., "Relation Between Particle Erosion and Lamellar Microstructure for Plasma Sprayed Alumina Coatings", Wear, Volume 260, (2006), pp.1166-1172.

**93.** Pfender, E., "Fundamental Studies Associated with the Plasma Spray Process", Surf. Coat. Technol., Volume 34 (1988), pp.1.

**94.** Knotek, O., In: Bhushah, R.F., (Ed.), Handbook of Hard Coatings Deposition Technologies, Properties and Applications, (2001), pp.92.

**95.** Guo, D.Z., Li, F.L.,Wang, J.Y, Sun, J.S., "Effects of Post-Coating Processing on Structure and Erosive Wear Characteristics of Flame and Plasma Spray Coatings", Surf. Coat. Technol., Volume 73, (1995), pp. 73.

**96.** Restall, J. E., Proc. 3rd Conf. on G as Turbine Materials in a Marine Environment, Bath, Ministry of Defence, London, Session V, Paper 10, (1976).

**97.** Galsworthy, J. C., Restall, J. E. and Booth, G. C., In: Brunetaud, R., Coutsouradis, D., Gibbons, T. B., Lindblom, Y., Meadowcroft D. B. and Stickler, R. (eds.), Proc. Conf.on High Temperature Alloys for Gas Turbines, Liege, October 4 - 6, (1982), pp. 207.

**98.** Tabakoff, W., "Erosion Resistance of Superalloys and Different Coatings Exposed to Particulate Flows at High Temperature", Surf. Coat. Technol., Volume 120– 121, (1999), pp.542.

**99.** Ninham, A.J., Levy, A.V., "The Erosion of Carbide-Metal Composites", Wear, Volume 121, (1988), pp. 347-361.

**100.** Shipway, P.H., Hutchings, I.M., "Measurement of Coating Durability by Solid Particle Erosion", Surf. Coat. Technol.,Volume 71, (1995), pp.1.

**101.** Brunton, J.H., Rochester, M.C., Preece, C.M., 'Erosion of Solid Surfaces by the Impact of Liquid Drops", Erosion, Treatise on Materials Science and Technology, Volume 16, Academic Press, New York, (1979), pp. 185–248.

**102.** Lesser, M.B., Field, J.E., "The Impact of Compressible Liquids" Ann. Rev. Fluid Mech., Volume 15 (1983), pp. 97–122.

**103.** Field, J .E., ELSI conference: Invited lecture, "Liquid Impact: Theory, Experiment, Applications", Wear, Volume 233–235, (1999), pp. 1–12.

**104.** Lee, M.K., Kim, W.W., Rhee, C.K., Lee, W.J., " Liquid Impact Erosion Mechanism and Theoretical Impact Stress Analysis in TiN- Coated Steam Turbine Blade Materials", Metal. Mater. Trans., Volume A, No. 30 (1999), pp.961–968.

**105.** Angle, P.A., Impact Wear of Materials, Elsevier; New York, (1976).

**106.** Tucker, R.C. Jr., "On the Relationship Between the Microstructure and the Wear Characterstics of Selected Thermal Spray Coatings", Proceeding of ITSC, Kobe, Japan, (1995), pp. 477 – 482.

**107.** Alonso, F., Fagoaga, I. and Oregui, P., "Erosion Protection of Carbon – Epoxy Composites by Plasma Sprayed Coatings", Suface and Coatings Technology, Volume 49, Issues 1 – 3, (1991), pp.482 – 488.

**108.** Tabakoff, W., Shanov, V., "Erosion Rate Testing at High Temperature For Turbo Machinery Use", Surface and Coatings Technology, Volume 76 – 77, Part I, (1995), pp. 75 – 80.

**109.** Hawthrone, F.M, Erickson, L.C., Ross, D., Tan, H. and Trockzynsko, T., "The Microstructural Dependence of Wear and Indentation Behaviour of Some Plasma- Sprayed Alumina Coatings", Wear, Volume 203 – 204, (1997), pp. 709.

**110.** Zhang, X.S., Clyne, T.W. and Hutchings, I. M., Surf. Engg., Volume 13, No. 5, (1997), pp.393.

**111.** Oka, Y.I., Okamara, K., Yoshida, T., "Practical Estimation of Erosion Damage Caused by Solid Particle Impact: Effects of Impact Parameters on a Predictive Equation", Wear, Volume 259, (2005), pp.95-101.

**112.** Roberto, Jose, Branco, Tavares, Gansert, Robert , Sampath, Sanjay , Christopher, C. Berndt , Herman, Herbert –"Solid Particle Erosion of Plasma Sprayed Ceramic Coatings ", Materials Research, Volume 7, No.1. (2004), pp. 147-153.

**113.** Maozhong, Yi, Baiyun, Huang and Jiawen, He, "Erosion Wear Behavior and Model of Abradable Seal Coating", Wear, 252, (2002), pp.9-15.

**114.** Chen, H., Lee, S.W., Du, Hao, Ding, Chuan. X. and Cho, Chu.l Ho; " Influence of Feed Stock and Spraying Parameters on the Deposition Efficiency and Microhardness of Plasma Sprayed Zirconia Coatings", Materials Letter, Volume 58, Issues 7 – 8, (2004), pp.241 – 1245.

**115.** Aglan, H. A. and Chenock, Jr, T. A. (1993). Erosion Damage Features of Polyimide Thermoset Composites, SAMPEQ, 41–47.

**116.** Nicholls, J.R., Deakin, M.J., Rickerby, D.S., "A Comparison Between the Erosion Behaviour of Thermal Spray and Electron Beam Physical Vapor

Deposition Thermal Barrier Coatings", Wear, Volume 233–235, (1999), pp. 352–361.

**117.** Sarikaya Ozkan, "Effect of Some Parameters on Microstructure and Hardness of Alumina Coatings Prepared by Air Plasma Spraying Process", Surface and Coatings Technology, Volume 190, (2005), pp.388-393.

**118.** Lima, C.R.C., Trevisan, R.E., "Graded Plasma Spraying of Premixed Metal Ceramic Powders on Metallic Substrates", J.Themal Spray Tech., Volume 62, (1997), pp. 199-204.

**119.** Lalleman G . – Tallaron, " Study of Microstructure and Adhesion of Spinelles Coatings Formed by Plasma Spraying", Ph. D. Thesis No. 96 – 58 (1996), E.C. Lyon, France.

**120.** Guilmad, Y., Denape, J. and Patil, J. A., " Friction and Wear Thresholds of Alumina-Chromium Steel Pairs Sliding at High Speeds Under Dry and Wet Conditions", Trib. Int. Volume 26, (1993), pp. 29.

**121.** Zhang, Z., Friedrich, K., Artificial Neural Network Applied to Polymer Composites: A Review, Comp. Sci. Technol., Volume 63, (2003), pp.2029-2044.

**122.** Rajasekaran, S., Vijayalakshmi, Pai G. A., Neural Networks, Fuzzy Logic And Genetic Algorithms—Synthesis and Applications – Prentice Hall of India Pvt. Ltd., New Delhi, (2003).

**123.** Rao, V. and Rao, H., 2000, C++ Neural Networks and Fuzzy Systems, BPB Publications.

**124.** Bullard, D. E., Lynch, D. C., Davenport, W. G., In: Thermal Plasma Applications in Materials and Metallurgical Processing, (Ed.) N. El-Kaddah, The Minerals, Metals and Materials Society, (1992), pp.175.

**125.** Ctibor, P., Neufuss, K., Zahalka, F., Kolman, B., "Plasma Sprayed Ceramic Coatings Without and With Epoxy Resin Sealing Treatment and Their Wear Resistance", Wear, Volume 262, (2007), pp.1274-1280.

**126.** Johner, H., Wilms, V., Schweltzer, K. K., Adam, P., " Experimental and Theoritical Aspects of Thick Themal Barrier Coatings for Turbine Applications", Thermal Spray: Advances in Coatings Technology , David L. Houck (Ed.) Published by ASM Int. USA (1987), pp.155– 166.

**127.** Patnaik, Amar, Satpathy, Alok, Mahapatra, S.and Dash, R., "Modeling and Prediction of Erosion Response of Glass Reinforced Polyster Fly ash Composites", Journal of Reinforced Plastics and Composites, (in press).

**128.** Prasad, B.K., Das, S., Jha, A.K, Modi, O.P., Dasgupta, R., Yegneswaran, A.H., "Factors Controlling the Abrasive Wear Response of a Zinc Based Alloy Silicon Carbide Particle Composite", Composites, PartA; Volume 28A, (1997), pp. 301–308.

**129.** Chua, M.S., Rahman, M., Wong, Y.S., Loh, H.T., "Determination of Optimal Cutting Conditions Using Design of Experiments and Optimization Techniques", Int. J. Mach Tools Manuf., Volume 32, No. 2, (1993), pp. 297–305.

**130.** Taguchi, G., Introduction to quality engineering, Tokyo: Asian Productivity Organization, (1990).

**131.** Yang, W.H., Tarn, Y.S., "Design Optimization of Cutting Parameters for Turning Operations Based on the Taguchi Method", J. Matern. Process Technol., Volume 84, (1998), pp. 121–129.

**132.** Phadke, M.S., Quality engineering using Robust design, AT&T, Bell Laboratories Report. New Jersey: Prentice-Hall International Editions, (1989).

**133.** Sparks, A.J., Hutchings, I.M., "Transitions in Erosive Wear Behaviour of Glass Ceramic", Wear, Volume 149, (1991), pp. 99-110.

**134.** J.E.Ritter (ed.), Erosion of Ceramic Materials, Trans. Tech. Publications, Zurich, Switzerland, (1992).

**135.** Sundarajan, G., Roy, M. and Venkataraman, B., "Erosion Efficiency – A New Parameter to Characterize the Dominant Erosion Micromechnism", Wear, Volume 140, (1990), pp. 369-381.

**136.** Lishizhou, Dong ,XiangLin, Erosion wear and Fretting Wear of Materials (in Chinese), Publisher of Mechanical Industry, Beijing, (1987).

**137.** Srinivasan, Sreeram and Scattergood, Ronaldo O., "Effect of Erodent Hardness on Erosion of Brittle Materials", Wear, Volume 128, (1988), pp. 139-152.

# PUBLICATIONS

1. "Evaluation of Erosion Wear of a Ceramic Coating with Taguchi Approach", S.C.Mishra, S.Praharaj, Alok Satapathy, Journal of Manufacturing Engineering, 2009, (accepted).

2. "Deposition of Plasma Spray Coating Using Fly ash Premixed with Quartz", S.C.Mishra, S.Praharaj, Alok Satapathy, Communicated to Bulletin of Material Science.

3. "Structure Property characteristics of Plasma Spray Coating Made with Low Valued Materials", S.C.Mishra, S.Praharaj, Alok Satapathy, Communicated to Indian Journal of Engineering and Material Sciences.